Ghent University – Faculty of Science
Vlaams Instituut voor Biotechnologie (VIB)
Laboratory of Molecular Cancer Biology (LMCB)

Role of the microRNA Pathway in Retinoblastoma

David Nittner

Thesis submitted in partial fulfillment of the requirements for the degree of Doctor in Sciences: Biotechnology

Academic year 2011-2012
Promoter: Prof. Dr. Jean-Christophe Marine

Thesis submitted in partial fulfillment of the requirements for the degree of
Doctor in Sciences: Biotechnology

Closed defense: 6th June 2012
Public defense: 28th June 2012

Promoter:	Prof. Dr. Jean-Christophe Marine[1]
Examination Committee:	
Chairman	Prof. Dr. Johan Grooten[2]
Secretary	Prof. Dr. Jean-Christophe Marine[1]
Reading Committee	Prof. Dr. Geert Berx[3] Prof. Dr. Jan Cools[4] Dr. Geertrui Denecker[3] Prof. Dr. Frank Speleman[5]
Additional Members	Prof. Dr. Wim Declercq[6] Dr. Bram De Craene[3] Prof. Dr. Johannes Schulte[7]

1. Laboratory of Molecular Cancer Biology, VIB-KULeuven, Belgium
2. Laboratory of Molecular Immunology, Biomedical Molecular Biology, UGent, Belgium
3. Molecular and Cellular Oncology Unit, VIB Department for Molecular Biomedical Research, UGent, Belgium
4. VIB Department of Molecular and Developmental Genetics, K.U.Leuven, Belgium
5. Centre for Medical Genetics Ghent (CMGG), University Hospital Ghent, UGent, Belgium
6. Molecular Signalling and Cell Death Unit, VIB Department for Molecular Biomedical Research, UGent, Belgium
7. Department of Pediatric Oncology and Hematology, University Children's Hospital Essen, Essen, Germany

Acknowledgment

Chris, thank you so much for having given me the opportunity to work on this exciting project and also for your excellent support. The last 5 years have been a great pleasure for me and I am very glad to have had so many possibilities to travel abroad to study new techniques and attend international meetings.

For the financial support I want to thank VIB who supported me over the last 5 years. I especially want to thank Marijke Lein and Mark Veugelers at VIB HQ for all their help and efforts.

Jody, thanks for all your support and your help over the last 5 years. I learned a lot and enjoyed working in your lab.

A big thank you goes to all LMCB members who made the last couple of years unforgettable for me. Thank you for all your help throughout these past few years and the great atmosphere in the lab which made the work so much more enjoyable every day. You guys were always there when I needed you.

Irina, thank you so much for all the time during the Dicer project. Without you, the project would not have existed. It was a great opportunity for me to take over your project and learn from you.

Aleks, thank you so much for everything. I don't even know where to begin. It was great to work with you on the Suvar project, even if the outcome was not what we hoped for. But nevertheless, I am happy for all the things you taught me during that time… and all the countless zombie links you sent me via email.

Fred, thank you for all the *in vitro* work you contributed to the project and all your help with the mice. You always had a helping hand ready when I needed it. I will miss all the discussions about the project when you are gone. Hopefully we will meet again at the next 20 km of Brussels or the BIFFF.

Jessika, thanks for the translations for my thesis. I really appreciate the time you took. It was great having you as my "office neighbor".

Laura, thanks for all the help with my numerous statistical questions. I could always rely on you.

Aga and Sarah, thanks for showing me how to work with mice, how to hold and inject them, and all the rest what made my time in Ledeganck so much easier.

Rajesh, thanks for the great time in the lab. Now I even know the rules to cricket.

Trui, thanks for your help during the Dicer project. I also really appreciate that you were part of my jury and are very grateful for your valuable comments.

Odessa and Greet, thanks for all the help with the mice. Especially in the last months during writing and preparing my PhD thesis, it would not have been possible without you.

Flavie, thanks for all your effort with organizing the lab meetings and journal clubs and your flexibility when I (usually) had to change the date.

Michael, thanks for always knowing how to order things and answering my countless questions on where to find this and that in the lab during all the times we moved.

Morvarid, thanks for all the help during my PhD and especially during the PhD defense. I could always ask you what to do and you always helped me.

Dieter, Natacha, Natalie, and Rose, thanks for all the help with PCRs, stainings, and other countless things in the lab which helped me to safe so much time.

I want to thank Pieter Mestdagh, Jo Vandesompele, and Frank Speleman for all their work with the miRNA profiling for my project.

Thanks also to Johannes Schulte and Alexander Schramm for sharing the data of the human retinoblastoma samples with us.

Thanks to Michael Dyer who gave me the opportunity to learn from his expertise in performing all the experiments with mouse retinae.

Thanks to Aart G. Jochemsen for his help with the Y79 cell lines.

Thanks to G. Hannon for providing the *Dicer1* floxed mice.

Last but not least, I want to thank my family very much for their constant support during all of my studies. Thank you to my parents, who always believed in me. I also want to express my gratitude towards Anne-Leen's family, who were also always there for me and helped us out with countless days of babysitting. Thank you, Anne-Leen, for all your help. You always supported me, from preparing my applications for the VIB Scholarship for International Ph. D. students to helping correcting my thesis and all other help during this stressful time of writing my thesis.

Table of Contents

1. Summary

1.1 Summary

Retinoblastoma is the most prevalent intraocular malignant tumor among very young children (Kivelä 2009, Mahajan et al. 2011). Most of the children are younger than two years when they are diagnosed with retinoblastoma (Young et al. 1999). The initial step for retinoblastoma formation is a mutation in the retinoblastoma gene, *RB1*, which is either sporadic or heritable. Besides the involvement of the tumor suppressor *RB1*, recent studies also revealed a link between retinoblastoma development and the p53 pathway through involvement of its negative regulators *Mdm2* and *Mdm4* (Laurie et al. 2006).

The mouse tumor model we use to study the molecular mechanisms of retinoblastoma, relies on the absence of both *Rb1* and the *Rb1* family member *p107*. As a consequence of the *Rb1/p107* deficiency, these mice develop retinoblastoma late in life. Additional loss of *Trp53* (or *p53*) in these mice further accelerates tumor formation and increases the aggressiveness of the tumor spectrum (Zhang et al. 2004b, Laurie et al. 2006).

The p53 tumor suppressor is commonly compromised in human cancers – either by direct mutation within the *p53* gene (*TP53*) or by deregulation of its upstream regulators or downstream effectors such as *Mdm2* and *Mdm4* (Marine et al. 2006, Toledo and Wahl 2006). Moreover, mutations in *p53* are often associated with aggressive tumor development and poor prognosis in disease outcome (Soussi and Béroud 2001).

Therefore, identification of p53 interactors crucial for the survival of *p53*-compromised mutant cells might highlight potential novel cancer cell-specific drug targets. Those targets would have the benefit that therapeutically targeting these p53 interactors would lead to synthetic lethality in *p53*-deficient cancer cells but leaving healthy tissue with an intact p53 pathway unharmed.

In this work we show that homozygous loss of *Dicer1*, a central enzyme in the microRNA processing machinery and a haploinsufficient tumor suppressor (Lambertz et al. 2010, Kumar et al. 2009), prevents retinoblastoma formation in mice by synthetic lethal interaction with *p53*. Although loss of *Dicer1* is tolerated during normal retinogenesis and in retinoblastoma-tumor initiating cells with an intact p53 pathway, *Dicer1* deficiency is synthetic lethal upon *p53* inactivation in tumor initiating cells. However, oncogenic stress,

such as *Rb1/p107* inactivation in the mouse model we used, is required for the *Dicer1*/*p53* synthetic lethality.

Importantly, the synthetic lethal effect of *Dicer1* and *p53* can fully be replaced by deletion of the oncogenic microRNA cluster *miR-17~92* instead of *Dicer1*, as we show that inactivating the *miR-17~92* cluster in tumor-prone mice deficient of *p53* suppresses tumorigenesis. Accordingly, *in vitro* co-silencing of *miR17/20a* and *p53* cooperatively decreases the viability of pre-formed human retinoblastoma cells.

Taken together, we provide important insights into the genetic mechanisms explaining why *Dicer1* is not lost during tumorigenesis and identified *miR-17~92* as a first microRNA cluster of which loss is synthetic lethal with *p53*. Consequently, while inhibition of *Dicer1* should be considered with caution, microRNAs such as miR-17/20a should be explored as a highly selective therapeutic approach for the treatment of retinoblastoma.

Ultimately, the question should be addressed, whether there are other tumor systems in which the *miR-17~92* cluster, or any other microRNAs, would show a synthetic lethal interaction with *p53* and could therefore be an important new avenue of research in fighting diseases with a compromised p53 pathway.

1.2 Samenvatting

Retinoblastoma is de meest voorkomende intraoculaire maligne tumor bij kinderen (Kivelä 2009, Mahajan et al. 2011). De meerderheid van de kinderen zijn jonger dan twee jaar op het moment van diagnose (Young et al. 1999). De initiële stap naar retinoblastomavorming is een mutatie in het retinoblastomagen, *RB1*. Deze mutatie is weinig voorkomend of overerfbaar.

Naast de betrokkenheid van de tumorsuppressor, *RB1* tonen recente studies de link aan tussen retinoblastomaontwikkeling en de p53-signalisatieweg door de betrokkenheid van zijn negatieve regulatoren, *Mdm2* and *Mdm4* (Laurie et al. 2006).

Het muismodel dat we gebruiken om de moleculaire mechanismen van retinoblastoma te bestuderen is afhankelijk van de afwezigheid van zowel *Rb1* en het *Rb1*-familielid, *p107*. Als gevolg van de *Rb1/p107*-afwezigheid, ontwikkelen deze muizen retinoblastoma laat in het leven. Bijkomend verlies van *Trp53* (of *p53*) in deze muizen versnelt verder de tumorontwikkeling en verhoogt de agressiviteit van het tumorspectrum (Zhang et al. 2004b, Laurie et al. 2006).

De tumorsuppressor, p53 is vaak aangetast in menselijke kankers, dit door directe mutatie binnen het *p53*-gen of door ontregeling van opwaartse of neerwaartse effectoren zoals *Mdm2* and *Mdm4* (Marine et al. 2006, Toledo and Wahl 2006). Bovendien zijn mutaties in *p53* dikwijls geassocieerd met agressieve tumorontwikkeling en slechte prognose in de afloop van de ziekte (Soussi and Béroud 2001).

Zodoende kan identificatie van p53-interactoren, die noodzakelijk zijn voor de overleving van cellen met gewijzigd *p53*, nieuwe celspecifieke doelwitten onthullen waartegen nieuwe therapeutische middelen kunnen ontwikkeld worden. Kankermedicijnen gericht tegen deze p53-interactoren zou leiden tot synthetische letaliteit in *p53*-deficiënte kankercellen maar zou gezond weefsel met een intacte p53-signalisatieweg ongedeerd laten.

In dit werk tonen we aan dat homozygotisch verlies van *Dicer1*, een centraal enzyme in de biogenese van microRNA's en een haploinsufficiente tumorsuppressor (Lambertz et al. 2010, Kumar et al. 2009) retinoblasomavorming in muizen voorkomt door zijn synthetisch letale interactie met p53. Hoewel tijdens de normale retinogenese en in startende retinoblastomatumorcellen met een intacte p53-signalisatieweg het verlies van *Dicer1* tolerant is, is een Dicer1-tekort synthetisch lethaal bij *p53*-inactivatie in tumor-initiërende cellen. Oncologische stress zoals *Rb1/p107*-inactivatie in het gebruikte muismodel is hoe dan ook nodig voor de *Dicer1*/*p53*-synthetische letaliteit.

Niet onbelangrijk is dat het synthetisch letaal effect van *Dicer1* en *p53* volledig kan worden herhaald door de deletie van de oncologische microRNA-cluster, *miR-17~92* in plaats van *Dicer1*. Zo tonen we aan dat in *p53*-deficiënte muizen, vatbaar voor tumoren de inactivatie van de *miR-17~92*-cluster de tumorontwikkeling onderdrukt. Ook *in vitro* zien we een verminderde leefbaarheid van humane retinoblastomacellen wanneer we *miR17/20a* en *p53* gelijktijdig uitschakelen.

Alles samenvattend leveren we belangrijke inzichten in de genetische mechanismen die verklaren waarom *Dicer1* niet verloren is tijdens de tumorontwikkeling en identificeren we *miR-17~92* als eerste microRNA-cluster die een synthetisch letale interactie vertoont met *p53*. Derhalve moet de remming van *Dicer1* voorzichtigheid overwogen worden, terwijl verder onderzoek van de microRNA's, miR-17/20a nodig is voor een zeer selectieve therapeutische benadering in de behandeling van retinoblastoma.

Tenslotte moet men zich afvragen of er andere tumorsystemen zijn waarbij de *miR-17~92*-cluster of andere microRNA's synthetische letaliteit vertonen met *p53* en

bijgevolg kunnen leiden tot een nieuwe onderzoeksweg naar de strijd tegen ziekten met een gecompromitteerde p53-signalisatieweg.

2. Introduction

2.1 The microRNA pathway

2.1.1 Non-coding RNAs are crucial for normal development and for disease

Protein-coding genes account for 2% of the genome (Alexander et al. 2010). But although the rest of the genome does not give rise to proteins, there are many non-coding genomic regions which have a crucial functional role for normal development and for disease. Non-coding RNAs (ncRNAs) are a relatively new class of RNA which contribute to normal development and to many different human diseases (van Kouwenhove et al. 2011, Nikitina et al. 2012). There are many different types of ncRNAs (see Table 2.1). The first identified and also most studied type of ncRNAs are microRNAs (miRNAs) (Lee et al. 1993, Wightman et al. 1993).

2.1.2 Biogenesis of miRNA

miRNAs are small non-coding RNAs with a length of 19-24 bp and are evolutionarily well conserved. They regulate gene expression post-transcriptionally by either inducing degradation or repressing translation of their target mRNA molecules. The general – "canonical" – biogenesis of miRNAs starts from primary precursor miRNAs (pri-miRs) which are transcribed by RNA polymerase II or III (see Figure 2.1). These pri-miRs contain a so called stem-loop structure in which the sequences are not perfectly complementary. This motif is recognized by a ribonuclease Drosha together with the dsRNA-binding protein (dsRBP) DGCR8 (together they are called Pasha) in the nucleus. The pri-miRNA is processed into a ~70-nucleotide precursor miRNA (pre-miR) by a mechanism called cropping. This pre-miR is now exported into the cytoplasm with the help from Exportin 5 (XPO5). In the cytoplasm, the pre-miR now binds to another dsRBP (TRBP) in complex with the ribonuclease Dicer1, and is processed into a double-stranded miRNA/miRNA* to its mature length of ~20 bp. This process is called dicing. One strand of the miRNA/miRNA* duplex – the guide strand – is incorporated together with Argonaute 2 (Ago2) into the miRNA-induced silencing complex (miRISC) whereas the other strand is released and degraded. The mature miRNA strand can then either silence its target mRNA by translational repression and/or

deadenylation within the miRISC or direct an endonucleolytic cleavage (slicing) with the help of the AGO2 protein. In most cases, the grade of complementarity of the "seed" sequence of the miRNA (positions 2 to 8 from the 5' end of the miRNA) to the "seed match" (3' UTR of the target mRNA) is responsible for the specificity of miRNA targeting (reviewed in Lujambio and Lowe 2012, Winter et al. 2009).

Besides the common mechanisms of silencing mRNA of target genes described above, miRNAs were also found to be able to target DNA, ribonucleoproteins, or even increase expression of its target mRNA (Garzon et al. 2010).

Table 2.1: Types of ncRNAs.
From Esteller 2011.

Name	Size	Location	Number in humans	Functions	Illustrative examples	Refs
Short ncRNAs						
miRNAs	19–24 bp	Encoded at widespread locations	>1,424	Targeting of mRNAs and many others	miR-15/16, miR-124a, miR-34b/c, miR-200	3–8
piRNAs	26–31bp	Clusters, intragenic	23,439	Transposon repression, DNA methylation	piRNAs targeting RASGRF1 and LINE1 and IAP elements	13–19
tiRNAs	17–18bp	Downstream of TSSs	>5,000	Regulation of transcription?	Associated with the CAP1 gene	37
Mid-size ncRNAs						
snoRNAs	60–300 bp	Intronic	>300	rRNA modifications	U50, SNORD	20–22
PASRs	22–200 bp	5′ regions of protein-coding genes	>10,000	Unknown	Half of protein-coding genes	10
TSSa-RNAs	20–90 bp	–250 and +50bp of TSSs	>10,000	Maintenance of transcription?	Associated with RNF12 and CCDC52 genes	35
PROMPTs	<200 bp	–205 bp and –5 kb of TSSs	Unknown	Activation of transcription?	Associated with EXT1 and RBM39 genes	36
Long ncRNAs						
lincRNAs	>200 bp	Widespread loci	>1,000	Examples include scaffold DNA–chromatin complexes	HOTAIR , HOTTIP , lincRNA-p21	2,28–30
T-UCRs	>200 bp	Widespread loci	>350	Regulation of miRNA and mRNA levels?	uc.283+, uc.338, uc160+	31–34
Other lncRNAs	>200 bp	Widespread loci	>3,000	Examples include X-chromosome inactivation, telomere regulation, imprinting	XIST, TSIX, TERRAs, p15AS , H19, HYMAI	2,23–25

*There is not necessarily a clear delineation between classes of non-coding RNA (ncRNA); for example, X-inactivation specific transcript (*XIST) and its antisense transcript TSIX could be considered as large intergenic non-coding RNAs (lincRNAs). In the 'Location' column, '–' represents the number of base pairs upstream of the transcription start site (TSS) and '+' represents the number of base pairs downstream of the TSS. CAP1, CAP, adenylate cyclase-associated protein 1; CCDC52, coiled-coil domain containing 52 (also known as SPICE1); EXT1, exostosin 1; HOTAIR, homeobox (HOX) transcript antisense RNA; HOTTIP, HOXA distal transcript antisense RNA; HYMAI, hydatidiform mole associated and imprinted; IAP, intracisternal A-particle; lncRNA, long non-coding RNA; miRNAs, microRNAs; piRNAs, PIWI-interacting RNAs; PASRs, promoter-associated small RNAs; PROMPTs, promoter upstream transcripts; RASGRF1, RAS-protein-specific guanine nucleotide-releasing factor 1; RBM39, RNA-binding motif protein 39; RNF12, ring finger protein 12 (also known as RLIM); snoRNAs, small nucleolar RNAs; TERRAs, telomeric repeat containing RNAs; tiRNAs, transcription initiation RNAs; TSSa-RNAs, TSS-associated RNAs; T-UCRs, transcribed ultraconserved regions.

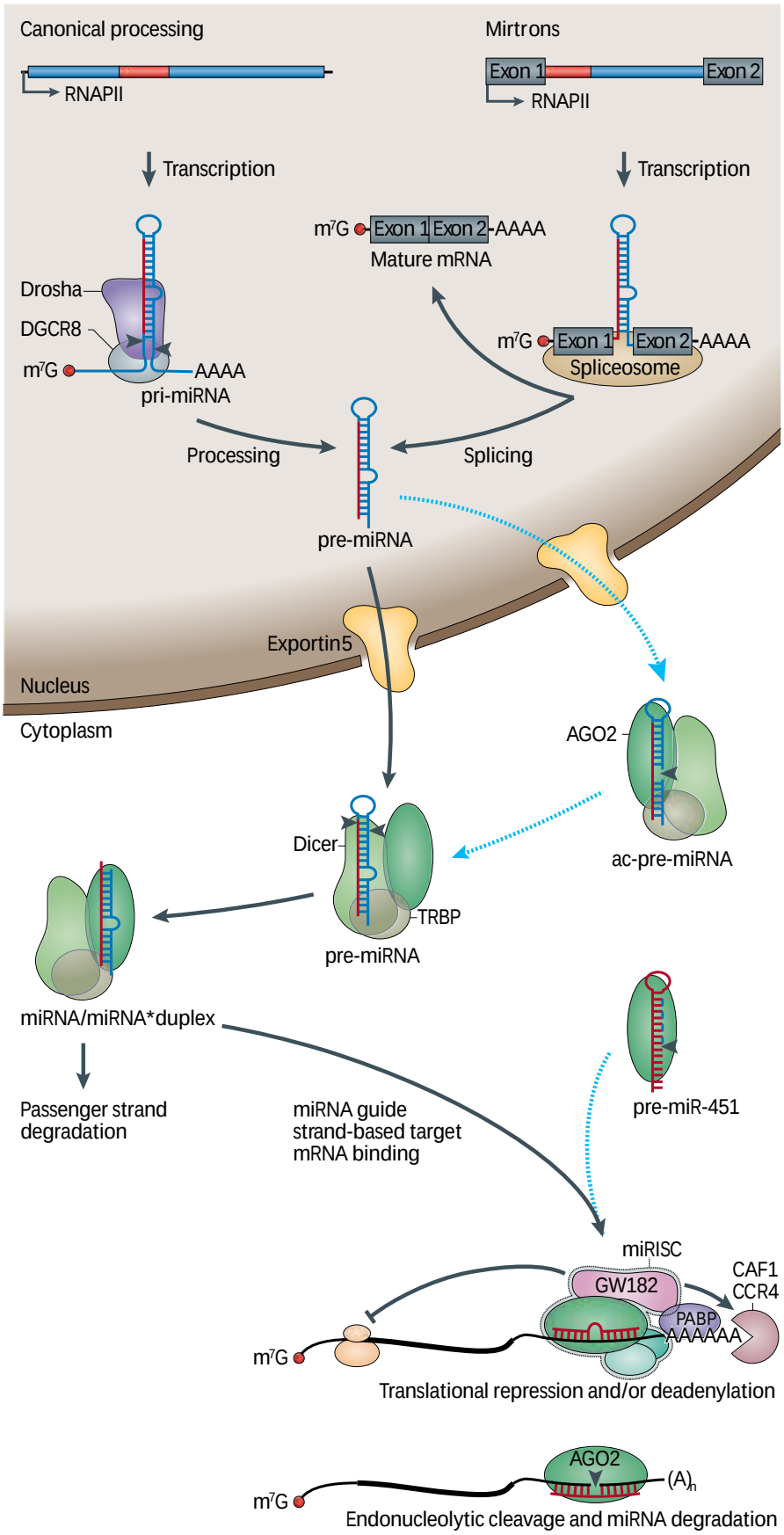

Figure 2.1: The biogenesis of miRNAs.
For detailed description of the biogenesis of miRNAs: see text (figure modified from Krol et al. 2010).

The above-described canonical pathway is used for the processing of most miRNAs. There are however many more variations of miRNA maturation (Figure 2.2). These include the Drosha-independent form of pri-miRNA processing where intron-derived miRNAs (mirtrons) are spliced by the splicosome with bypassing the cleavage by Drosha (Ruby et al. 2007, Okamura et al. 2007, Berezikov et al. 2007). Other examples for Dicer1-mediated but Drosha-independent miRNAs are some miR-tRNAs (Babiarz et al. 2008) and also some small nucleolar RNAs (snoRNAs) with miRNA-like functions (Ender et al. 2008).

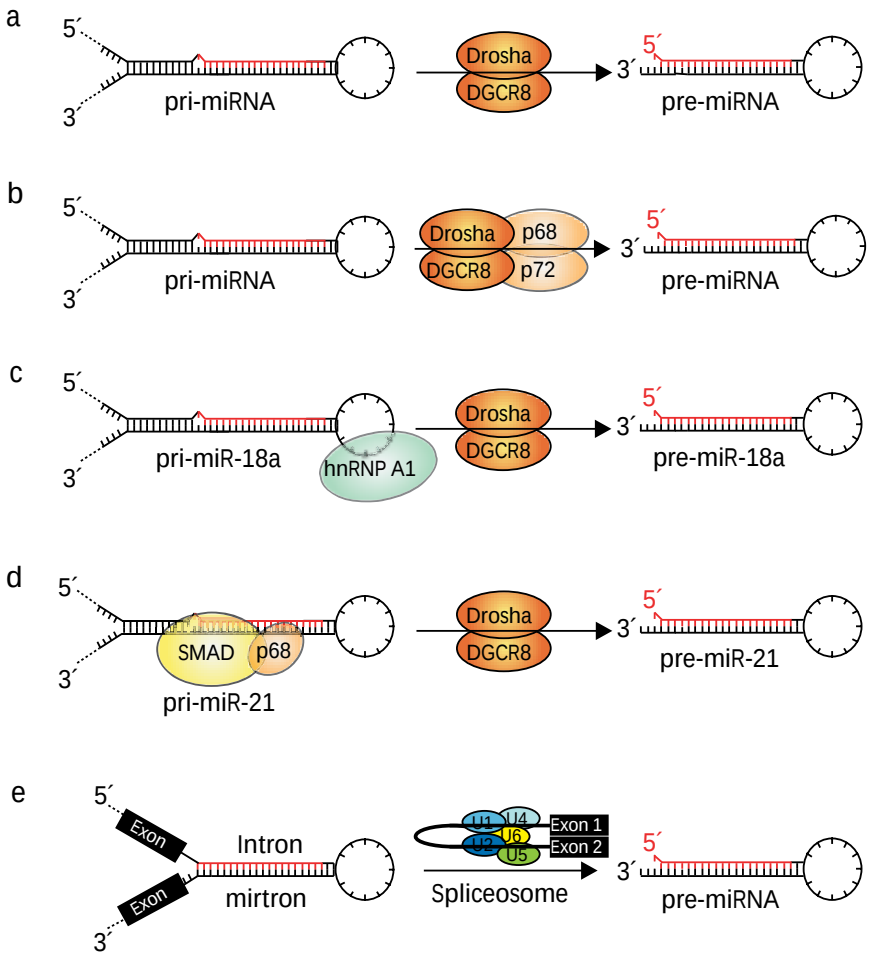

Figure 2.2: Canonical and non-canonical ways of pri-miRNA processing.
(A) Canonical maturation process involving the cleavage of the pri-miRNA by the microprocessor complex Drosha-DGCR8 and release of the pre-miRNA. (B) For effective cleavage, some miRNAs require additional factors like p68 and p72 for more specificity. See also Figure 2.10 for more details. (C) For processing of pri-miR-18, hnRNP A1 has to interact with the pri-miR to facilitate the cleavage by Drosha-DGCR8. (D) Cleavage of pri-miR-21 depends on binding of SMAD, induced by TGFβ signaling. (E) Drosha-DGCR8 processing can be completely replaced by the splicing mechanism of the spliceosome itself if the released and debranched intron (called mirtrons) resembles the length and hairpin structure of a pre-miRNA (figure modified from Winter et al. 2009).

2.1.3 Dicer1-independent maturation of pre-miRNAs

More recently, a Dicer1-independent form of miRNA maturation was also found (Cifuentes et al. 2010, Cheloufi et al. 2010, Yang et al. 2010). The biogenesis of the highly conserved miR-451 does not depend on the cleavage by Dicer1. Instead, the pre-miRNA-451 only binds Ago2 which cleaves the paired mRNA* passenger strand 10 nucleotides away from the 5' end of the miRNA guide strand incorporated into the Ago2 protein. It is suggested that polyuridylation and nuclease-mediated removal of uridines and template nucleotides is followed by the Ago2 cleavage to generate the mature miRNA (Figure 2.3).

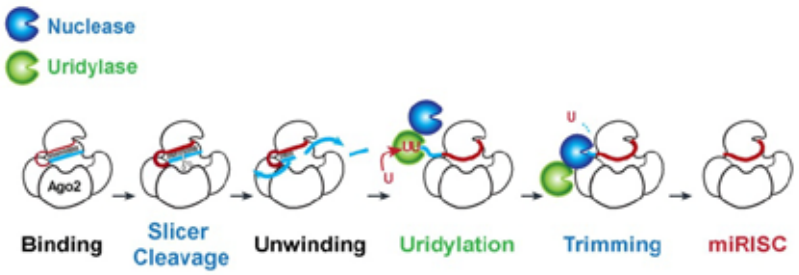

Figure 2.3: Model for Ago2-mediated pre-miRNA processing.
Pre-miRNA-451 can be processed by Ago2 independently of Dicer1. Ago2 is able to cleave the bound double-stranded pre-miRNA (miRNA/miRNA*) by itself followed by unwinding, uridylation, trimming of uridines and nucleotides to give rise to the mature miRNA (figure modified from Cifuentes et al. 2010).

Interestingly, processing of miRNAs by Ago2 alone instead of a Dicer1-mediated cleavage is determined by the secondary structure of the hairpin and not only by the sequence of the miRNA itself. Cifuentes and colleagues were able to mimic the structural traits of pre-miR-451 and applied them to pre-miR-430. Solely by adapting the structure, pre-miR-430 was now Dicer1-independently processed by Ago2 to a fully functional mature miRNA which could rescue the morphogenesis defects which normally occur upon loss of *Dicer1* (Cifuentes et al. 2010).

These findings might also have implications for the normally Dicer1-dependent processing of the canonical miRNAs. A change in structure of canonical pre-miRNAs could circumvent the need of miRNAs to be processed by Dicer1 and could therefore induce cleavage and maturation by Ago2. In this scenario, miRNA processing would be possible, even if *Dicer1* is lost or mutated.

2.1.4 Genetic defects in miRNAs are a common hallmark of disease

MicroRNAs are well-known to be able to influence and control normal processes like differentiation, cellular proliferation, and apoptosis by repressing many target genes involved in these processes. Importantly, more and more evidence shows that miRNAs also have crucial functions in human diseases. Differential expression of miRNAs, and therefore controlling of gene expression, is well-known in many types of cancer (Calin et al. 2002, Lu et al. 2005, He et al. 2005). They can either act as tumor suppressors or as oncogenes (Table 2.2 and Calin et al. 2002, Esquela-Kerscher and Slack 2006). When acting as tumor suppressors, miRNAs are usually deleted or downregulated, while in the role of oncogenes, they are commonly overexpressed.

The miR-34 family is an example for such a tumor suppressor function. miR-34 is downregulated in neuroblastoma (Cole et al. 2008), pancreatic cancer cell lines (Chang et al. 2007), non-small cell lung cancer (Bommer et al. 2007), and several other cancer types (Table 2.2). Interestingly, miR-34 is a direct target gene of p53 (He et al. 2007). It was shown that activation of miR-34 can induce apoptosis, cell-cycle arrest, and senescence, and inhibit migration through targeting and degrading genes involved in those processes (summarized in Hermeking 2009). Downregulation of miR-34 in many cancers therefore comes with no surprise, since inhibition of apoptosis, circumvention of senescence, or enhanced migration potential present typical hallmarks of cancer and metastasis (Hanahan and Weinberg 2000, Hanahan and Weinberg 2011).

The probably best known family of miRNAs acting as oncogenes is the *miR-17~92* cluster, also called oncomiR-1 (He et al. 2005). It is located at chromosome 13q31.3, a region which is amplified in several hematopoietic cancers and solid tumors such as diffused B-Cell lymphoma (DLBCLs), lung carcinoma, follicular lymphomas, and Burkitt's lymphomas (Ota et al. 2004). Overexpression of *miR-17~92* has also been observed in many other tumor types (Volinia et al. 2006, Petrocca et al. 2008a, He et al. 2005). Since it negatively regulates proteins involved in blocking both proliferation (p21) and angiogenesis (CTGF, Tsp1), and also inducing apoptosis (Pten, Bim), upregulation of *miR-17~92* as seen in tumors leads to induction of proliferation and/or angiogenesis and also a block of apoptosis (Olive et al. 2010). Again, processes which are typical hallmarks of cancer and metastasis. More about the *miR-17~92* cluster in section 2.1.5, page 17.

Table 2.2: Key miRNAs involved in cancer.
Figure modified from Lujambio and Lowe 2012.

MicroRNA	Function	Genomic location	Mechanism	Targets	Cancer type	Mouse models	Clinical application
miR-17 -92 cluster	Oncogene	13q22	Amplification and transcriptional activation	BIM, PTEN, CDKN1A and PRKAA1	Lymphoma, lung, breast, stomach, colon and pancreatic cancer	Cooperates with MYC to produce lymphoma. Overexpression induces lymphoproliferative disease	Inhibition and detection
miR-155	Oncogene	21q21	Transcriptional activation	SHIP1 and CEBPB	Chronic lymphocytic leukaemia, lymphoma, lung, breast and colon cancer	Overexpression induces pre-B-cell lymphoma and leukaemia	Inhibition and detection
miR-21	Oncogene	17q23	Transcriptional activation	PTEN, PDCD4 and TPM1	Chronic lymphocytic leukaemia, acute myeloid leukaemia, glioblastoma, pancreatic, breast, lung, prostate, colon and stomach cancer	Overexpression induces lymphoma	Inhibition and detection
miR-15a/16-1	Tumour suppressor	13q31	Deletion, mutation and transcriptional repression	BCL2 and MCL1	Chronic lymphocytic leukaemia, prostate cancer and pituitary adenomas	Deletion causes chronic lymphocytic leukaemia	Expression with mimics and viral vectors
let-7 family	Tumour suppressor	11 copies (multiple locations)	Transcriptional repression	KRAS, MYC and HMGA2	Lung, colon, stomach, ovarian and breast cancer	Overexpression suppresses lung cancer	Expression with mimics and viral vectors
miR-34 family	Tumour suppressor	1p36 and 11q23	Epigenetic silencing, transcriptional repression and deletion	CDK4, CDK6, MYC and MET	Colon, lung, breast, kidney, bladder cancer, neuroblastoma and melanoma	No published studies	Expression with mimics and viral vectors
miR-29 family	Oncogene	7q32 and 1q30	Transcriptional activation	ZFP36	Breast cancer and indolent chronic lymphocytic leukaemia	Overexpression induces chronic lymphocytic leukaemia	No published studies
	Tumour suppressor		Deletion and transcriptional repression	DNMTs	Acute myeloid leukaemia, aggressive chronic lymphocytic leukaemia and lung cancer		No published studies

BCL2, B-cell lymphoma protein-2; BIM, BCL-2-interactiing mediator of cell death; CDKN1A, cyclin-dependent kinase inhibitor 1A; CEBPB, CCAAT/enhancer binding protein β; HMGA2, high mobility group AT-hook 2; CDK4, cyclin-dependent kinase 4; CDK6, cyclin-dependent kinase 6; DNMT, DNA methyltransferase; MCL1, myeloid cell leukaemia sequence 1; PTEN, phosphatase and tensin homologue; PRKAA1, protein kinase, AMP-activated, alpha 1 catalytic subunit; PDCD4, programmed cell death 4; SHIP1, Src homology 2 domain-containing inositol 5-phosphatase 1; TPM1, tropomyosin 1; ZFP36, zinc finger protein 36.

miRNAs are globally downregulated in cancer cells

It is noteworthy that somatic mutations in the seed sequence of tumor-suppressor miRNAs, which could abrogate the suppressive/degrading function of those miRNAs, is very rare (Diederichs and Haber 2006). Instead, it seems that the levels of miRNAs (upregulation/downregulation) *per se* are much more crucial in the control of cancer development. Although several oncogenic miRNAs are upregulated in cancer, it is generally accepted that the overall levels of miRNAs are decreased in cancer cells (Chang et al. 2008, Thomson et al. 2006). An explanation for this phenomenon might be the MYC oncoprotein-induced repression of several miRNAs (Chang et al. 2008). MYC is overexpressed in many cancers and by downregulating the expression levels of tumor suppressor miRNAs, MYC might even further implement its oncogenic function.

Another explanation for the downregulated state of miRNAs in cancer might be the fact that levels of proteins involved in the biogenesis of miRNAs are often low (Thomson et al. 2006). In a reverse experiment, we and others (Lambertz et al. 2010, Kumar et al. 2009) could show that downregulation of *Dicer1* (and Drosha, Kumar et al. 2007) itself can promote tumorigenesis. This data is supported by the fact that reduced levels of Dicer1 and Drosha are associated with poor clinical prognosis in ovarian cancer (Merritt et al. 2008).

Taken together, relatively small changes in miRNA levels might have a huge impact on tumor development and homeostasis.

miRNAs as cancer diagnostic tool

Besides the role of miRNAs in cancer initiation, there are also reports that miRNAs can influence cancer progression and metastasis (Ma et al. 2007, Tavazoie et al. 2008, Ma et al. 2010, Valastyan et al. 2009). In breast cancer, mir-10b is found to be highly expressed in metastatic breast cancer cells and can positively regulate cell migration and invasion. Further experiments have shown, when overexpressed in non-metastatic breast tumors, miR-10b can by itself trigger initiation of robust invasion and metastasis (Ma et al. 2007).

Similar to protein-coding genes, miRNAs can act as either oncogenes or tumor suppressors in a tissue-specific manner. Depending on the tissue in which they are expressed, miRNAs can target different sets of genes, resulting in a different outcome of the cell physiology. As shown for the miR-29 family, their tumor-suppressive effect in lung tumors stands in sharp contrast to the oncogenicity in breast cancer. It is suggested that targeting either the DNA methyltransferases DNMT3A and DNMT3B or ZFP36 leads to such different

outcomes (Figure 2.5 and Fabbri et al. 2007, Gebeshuber et al. 2009, Mott et al. 2007, Pekarsky et al. 2006).

Taken together the importance of miRNAs in cancer, the tissue-specificity of their expression pattern and resulting differences in output, combined with the fact that several oncogenic miRNAs are highly overexpressed in tumors, could make them a powerful diagnostic tool for cancer. In the context of prostate cancer, elevated levels of miR-141 measured in blood plasma could distinguish patients with prostate cancer from healthy control individuals (Mitchell et al. 2008). Not only are circulating miRNAs in human plasma very stable and protected from endogenous RNase activity (Mitchell et al. 2008), they also are remarkably stable in formalin-fixed tissue (Nelson et al. 2006, Li et al. 2007, Xi et al. 2007). In the near future, therefore it should become feasible to detect elevated miRNA levels in human plasma and use them as a prediction for possible cancer initiation/progression or to correlate high miRNA levels in tissue sections with disease outcome, cancer classification, treatment decisions, and treatment efficacy.

miRNAs as targets of new potential cancer therapies

As the expression of miRNAs is frequently deregulated in human cancer (reviewed in Esquela-Kerscher and Slack 2006, Calin and Croce 2006) and miRNA expression itself and their pattern of target genes is commonly tissue-specific in human cancer (Lu et al. 2005, Fabbri et al. 2007, Gebeshuber et al. 2009), miRNAs have a great potential as new drug targets in cancer but also other diseases (Figure 2.4).

That miRNA inhibition can decrease angiogenesis resulting in a decreased tumor burden was shown for miR-132 (Anand et al. 2010). miRNA-132 is present in the endothelium of human tumors but undetectable in normal endothelium. In tumors, upon being highly expressed, miR-132 suppresses p120RasGAP expression and induces neovascularization. Upon delivery of the oligonucleotide anti-miR-132 to tumor endothelium with the help of nanoparticles that specifically target tumor neo-vasculature (Hood et al. 2002, Murphy et al. 2008), angiogenesis was successfully suppressed in mice and resulted in a decreased tumor burden.

Taking miR-132 as an example of successfully and tissue-specifically administering miRNAs to tumors to reduce the tumor burden, it should be clear that influencing expression levels of miRNAs might be key in miRNA-targeted therapy. But besides repressing miRNAs by using anti-miRs (complementary antisense oligonucleotides), other techniques have been

reported as well. Using miR-sponges, oligonucleotide constructs with specific multiple complementary miRNA binding sites in tandem, individual miRNAs could be depleted in different model organisms (Valastyan et al. 2009, Loya et al. 2009, Zhu et al. 2011). Furthermore, antagomirs, siRNA, and locked nucleic acids (summarized in Garzon et al. 2010) are other known methods to inhibit oncogenic miRNAs and therefore eventually blocking or reducing cancer formation or progression.

Another strategy for miRNA-targeted therapy is the restoration of expression of miRNA with tumor-suppressor function. This can be either achieved by synthetic miRNA mimics or viral delivery of miRNAs (Garzon et al. 2010). In both cases, mouse models were successfully used to show that upon reconstitution of miRNAs, the tumor burden was decreased (Kota and Balasubramanian 2010, Bonci et al. 2008).

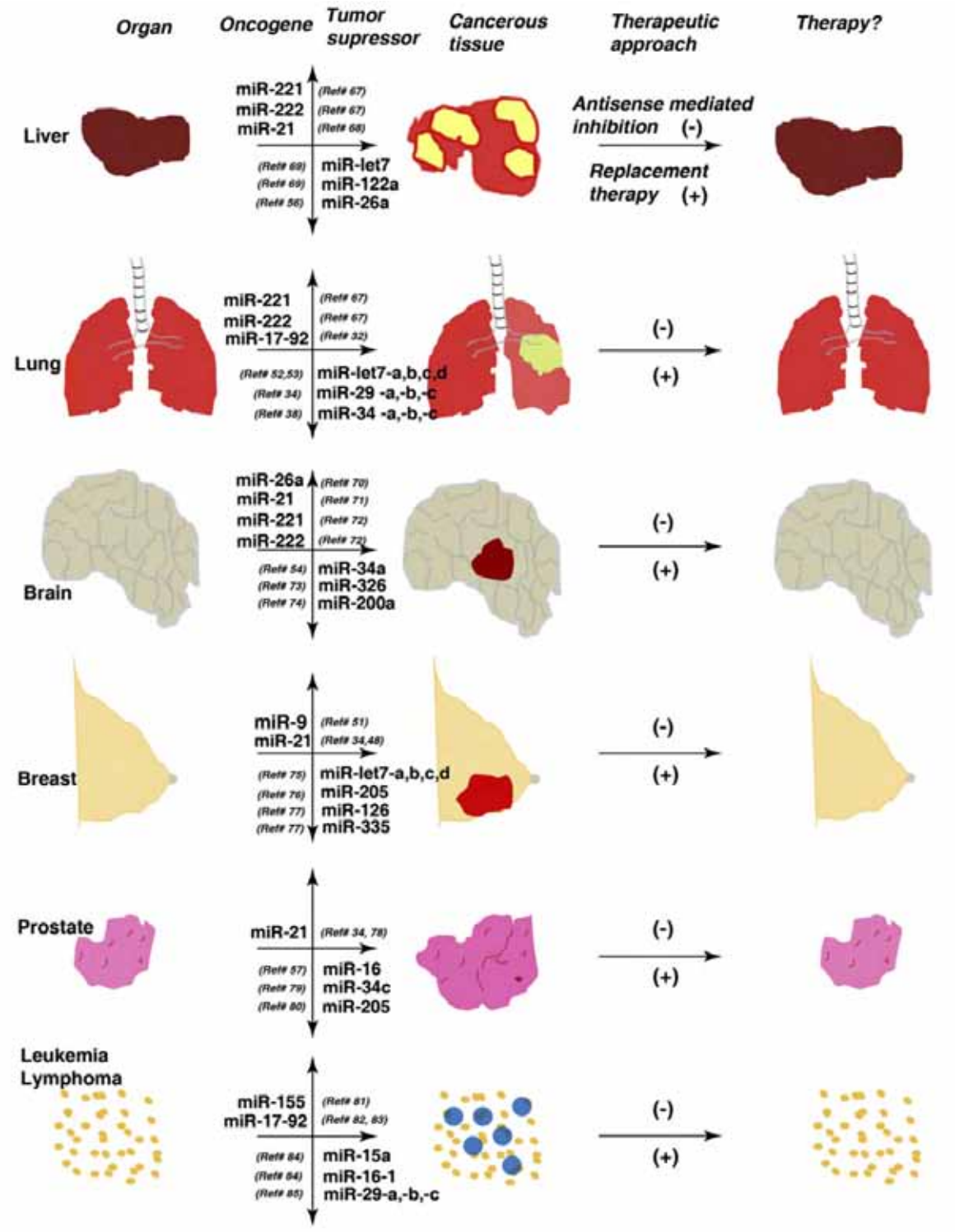

Figure 2.4: Potential miRNA targets for cancer therapy.

Overview of miRNAs that are reported to be upregulated (upward arrow) or downregulated (downward arrow) in different forms of cancer and could be correlated with alterations in cell growth, apoptosis, or invasiveness of these cancer cells. For possible cancer therapy, expression of miRNA with oncogenic function could be downregulated (-) by different methods described in the text. Tumor suppressor miRNAs on the other hand could be targeted by reconstitution therapy (+) with viral overexpression or synthetic miRNA mimics (figure modified from Kota and Balasubramanian 2010).

miRNAs can influence the cancer epigenome and *vice versa*

Many studies are indicating that miRNAs are also able to change and control epigenetic modifications such as DNA methylation patterns, histone modifications, and chromatin remodeling (Figure 2.5). Changes of those epigenetic marks, either globally or gene-specific, define the cancer "epigenome" (Portela and Esteller 2010). Thus miRNAs are also able to change processes of cancer initiation and progression by targeting components of the epigenetic machinery. One example includes the already mentioned miR-29 family which targets the DNA methyltransferases DNMT3A and DNMT3B in lung cancer and therefore is acting as tumor suppressor (Fabbri et al. 2007 and Figure 2.5). Other examples compromise the commonly lost in prostate cancer miR-101 which inhibits the histone methyltransferase EZH2, known to be overexpressed in aggressive solid tumors (Varambally et al. 2008) and others shown in Figure 2.5 (miR-449a, miR-9*, miR-124).

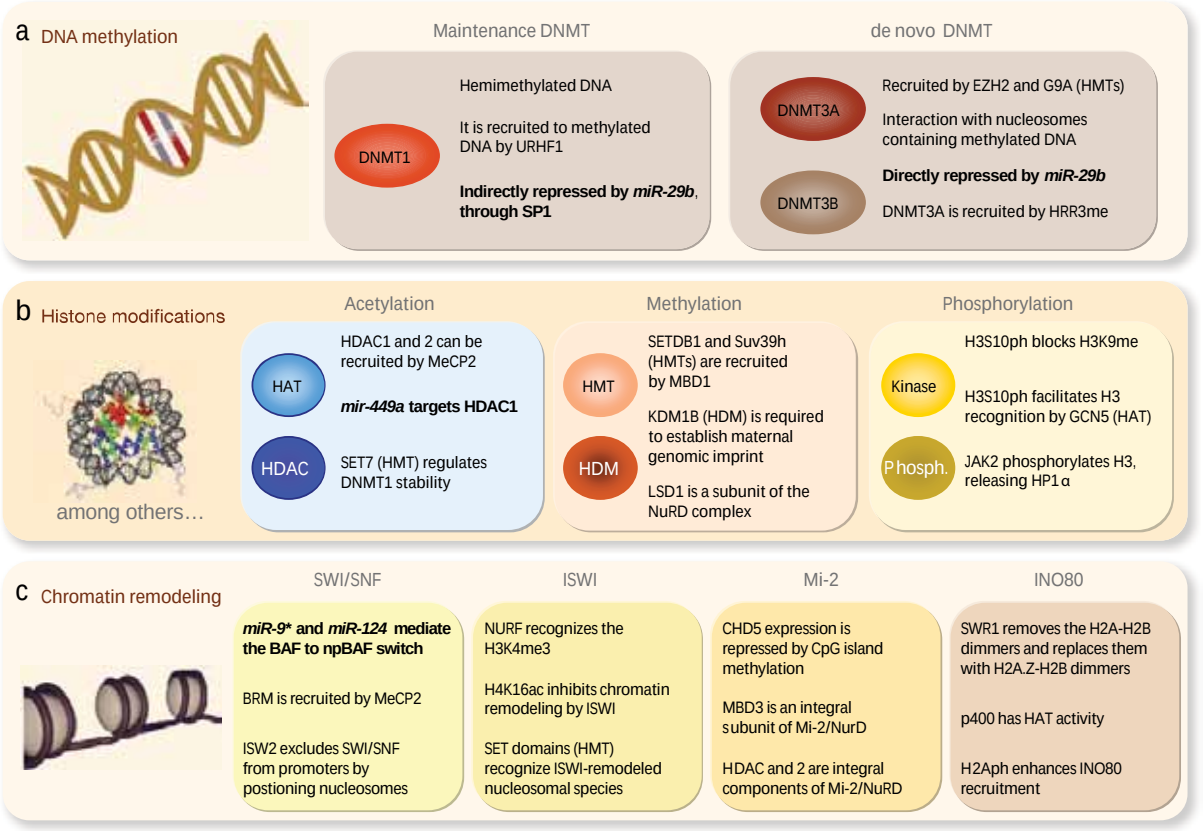

Figure 2.5: Epigenetic machinery and interplay among epigenetic factors.
DNA methylation (A), histone modifications (B), and chromatin remodeling (C) are epigenetic marks which are catalyzed by different epigenetic complexes. Their main families and interaction partners are shown. Examples of miRNAs which regulate or are involved in those epigenetic complexes, are indicated in bold (figure modified from Portela and Esteller 2010).

Interestingly, changes in epigenetic marks such as DNA methylation and histone modifications can also influence the expression of miRNAs. It was shown for miR-127 – normally downregulated in cancer cells – that, upon inhibition of DNA methylation and histone deacetylation, miR-127 could be highly induced and downregulate its target, the proto-oncogene *BCL6* (Saito et al. 2006). The reason for miR-127 downregulation in cancer cells is the fact that it is embedded in a CpG island that, in cancer, becomes hypermethylated and therefore silenced. Removing the methylation marks therefore activates transcription of miR-127.

Other examples of miRNAs influenced by epigenetic changes are miR-181a, miR-181b, miR-200b, miR-200c, and miR-203 which are epigenetically repressed by PCR2, a polycomb repressive complex that contains EZH2 which methylates histone H3 on lysine 27 (H3K27) (Cao et al. 2011).

2.1.5 The *miR-17~92* cluster

The *miR-17~92* cluster, also known as OncomiR-1 (He et al. 2005), consists of six tandem stem-loop hairpin structures that encode for six mature miRNAs (miR-17, miR-18a, miR-19a, miR-19b-1, miR-20a, miR-92a-1) and belongs to a family of polycistronic miRNA genes which are highly conserved among different species (Tanzer and Stadler 2004). Other members of this family are the *miR-106a~363* and *miR-106b~25* clusters. Together, these three clusters can express 15 miRNAs which can also be grouped according to their seed sequences determining their target genes. miRNAs of the same seed group are predicted to target largely overlapping set of genes (Figure 2.6 and Ventura et al. 2008, Sage and Ventura 2011).

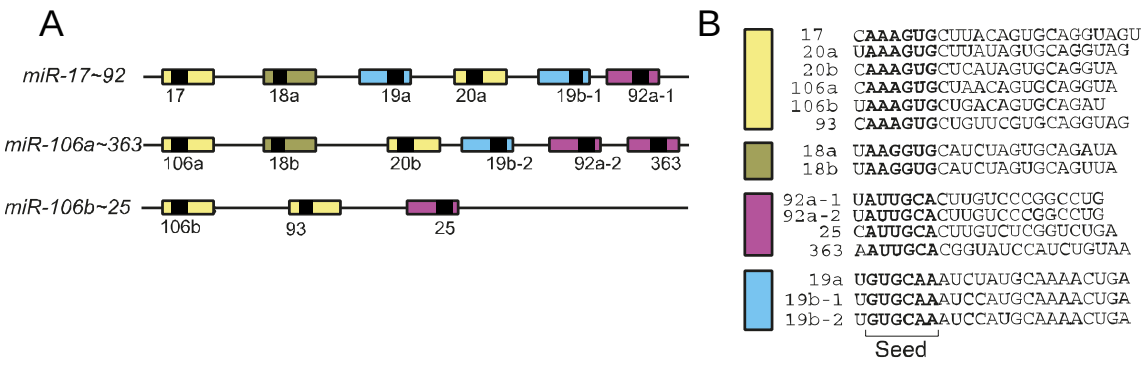

Figure 2.6: Schematic representation of the *miR-17~92* cluster.
(A) Schematic of the *miR-17~92* cluster and its two paralogs, *miR-106a~363* and *miR-106b~25*. Pre-miRNAs are indicated as color-coded boxes. Black boxes correspond to the mature miRNA. The color code identifies miRNAs with the same seed sequence. (B) Sequence comparison of the 15 miRNAs encoded by these three miRNA clusters. miRNAs with the same seed sequence (bold) are grouped together and color-coded according to (A). miRNAs of the same seed group are predicted to target largely overlapping gene sets (figure modified from Ventura et al. 2008 and Sage and Ventura 2011).

The *miR-17~92* cluster is crucial for mammalian development

Targeted deletions in the *miR-17~92*, *miR-106a~363* and *miR-106b~25* clusters in mice have shown that the *miR-17~92* cluster is important for mammalian development while *miR-106a~363* and *miR-106b~25* are dispensable (Ventura et al. 2008). B-cell development, particularly the transition from pro-B to pre-B state, highly depends on *miR-17~92*. Loss of *miR-17~92* leads to enhanced apoptosis in the pro-B-cells during fetal but also adult B-cell development. Other developmental defects resulting from deletion of *miR-17~92* are lung hypoplasia and ventricular septal defects (Ventura et al. 2008). It was also shown that there is a functional interaction between *miR-17~92* and *miR-106b~25* since loss of both clusters resulted in a more severe developmental defect compared to loss of *miR-17~92* alone. Additionally, loss of both clusters *miR-17~92* and *miR-106b~25*, as well as loss of all three clusters combined, resulted in higher levels of apoptosis in the fetal liver, the ventral horns of the spinal cord, and the lateral ganglionic eminences (Ventura et al. 2008). It is worth mentioning that *miR-17~92* and *miR-106b~25* show very similar expression levels and tissue distribution. This suggests that, depending on the tissue, it might be possible that *miR-106b~25* compensates for the loss of *miR-17~92*, explaining why loss of both, *miR-17~92* and *miR-106b~25*, shows more severe effects.

Recently, *miR-17~92* was also found to be important for growth and skeletal development in humans (de Pontual et al. 2011). It was shown that a subset of patients with the Feingold syndrome – an autosomal dominant syndrome causing microcephaly, relative short stature, and digital anomalies (Feingold et al. 1997, Celli et al. 2003) – have germline

hemizygous deletions of a specific gene locus that includes the *miR-17~92* cluster. Loss of *miR-17~92* in those patients therefore mimicked the loss-of-function mutations of MYCN, the gene that is responsible for the Feingold syndrome in the majority of the cases (van Bokhoven et al. 2005, Marcelis et al. 2008).

miR-17~92 is overexpressed in a wide variety of tumors

The *miR-17~92* cluster is the first cluster of miRNAs which was found to be overexpressed in cancer, hence the name OncomiR-1 (Ota et al. 2004, He et al. 2005). In 2004, a focal amplification of the *miR-17~92* locus in diffuse large B-cell lymphoma (DLBCL) was reported for the first time (Ota et al. 2004). Since then, overexpression of the *miR-17~92* cluster has been found in a wide range of blood cancer and solid tumors such as small cell lung cancer (Hayashita et al. 2005, Matsubara et al. 2007), colon cancer (Dews et al. 2006), medulloblastoma (Uziel et al. 2009), and neuroblastoma (Schulte et al. 2008, Mestdagh et al. 2010).

A study of Conkrite et al. (Conkrite et al. 2011) which was published in parallel with our work on the *miR-17~92* cluster in retinoblastoma, additionally confirmed our finding that *miR-17~92* is also overexpressed in retinoblastoma (shown later in this thesis in section 4.4, page 62).

Pleiotropic functions of *miR-17~92* are achieved by repressing specific targets

Levels of E2F and MYC (and/or MYCN) are known to be elevated in many cancer cells. For example, E2F activity is high in *RB1* mutant cells such as retinoblastoma cells because E2F is normally repressed by RB1. Also, levels of the MYC oncogene were shown to be high in mouse and human retinoblastomas (Lee et al. 1984, MacPherson et al. 2007) and neuroblastoma (Schulte et al. 2008, Kohl et al. 1983). Both, E2F1 and MYC, are known to transcriptionally target *miR-17~92* directly (O'Donnell et al. 2005, Sylvestre et al. 2007, Woods et al. 2007) and might therefore be responsible for elevated levels of *miR-17~92* in these tumors.

The mechanisms through which elevated levels of *miR-17~92* lead to its oncogenic activity and accelerate tumorigenesis are at the center of many different studies in various tumor models (Figure 2.7). It was previously shown that *miR-17~92* can (i) promote proliferation by inhibition of p21/p57 (Petrocca et al. 2008b, Ivanovska et al. 2008, Conkrite et al. 2011), (ii) increase cell survival by suppressing apoptosis through inhibition of PTEN/BIM (Mu et al. 2009, Olive et al. 2009, Mavrakis et al. 2010), (iii) increase

angiogenesis by blocking CTGF/Tsp1 (Dews et al. 2006), and (iv) create resistance to TGFβ signaling by inhibition of SMAD2/SMAD4/TGFβR2 (Mestdagh et al. 2010).

However, the molecular basis of the pleiotropic functions of the *miR-17~92* cluster is not yet fully understood. As mentioned before, expression levels of the *miR-17~92* cluster are highly tissue-specific. Additionally, each mature miRNA of the six members of the *miR-17~92* cluster might also show different expression levels individually, since upon cleavage of the *miR-17~92* pri-miRNA by Drosha, each of the members of this cluster could theoretically be processed independently. Thus, maturation of individual members of the *miR-17~92* cluster might contribute to the complex regulatory network of this cluster. An example of selective elevation of expression levels of individual miRNAs of the *miR-17~92* cluster is the VEGF-mediated upregulation of *miR-17*, *miR-18*, and *miR-20*. Only those three members were found to participate in the control of angiogenic phenotypes upon VEGF upregulation (Suárez et al. 2008).

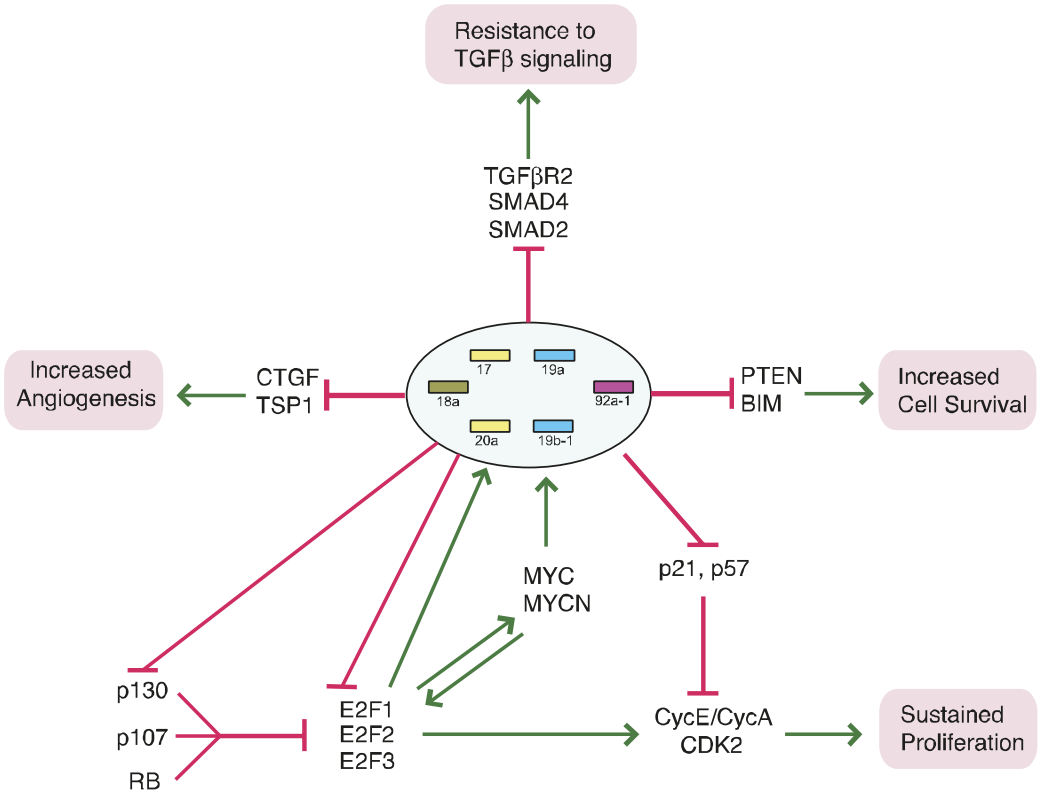

Figure 2.7: The pleiotropic functions of *miR-17~92* are achieved by repressing specific targets.
The *miR-17~92* cluster has many pleiotropic functions and oncogenic activities which are tightly controlled in a complicated regulatory network. Depending on cell type and physiological context, *miR-17~92* can (i) promote proliferation by inhibition of p21/p57, (ii) increase cell survival by suppressing apoptosis through inhibition of PTEN/BIM, (iii) increase angiogenesis by blocking CTGF/Tsp1, and (iv) create resistance to TGFβ signaling by inhibition of SMAD2/SMAD4/TGFβR2 (figure modified from Sage and Ventura 2011 and Osada and Takahashi 2011).

One of the mechanisms of how the *miR-17~92* cluster is possibly involved in the cell-cycle regulation is through a finely tuned auto-regulatory feedback loop involving E2F, MYC, and *miR-17~92*. On the one hand, it was reported that E2F1 is a target of both miR-17 and miR-20 and that both E2F2 and E2F3 are targets of miR-20 alone (O'Donnell et al. 2005). On the other hand, E2F directly activates transcription of *miR-17~92* (Woods et al. 2007). Additional experiments in fibroblasts have demonstrated that inhibition of miR-17/miR-20a leads to G1 checkpoint activation due to accumulation of DNA double-strand breaks through activation of E2F1 transcription factor (Pickering et al. 2009). Taken together, these data suggest that the MYC-regulated miRNAs miR-17/miR-20a might play an important role in controlling the right timing of E2F1 expression and therefore bypassing the G1 checkpoint caused by accumulation of E2F1. Consequently, an amplified *miR-17~92* cluster, and therefore high levels of miR-17/miR-20a in cancer cells, might dampen the positive E2F/MYC feedback loop and reduce the apoptotic potential of E2F1, leading to an enhanced proliferative signal (Figure 2.7 and Osada and Takahashi 2011, Olive et al. 2010). Whether high levels of E2F and MYC are a cause or a consequence of high *miR-17~92* levels in human cancers, is, however, not known. Further studies are required to find the cause of deregulation of *miR-17~92*/E2F/MYC in human cancers and to develop drugs to restore the non-pathological cell homeostasis.

miR-17~92 is a target of p53 and *vice versa*

Studies in colon cancer cell lines also revealed a direct interaction between the *miR-17~92* cluster and the p53 tumor suppressor protein (Yan et al. 2009). Yan et al. suggested that, in cells under hypoxia, p53 can bind to a potential p53-binding site in the proximal region of the *miR-17~92* promoter and repress transcription of *pri-miR-17~92*. Reduced levels of *miR-17~92* mediated by p53 might therefore give rise to apoptosis under hypoxic conditions, eventually via PTEN/BIM. Transcriptional repression of *miR-17~92*, induced by p53, is mediated through inhibition of TATA-binding protein (TBP) recruitment to the *miR-17~92* promoter. Both, TBP and p53, have overlapping binding sites within the *miR-17~92* promoter and are competing with each other. Whereas binding of TBP results in *miR-17~92* expression, replacement of TBP by p53 within the *miR-17~92* promoter results in repression (Figure 2.9 and Yan et al. 2009).

Very recently, *p53* was also identified as a possible target of miR-92a, a member of the *miR-17~92* cluster, linking overexpression of individual members of the *miR-17~92* in

chronic lymphocytic leukemia (CLL) patients with the downregulation of *p53* and therefore contributing to the oncogenic phenotype (Li et al. 2012).

Besides the possible direct regulation of *p53* by members of the *miR-17~92* cluster, *p53* is also indirectly regulated by *miR-17~92* via the PTEN-PI3K-AKT-MDM2-p53 pathway (schematic in Figure 2.9). Upregulation of *miR-17~92* would lead to a block in PTEN expression and to activation of the PI3K-AKT signaling pathway, and thereby suppressing p53 function via MDM2 (Zhou et al. 2001, Mayo and Donner 2001, Xiao et al. 2008, Lenz et al. 2008).

2.2 The p53 tumor suppressor

2.2.1 p53 is an important regulator of the miRNA pathway

Very little is known about the interaction of p53 with the *miR-17~92* cluster and their contribution to disease phenotypes. But many studies have shown that the p53 tumor suppressor protein is a key regulator of miRNA processing in general (Figure 2.9, Figure 2.10 and Suzuki et al. 2009, Suzuki and Miyazono 2010, Boominathan 2010b, Boominathan 2010a, Feng et al. 2011).

The p53 tumor suppressor protein and its canonical pathway and regulation

p53, also known as "the guardian of the genome", is a well-studied tumor suppressor which is connected to virtually all types of cancer, either by direct mutation within the *p53* gene or by mutation/deletion of its upstream regulators or downstream effectors such as *Mdm2* and *Mdm4* (Levine et al. 2004, Olivier et al. 2004, Toledo and Wahl 2006, Marine et al. 2006). Mutations in *p53* are often associated with aggressive tumors and poor prognosis in the outcome of a disease (Soussi and Béroud 2001, Soussi 2007).

p53 is a core regulator in a signaling pathway, starting from a wide variety of intracellular and extracellular stress signals detected by the cell and passed on to p53 by various mediators. Stabilized and activated, p53 then transcriptionally activates or, very rarely, represses numerous target genes – the downstream effectors – which cause a variety of cellular responses, usually involved in tumor suppression by promoting growth arrest and apoptosis (Figure 2.8 and reviewed in Vogelstein et al. 2000, Kruse and Gu 2009, Levine and Oren 2009, Vousden and Lane 2007, Vousden and Ryan 2009).

Besides its canonical function as a transcriptional activator, p53 was recently shown to have transcriptional-independent – cytoplasmic – activities such as regulation (inhibition is controversial) of autophagy (Tasdemir et al. 2008), transactivation-independent proapoptotic activities of p53 regulated by FOXO3a (You et al. 2006) or direct activation of Bax by p53, leading to mitochondrial membrane permeabilization and apoptosis (Chipuk et al. 2004).

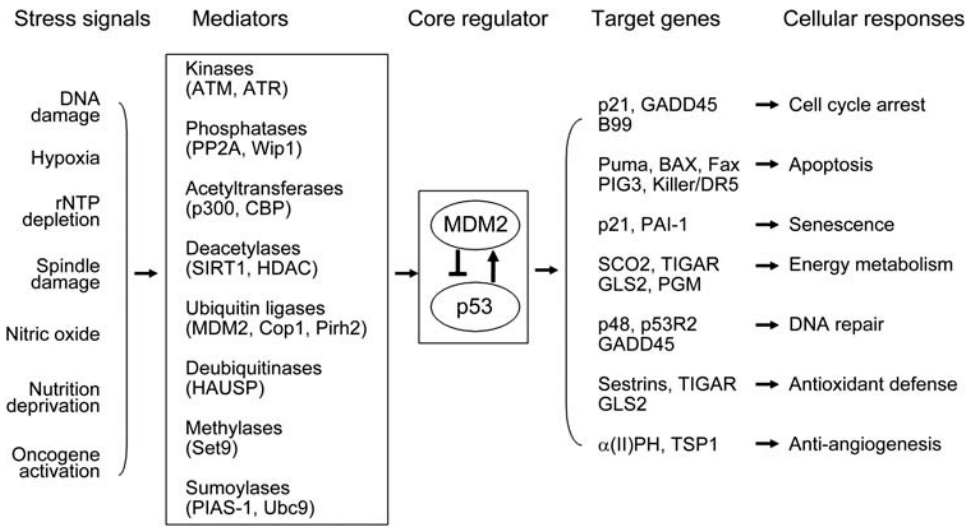

Figure 2.8: Signalling pathway of the p53 tumor suppressor.
Stress signals from within or outside of the cell are detected and passed on to p53 with the help of many different mediators (list shown is not exclusive). These signals lead to increased levels of p53 through degradation of its main negative regulator Mdm2. The accumulation and therefore activation of p53 leads to transcriptional activation of p53 target genes which can initiate various cellular responses to fulfill the tumor suppressive function of p53 (graph from Feng et al. 2011).

The classical stress signals activating p53 are DNA damage, rNTP depletion, spindle damage, telomere attrition, oncogene activation, nutrition deprivation, and hypoxia. The usually short-lived p53 protein is generally activated due to posttranslational modifications that cause its accumulation and stabilization and therefore increase in its transcriptional activities. Such modifications include phosphorylation, acetylation, methylation, ubiquitination, summolation, and neddylation.

Upon activation, p53 can act as a transcription factor and binds to specific DNA sequences, so called p53-responsive elements (RE), to regulate the transcription of its target genes like p21, Puma, TIGAR, or PAI-1, leading to a specific cellular response. These include cell cycle arrest, apoptosis, senescence, and DNA repair. So upon stress – also highly cell type dependent – p53 can induce cell cycle arrest, apoptosis, or senescence in order to prevent possible propagation of damaged or mutated cells which could initiate tumor formation (Levine et al. 2006, Vousden and Prives 2009).

Since p53 has such a crucial importance in not only preventing tumorigenesis, but also in being able to impede on embryonic development and stem cell homeostasis, p53 has to be tightly regulated. The core regulators of p53 are the two structurally related RING finger-domain containing proteins Mdm2 and Mdm4. Mdm2 usually inhibits p53 function by acting as an E3 ligase and ubiquitylating p53 to mark it for proteasomal degradation (Haupt et al. 1997, Kubbutat et al. 1997). Mdm4 however, despite being structurally related to Mdm2, does not directly target p53 for degradation through ubiquitylation. Mdm4 rather assists Mdm2 in regulating the stability of p53 (Migliorini et al. 2002). Additionally, Mdm4 can also regulate p53 transcriptional activity independently of Mdm2 (Francoz et al. 2006, Maetens et al. 2007).

It is therefore not surprising that not only *p53* is crucial for tumor development, but that its negative regulators *Mdm2* and *Mdm4* are, too. Both were found to be upregulated in various cancers, thus keeping low levels of p53 in the cell to prevent apoptosis, senescence, or cell cycle arrest, hallmarks of cancer cells which have to be overcome in order to allow for formation of tumors. Among others, *Mdm2* was found to be overexpressed in non-small cell lung cancer (NSCLC) (Dworakowska et al. 2004), soft tissue tumors such as Ewing's sarcoma, leiomyosarcomas, lipomas, liposarcomas, malignant fibrous histiocytomas, malignant Schwannomas and other sarcomas (Momand et al. 1998, Ragazzini et al. 2004), and malignant melanoma (Muthusamy et al. 2006). Overexpression of *Mdm4* was found in various tumors such as breast carcinomas, and colon and lung cancers (Danovi et al. 2004), as well as pre-B lymphoblastic leukemias (Han et al. 2007). Most importantly for the study described in this thesis, both *Mdm2* and *Mdm4* were found to be overexpressed in retinoblastoma (Laurie et al. 2006). As a possible cause for p53 dysfunction that allows for tumor formation, *Mdm2* and *Mdm4* are potential targets for chemotherapeutical treatment (Danovi et al. 2004, Garcia et al. 2011, Laurie et al. 2006). Inhibition of negative regulators, such as *Mdm2* and *Mdm4*, could reactivate p53 in tumors with an otherwise *wild-type* form of p53 that could compromise survival of tumor cells.

However, tumors with a mutated form of p53 would not be suitable for such a therapy of p53-reactivation. In the latter case, one possible strategy of taking advantage of the mutated form of p53 in tumor cells would be the application of synthetic lethality (more about synthetic lethality in section 2.3, page 28). Finding a synthetic lethal partner of *p53* and chemically inhibiting this candidate would specifically remove the *p53* mutant cells and leave cells without *p53* mutation unharmed.

Transcriptional regulation of miRNA expression by p53

The p53 tumor suppressor is known as a transcription factor which can transcriptionally regulate a huge set of protein-coding target genes to elicit cellular responses mainly involved in tumor suppression. However, recent studies of different groups unraveled a new mechanism, connecting p53 with the miRNA pathway to suppress tumorigenesis. miRNAs with tumor suppressive function were found to be direct transcriptional targets of p53. Expression of the miR-34 family, consisting of miR-34a, miR-34b, and miR-34c and encoded by two different genes, was first found to be directly regulated by p53 (Chang et al. 2007, He et al. 2007, Raver-Shapira et al. 2007, Tazawa et al. 2007, Tarasov et al. 2007, Corney et al. 2007). It was further shown that, on the one hand, ectopic expression of miR-34a would lead to p53-mediated apoptosis, cell cycle arrest, and senescence, while on the other hand, inactivation of endogenous miR-34a inhibits p53-dependent apoptosis in cells. miR-34 can induce apoptosis or decrease cell proliferation by repressing the expression of specific targets involved in survival, cell cycle regulation, or cell proliferation. Among those targets are cyclin E2, cyclin-dependent kinases 4 and 6 (CDK4 and CDK6), and Bcl-2 (Figure 2.9).

The miR-34 family is not only directly regulated by p53, and thereby involved in the downstream pathway of p53, but it also regulates p53 activity upstream by suppressing the silent information regulator 1 (SIRT1) (Yamakuchi et al. 2008). SIRT1 is a negative regulator of p53 which deacetylates Lys382 of p53 and leads to repression of apoptosis (Luo et al. 2001). This interaction with SIRT1 creates a positive feedback loop between p53 and the miR-34 family, showing for the first time that miRNAs can function to enhance p53 signaling.

Interestingly, decreased expression of miR-34 could be found in various tumors such as NSCLC (Bommer et al. 2007), pancreatic cancer (Chang et al. 2007), and colon cancer (Tazawa et al. 2007), suggesting a tumor suppressive role of miR-34. This is in line with the previously mentioned findings that miR-34 and p53 build a positive feedback loop and therefore loss of either *p53* or the miRNA miR-34 would promote tumorigenesis.

Besides the miR-34 family, there are several other miRNAs of which expression is transcriptionally regulated by binding of p53 to their promoters, including *miR-192*, *miR-194*, *miR-215*, *miR-17-5p*, *miR-20a*, *miR-143*, *miR-145*, *miR-16-1*, and *miR-107* (Figure 2.9). Among those, miR-145 was reported to negatively regulate the oncogene c-Myc (Sachdeva et al. 2009). Overexpression of miR-145 would reduce c-Myc expression, leading to growth

inhibition and therefore functioning as a putative tumor suppressor. miR-107 can repress the expression of the hypoxia inducible factor 1 beta (HIF-1beta), thus blocking hypoxia signaling and angiogenesis (Yamakuchi et al.). Two other miRNAs, miR-192 and miR-215, were shown to be induced by p53 and cause cell cycle arrest (Braun et al. 2008, Georges et al. 2008) through targeting several regulators of DNA synthesis and the G1 and G2 cell cycle checkpoints (such as CDC7, MAD2L1, and CUL5).

Taken together, p53 is able to repress processes like cell proliferation, cell survival, and angiogenesis not only through transcriptional activation of the classical protein-coding downstream effectors but also trough activation of miRNAs with a tumor suppressive function (Figure 2.9).

p53 itself is directly and indirectly regulated by miRNAs

Besides involvement of the positive feedback loop p53/miR-34/SIRT1, there are also other miRNAs functioning as upstream regulators of p53 by either upregulating or downregulating p53 (Figure 2.9).

Among the miRNAs indirectly activating p53 and inducing p53-mediated apoptosis are miR-29 and miR-122. The miR-29 family members (miR-29a, miR-29b, miR-29c) repress p85a, a regulatory subunit of PI3 kinase (PI3K) (Park et al. 2009) which is an upstream regulator of AKT. AKT is known to negatively regulate p53 activity by phosphorylation and thereby activation of MDM2 (Zhou et al. 2001). Therefore miR-29 is able to upregulate p53 through the negative feedback loop between PI3K-AKT-MDM2-p53 and acting as a tumor suppressor. Downregulation in various cancers such as leukemia (Pekarsky et al. 2006) and lung cancer (Fabbri et al. 2007) illustrates its tumor suppressive function.

Several miRNAs such as miR-504 (Hu et al. 2010) and miR-125 (Le et al. 2009) can also directly target p53 and suppress apoptosis, thus showing oncogenic functions. miR-504 is able to bind to two binding sites in the 3'-UTR of human *p53* and negatively regulate its expression (Hu et al. 2010). Upregulation in cancer cells of either of those two miRNAs therefore impairs the tumor suppressive function of p53.

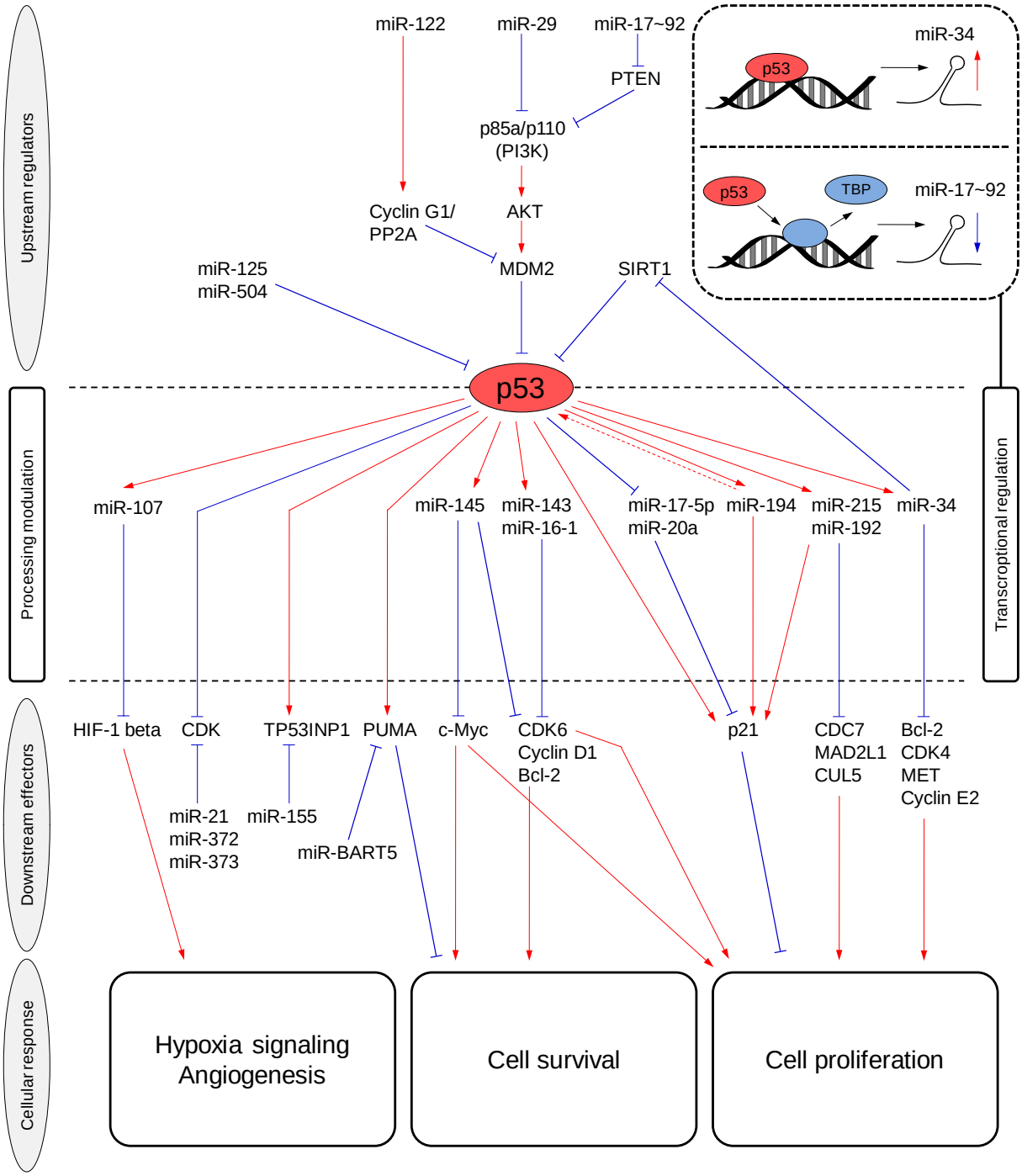

Figure 2.9: Interaction of the p53 pathway with the miRNA network.

The p53 tumor suppressor interacts with the miRNA pathway in various interconnected ways. (i) The p53 protein can transcriptionally regulate target miRNAs which can then further change the expression levels of several downstream effectors involved in cell proliferation, cell survival, and angiogenesis. (ii) Upstream regulators of p53, such as SIRT1 or Cyclin G1, can also be targeted by several miRNAs and therefore indirectly change levels of p53 and influence the cellular response. (iii) Several miRNAs, such as miR-125 and miR-504, can directly downregulate p53 and suppress apoptosis (Le et al. 2009, Hu et al. 2010) (figure based on Suzuki and Miyazono 2010 and Feng et al. 2011).

p53 regulates miRNA processing and maturation

In addition to its function as transcriptional activator of miRNAs, p53 can also promote post-transcriptional maturation of miRNAs (Figure 2.10 and Suzuki et al. 2009). For miR-143, miR-145, and miR-16-1 it was shown that p53 promotes Drosha-mediated processing, additionally requiring the interaction with p68 and p72 as well. These miRNAs negatively regulate important regulators of cell cycle and cell proliferation, such as K-Ras, CDK6, Bcl-2, and Cyclin D1 and are consequently decreased in various human cancers. Interestingly, transcriptionally inactive p53 mutants (such as R175H and R273H) were hindering the pri-miRNA maturation process by Drosha, resulting in low levels of those miRNAs.

Involvement in miRNA processing and maturation might therefore be an additional way of p53 to contribute to cancer progression independently of its transcriptional regulation properties.

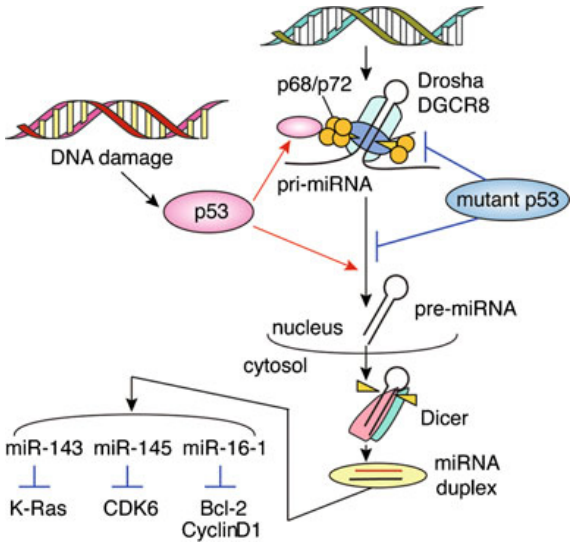

Figure 2.10: p53 is a regulator of miRNA biogenesis.
The p53 tumor suppressor is able to directly regulate miRNA biogenesis by interacting with the Drosha-p68-p72 processing complex in response to DNA damage and enhancing the post-transcriptional processing of miR-143, miR-145, and miR-16-1, leading to induction of growth-suppressive signals (schematic from Suzuki and Miyazono 2010).

2.3 Synthetic lethality

The principle of synthetic lethality was first described in 1946 (Dobzhansky 1946) and later in 1968 found in *Drosophila melanogaster* where simultaneous inactivation of two otherwise non-lethal genes *dor* and *ry* lead to embryonic lethality (Lucchesi 1968 and schematic in Figure 2.11).

The mechanism behind the synthetic lethal outcome can be either due to two genes involved in parallel redundant pathways or due to two genes that are important in the same essential pathway and consequently loss of the two genes would have a lethal effect (Ferrari et al. 2010).

Since the concept was first found, many studies identified new synthetic lethal interactions, mainly through genetic screens in yeast (Bender and Pringle 1991, Tong et al. 2001) and other model organisms and cell lines (Ma et al. 2012 and reviewed in Hartman et al. 2001, Ferrari et al. 2010). Finding new synthetic lethal interactions not only makes it possible to identify new features of essential processes in mammals and other organisms, it also gives us more insights about human genetic variation which helps us to understand genetic mutations and their contribution to different disease phenotypes, such as cancer. Especially with regards to mutations of a gene causing cancer in humans, identifying a synthetic lethal partner would help to selectively kill those cancer cells and making the synthetic lethal partner a promising drug target for chemotherapy.

Many synthetic lethal interactions were found in combination with important proteins involved in cell cycle regulation and cancer biology. Some of these proteins are Ha-RAS, Ki-RAS, proteins of the protein kinase networks (such as PI3K, EGFR, mTOR, Notch1, AKT-2), c-MYC, n-MYC, RB1, and p53 (reviewed in Weidle et al. 2011).

Since *p53* is the most frequently mutated gene in human cancers (Hainaut and Hollstein 2000, Petitjean et al. 2007), synthetic lethality in the context of *p53* loss of function is a very promising approach for anticancer drug development. Among others, synthetic lethal partners of p53 are CHK1, ATM, WEE-1, PKL-1, MK2, MYT-1, MAP-4, AMPK, GEF-H1, SGK2, PAK3, and ATR (Weidle et al. 2011, Ruzankina et al. 2009).

For example, the compound paclitaxel was found to target microtubule-associated protein-4 (MAP-4), transcriptionally repressed by p53, and selectively killing cells with transcriptionally inactive p53. However, in the case of wild-type p53, sensitivity to paclitaxel was reduced (Zhang et al. 1999, Murphy et al. 1996, Zhang et al. 1998).

More recently, checkpoint kinase Atr was identified as another synthetic lethal partner of *p53* in mice, emphasizing the importance of synthetic lethality not only for *in vitro* experiments but also *in vivo* (Ruzankina et al. 2009).

To our knowledge, nothing is known about synthetic lethal interactions of miRNAs and protein-encoding genes. Since there are multiple methods available to specifically downregulate or block expression and maturation of single miRNAs or miRNA families (anti-

miRs, miR-sponges (Valastyan et al. 2009, Loya et al. 2009, Zhu et al. 2011), antagomirs, siRNA, and locked nucleic acids (summarized in Garzon et al. 2010), miRNAs might represent an ideal target for cancer treatment in the context of synthetic lethality. Especially in case of synthetic lethal interactions of miRNAs with known tumor suppressors such as p53 which are lost or mutated in many cancers, targeting these miRNAs might be novel way of removing cancer susceptible or already formed tumor cells.

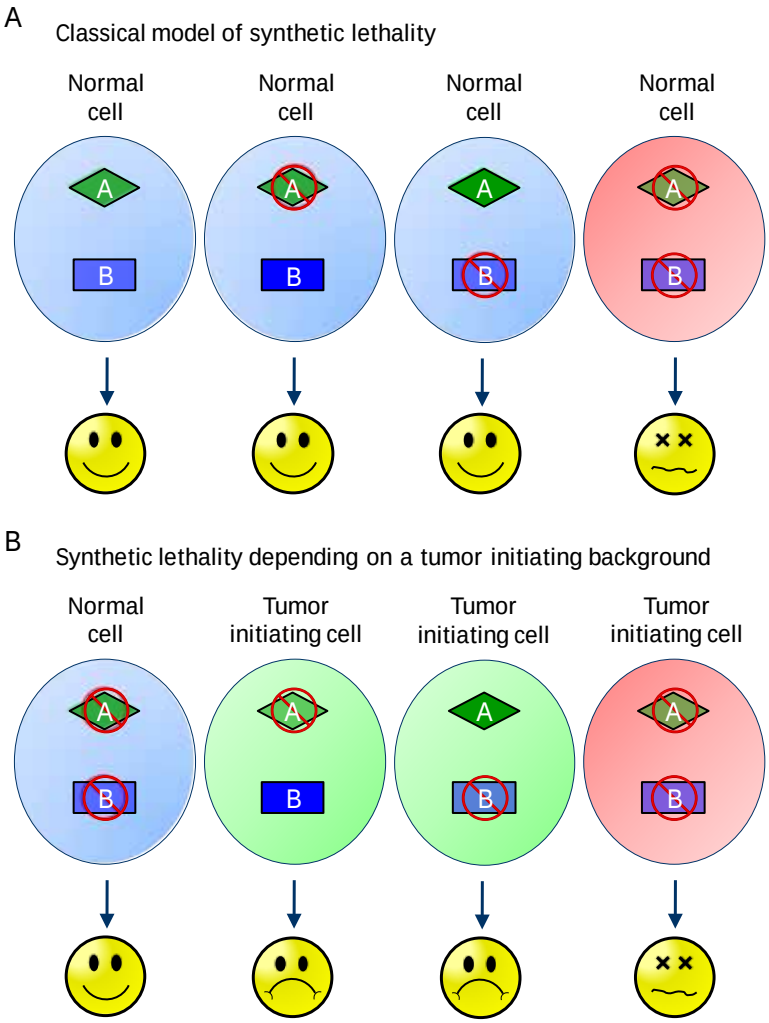

Figure 2.11: Principle of synthetic lethality.
(A) In the classical model of synthetic lethality inactivation of either gene A or B is tolerated by the cell and has no further consequences for its growth or metabolism. However, simultaneous inactivation of both genes A and B leads to cell death. (B) For therapeutic applications a synthetic lethal mechanism which is only applicable in tumor initiating cells but not in normal somatic non-mutated cells is desired. In such a scenario, concurrent inactivation of genes A and B (or inactivation of either gene) does not harm the cells. Inactivation of either gene A or B in a tumor initiating background has no or little viability (being "less fit") compromising effects on the cell. Then again, simultaneous inactivation of both genes A and B leads to cell death and therefore removal of the tumor initiating cells. The latter would enable tumor tissue to be removed by inhibition or removal of both genes A and B but would leave the surrounding healthy somatic tissue unharmed.

2.4 Biology of the eye and retina

2.4.1 Anatomy of the eye and retinal architecture

The retina consists of seven main cell types derived from a common progenitor. They compromise six cell types of neuronal origin, namely the photoreceptors (PR) (rods and cones), horizontal, amacrine, bipolar, and ganglion cells and one glial cell type known as the Müller glia (Figure 2.12 B). All different cell types are precisely organized into a discrete laminar structure forming the retina, situated at the back of the eye (Figure 2.12 A)

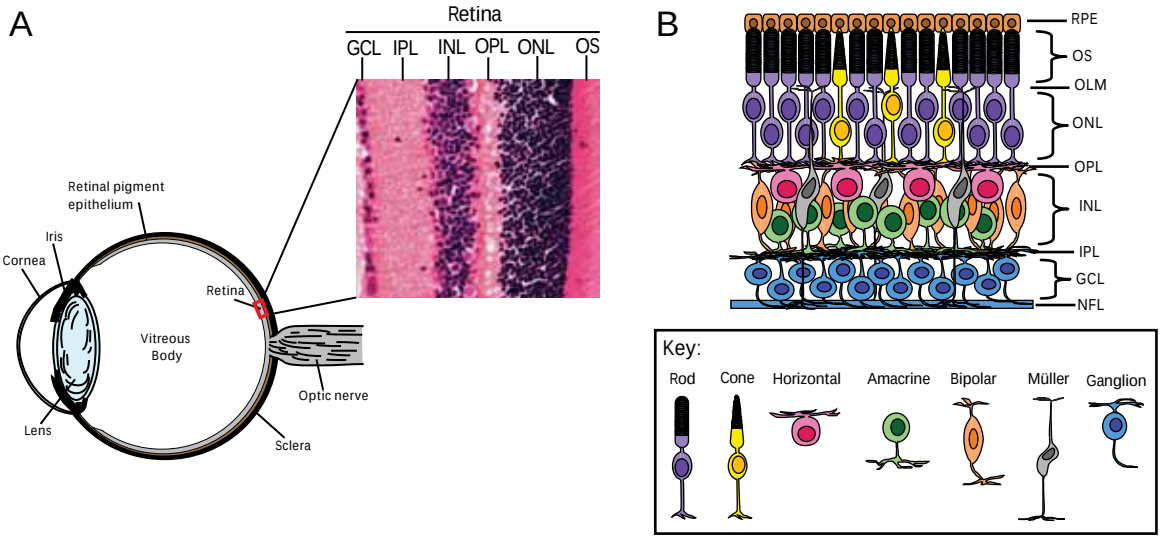

Figure 2.12: Anatomy of the eye and retinal architecture.
(A) Schematic of the human eye with enlarged view of the retina. Hematoxylin and Eosin staining of an adult mouse retina on the right shows the cytoarchitecture of a retina. (B) The retina is composed of six neuronal cell types and one glial cell type: the photoreceptors (PR) (rods and cones), horizontal, amacrine, bipolar, ganglion cells, and Müller glia (RPE: retinal pigmented epithelium, OS: outer segments, OLM: outer limiting membrane, ONL: outer nuclear layer, OPL: outer plexiform layer, INL: inner nuclear layer, IPL: inner plexiform layer, GCL: ganglion cell layer, NFL: nerve fiber layer). Figure modified from Poché and Reese 2009.

The retina can be sub-divided into different layers. Starting from the outermost region, adjacent to the retinal pigmented epithelium (RPE), there is (i) the outer nuclear layer (ONL), consisting of the light-sensing photoreceptors (PR) – the rods and cones. The rods and cones form specialized apical extensions at the outer limiting membrane (OLM) of the retina, forming the outer segments (OS) carrying the light-sensitive photopigments and all components for the visual transduction machinery that are needed for generating a neural signal upon response to light. Different cell types transfer the signal further through (ii) the outer plexiform layer (OPL), (iii) the inner nuclear layer (INL), (iv) the inner plexiform layer

(IPL) to the (v) ganglion cell layer (GCL). More specifically, upon receiving the signal from the outer retina, the bipolar cells stretching through the INL transmit the signal radially to the ganglion cell layer. The signal is thereby modulated within the OPL by horizontal cells, inhibitory interneurons also residing in the INL. The bipolar cells also make synapses with different amacrine cells and ganglion cells within the inner retina. Different amacrine cell types in the IPL further modulate retinal function through specific circuitry and signaling mechanisms. When the visual signal reaches the dendrites of retinal ganglion cells, it is further transmitted through their axons which form the (vi) nerve fiber layer (NFL) of the retina and transmit the signal to the visual centers of the brain. Additionally, the Müller glia cells, the primary glial cell population of the retina, are essential for the structure and the functional support of the other population of neurons. Their cell bodies are thereby extending across the whole retina, from the ONL to the GCL (reviewed in Poché and Reese 2009).

2.4.2 Retinal development

In contrast to the several months-long process of forming of the retina in the human embryo, retina formation takes only a few weeks in the mouse embryo (Figure 2.13). During this process, retinal progenitor cells divide and generate postmitotic transition cells with commitment to different neural and glial cell fates. Upon differentiation, the retinal progenitor cells form all synaptic connections necessary for correct visual signaling.

The mammalian retina is composed of seven main retinal classes (rod cells, cone cells, horizontal cells, amacrine cells, bipolar cells, Müller glia, and ganglion cells) which can be subdivided into roughly 55-60 functionally distinct cell types. The order in which the different classes of cell types emerge during retinal development is evolutionary conserved. For example, ganglion cells arise early during development while bipolar cells appear during later stages of retina formation.

Multipotent retinal progenitor cells normally change their cellular features in an unidirectional way to give rise to different cell types. Early progenitor cells, for example, are only able to differentiate into early-born cell types such as ganglion cells and cones but cannot differentiate into late-stage progenitor cells such as bipolar cells and Müller glia. Late-stage progenitor cells are on the other hand only able to differentiate into other late-born cell types such as bipolar cells but not to early-born cell types.

It should be noted that different cell types can originate at the same time point of development. Between embryonic days 13.5 (E13.5) and 17.5 (E17.5) in the mouse retina, cones, horizontal cells, and amacrine cells arise simultaneously. Spatial heterogeneity in

progenitor cells, such as syntaxin-positivity, was shown to play an important role in the process of deciding into which cell type the progenitor cell will differentiate. For example, syntaxin-positive cells were shown to be biased to differentiate into amacrine cells (reviewed in Dyer and Bremner 2005).

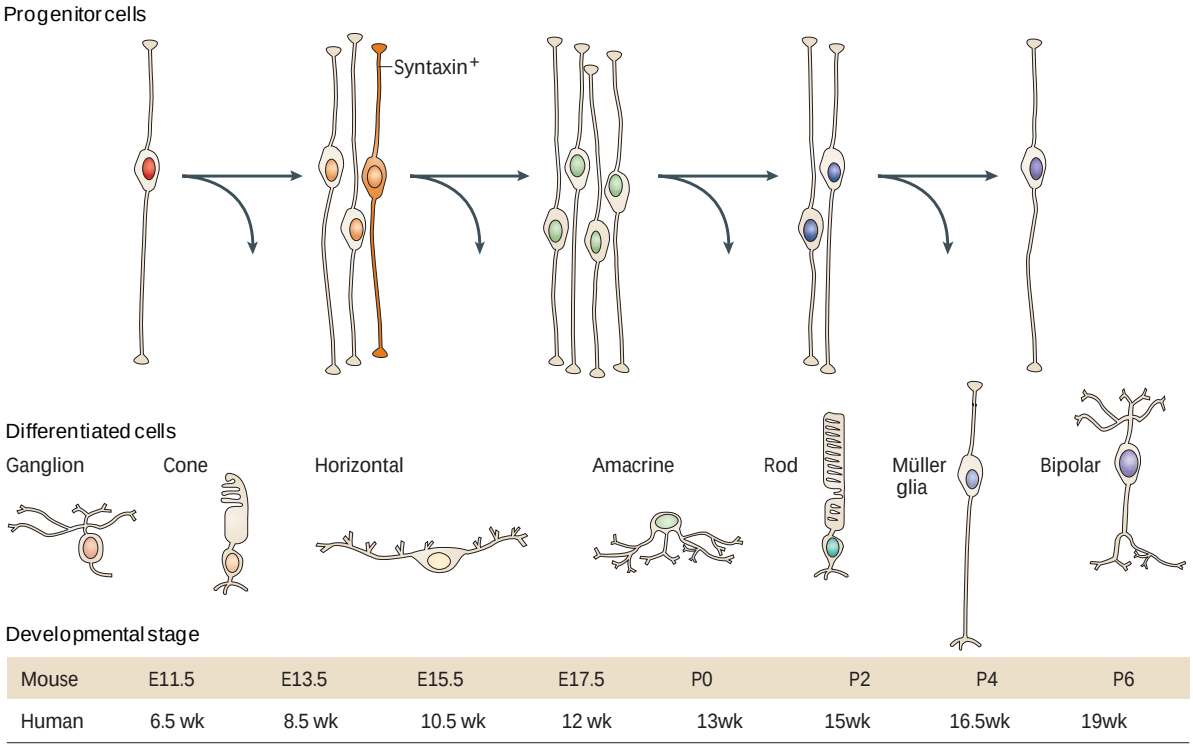

Mouse	E11.5	E13.5	E15.5	E17.5	P0	P2	P4	P6
Human	6.5 wk	8.5 wk	10.5 wk	12 wk	13wk	15wk	16.5wk	19wk

Figure 2.13: Retinal development.
Retinal formation takes several weeks (wk) in the mouse embryo and several months in the human embryo. The different cell types are represented by different colors: early-born cell types in red and late-born cell types in blue (figure modified from Dyer and Bremner 2005).

2.4.3 Retinoblastoma

Clinical features of retinoblastoma

Retinoblastoma is an intraocular ("in the eye") cancer mostly diagnosed in very young children. It occurs in 1 in 15 000 to 20 000 live births and is therefore the most common intraocular malignant tumor of childhood (Kivelä 2009, Mahajan et al. 2011). These numbers correspond to around 900 newly diagnosed cases of retinoblastoma in children worldwide each year (Kivelä 2009), including 300 new cases in the United States (Mahoney et al. 1990). The mean age of diagnosis is 13 months for bilateral (affecting both sides) and 25 months for unilateral (affecting one side only) retinoblastoma (Abramson et al. 1998). Unilateral cases (71.9%) are more common than bilateral cases (26.7%) (Tamboli et al. 1990, Broaddus et al.

2009). Two thirds (63%) of all children are two years or younger when they are diagnosed with retinoblastoma. 95% of all cases occur within the first 5 years of life (Figure 2.14 and Young et al. 1999).

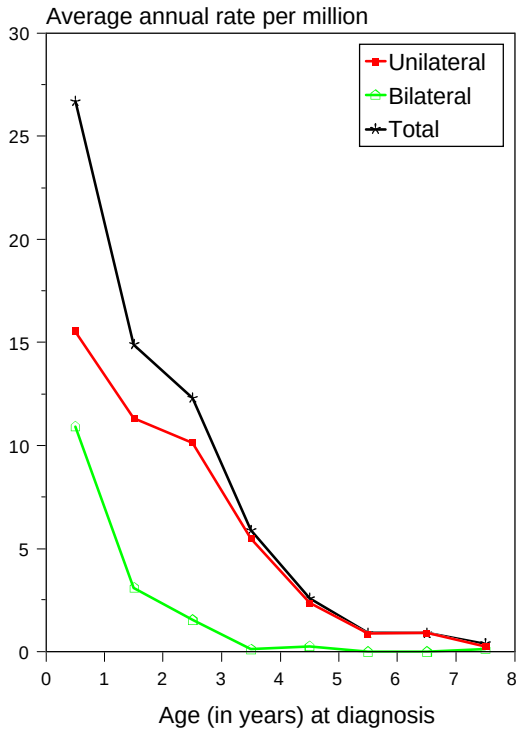

Figure 2.14: Age-specific incident rates of uni- and bilateral retinoblastoma (1976-84 and 1986-94).
Most cases of retinoblastoma occur in very young children. 63% of all children are two years or younger when they are diagnosed with retinoblastoma. 95% of all cases are seen within the first 5 years of life (data and graph from Young et al. 1999).

In regions such as Asia and Africa, the mortality rate is between 40 - 70%, whereas it is only 3 - 5% in Europe, Canada, or the USA (Kivelä 2009, MacCarthy et al. 2006, Nyamori et al. 2012, Leal-Leal et al. 2004, Rodrigues et al. 2004, Canadian-Retinoblastoma-Society 2009). Socio-economic factors and poor recognition of the seriousness of such an eye cancer are the reasons for the dramatic difference in mortality observed between western and developing countries (Canturk et al. 2010).

One of the most common first signs of retinoblastoma in a child is the presence of leucocoria (Abramson et al. 1998, Abramson et al. 2003, Goddard et al. 1999, Poulaki and Mukai 2009), the white tumor tissue covering the retina which reflects the light (Figure 2.15 A, B). Pictures of a person taken with a flash often give the effect of "red eyes". Reason for that is the reflection of the retina when hit by the flash at the right angle resulting in a red papillary light reflex. But upon early stages of retinoblastoma and formation of leucocoria

these "red eyes" appear white since the flash is reflected from the white tumor tissue in the eye instead of the retina itself (Figure 2.15 B).

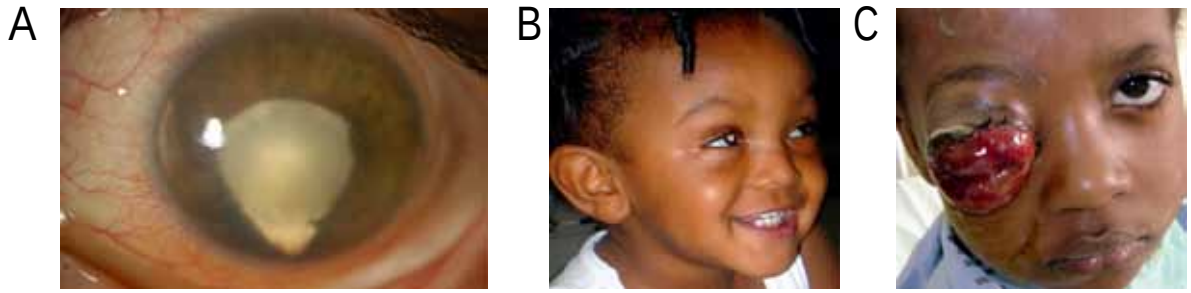

Figure 2.15: Detection of retinoblastoma.
(A) Leucocoria formation in the eye. White tumor tissue covering the retina is visible (Mahajan et al. 2011). (B) Early detection of retinoblastoma, the tumor is still contained within the eye. A white papillary light reflex makes early detection possible. (C) Proptosis of the eye at a very late detection stage of retinoblastoma (Dimaras et al. 2012).

Besides leucocoria, strabismus, poor visual tracking, glaucoma, spontaneous hyphema, pseudohypopyon, orbital cellulitis, or phthisis bulbi are other signs for the onset of retinoblastoma (Bowman et al. 2008, Owoeye et al. 2006, Mahajan et al. 2011).

Secondary nonocular malignancies are also observed in patients who survived the disease at a rate of 1% per year of life. These malignancies include osteogenic sarcoma of the skull and long bones, soft-tissue sarcoma, pinealoblastoma, cutaneous melanoma, and brain tumors among others (Mahajan et al. 2011). When bilateral retinoblastoma occurs together with pinealoblastoma it is referred to as "trilateral" retinoblastoma (Bader et al. 1980). The expression "trilateral" in combination with pinealoblastoma – cancer in the pineal gland – has its origins from the pineal function as a photoreceptor organ in lower animals. The pineal gland resembles the retina histologically and is described as a "third eye" (Bader et al. 1982).

Etiology of retinoblastoma

There are two forms of retinoblastoma: a genetic, heritable form (hereditary or germline mutation) and a non-heritable form caused by a somatic mutation (reviewed in Knudson 2001, Berger et al. 2011). Mutation in the germline accounts for 40% of all retinoblastomas (Knudson 1971). Inherited forms of retinoblastomas are usually bilateral (Knudson 1971, Richter et al. 2003) and very aggressive and are sometimes even associated with pinealoblastoma (together known as trilateral retinoblastoma) (Bader et al. 1982, Marcus et al. 1998). Unilateral retinoblastoma on the other hand is rarely passed on to the next generation (Knudson 1971; Richter et al. 2003).

Since children with unilateral retinoblastoma are usually diagnosed much later than children with the bilateral form, Alfred Knudson concluded that two hits – two mutational events – are the rate-limiting step for the development of retinoblastoma (Knudson 1971 and Figure 2.16). Several additional studies confirmed his "two-hit hypothesis" with the discovery of the first tumor-suppressor gene *RB1* at chromosome 13q14 in the 1980s (Comings 1973, Friend et al. 1986, Dryja et al. 1986, Lee et al. 1987), showing that loss of *RB1* is responsible for the initiation of retinoblastoma. Later it was also shown that loss of function of *RB1* can also be found in many other types of human cancers (Burkhart and Sage 2008, Talluri et al. 2010, Isaac et al. 2006, Longworth and Dyson 2010) such as lung and breast cancer (Harbour et al. 1988, Lee et al. 1988).

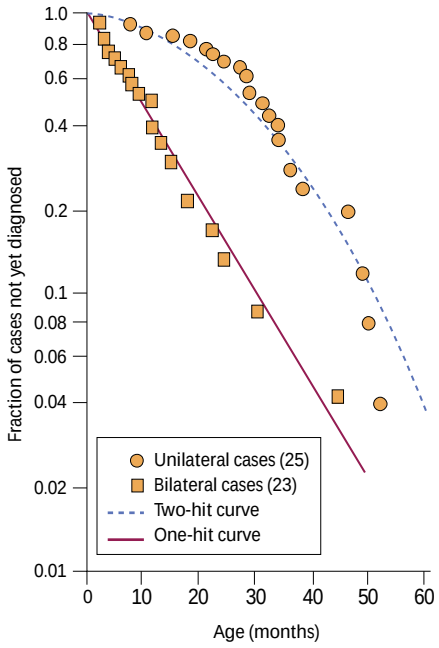

Figure 2.16: One-hit and two-hit curves for retinoblastoma.
Semilog plots of unilateral and bilateral retinoblastoma cases that are not yet diagnosed at plotted ages show that bilateral retinoblastoma cases match the expected shape of a one-hit curve. The unilateral cases on the other hand match the shape of a two-hit curve. Even though the bilateral cases also involve two mutations of *RB1*, they match the shape of a one-hit curve. This is due to the fact that in bilateral retinoblastoma one genetic mutation is always inherited and therefore only one additional mutation after birth is necessary to initiate tumor development (figure modified from Knudson 2001).

A biallelic mutation of the *RB1* gene initiates retinoblastoma formation, both in the heritable and non-heritable form of retinoblastoma (symbolized as constitutional *RB1* mutation M1 and somatic *RB1* mutation M2 in each allele in Figure 2.17). In the heritable form, all cells of the organism are predisposed due to a constitutional mutation in *RB1* (M1 in Figure 2.17). After this monoallelic loss of *RB1*, a second, now somatic mutation (M2 in Figure 2.17) in the other *RB1* allele in one or more developing fetal retinal cells will result in

complete loss of function of *RB1* and will therefore initiate tumor formation. Since it is very likely that the second mutation will occur in some of the rapidly dividing fetal retinoblasts, this cancer-susceptibility phenotype is dominantly inherited whereas the tumor initiation itself can be considered as a recessive trait. Then again, in the non-heritable form where initially all cells of the organism are *wild-type* for *RB1*, both mutations M1 and M2 covering both alleles have to happen in one and the same fetal retinoblast before it is completely differentiated in order to lose *RB1* and initiate the development of retinoblastoma. The higher probability of acquiring mutations in both *RB1* alleles in the heritable form of retinoblastoma therefore also explains the earlier detection and onset of retinoblastoma formation compared to the non-hereditable form. In the non-hereditary cases, a first mutation might have occurred in some retinoblasts but a second mutation might not arise before the retinal cell is completely differentiated. In this case, the mutated cells would be cancer-susceptible but would not directly give rise to tumors.

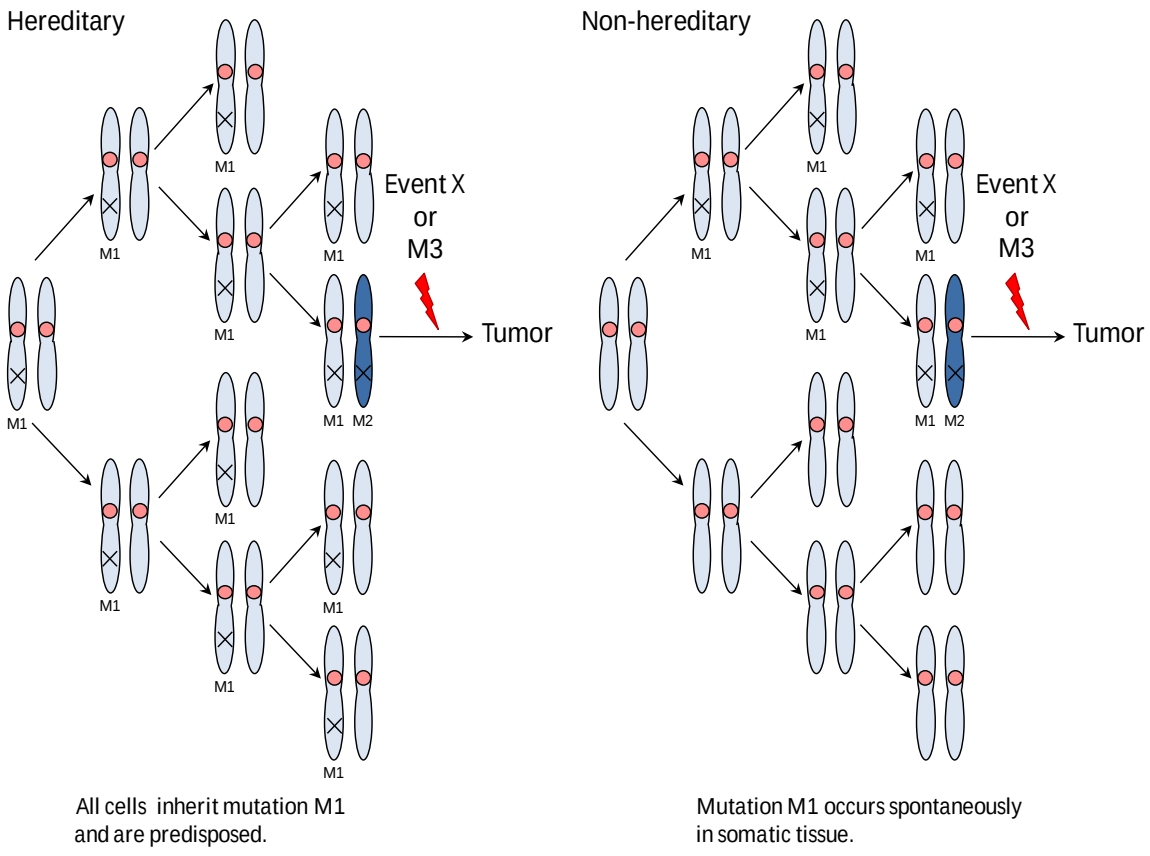

Figure 2.17: Genetics of the "two-hit" tumor formation in heritable and non-heritable retinoblastoma.
In the hereditary form of retinoblastoma, all cells and therefore all retinoblasts have one mutation and represent a so-called "one-hit" clone. In non-hereditary retinoblastoma, only one single precursor gets mutated and forms the one-hit clone, eventually giving rise to more one-hit clones before a mutation in the second allele can occur. The chances of accumulating a second mutation are therefore higher in the hereditary form. Consequently, acquiring a third mutation (event X or M3) resulting in the onset of tumor formation will be earlier compared to the non-hereditary form (figure modified from Knudson 2001 and Dimaras et al. 2012).

Molecular and genetic events in retinoblastoma progression

Indeed, virtually all patients harbor a mutation in the *RB1* locus. In hereditary cases (around 55%), all cells of the body carry a germline inactivated *RB1* allele and a somatic loss of the second allele occurs in retinal cells. In non-hereditary cases (the remaining 45% of all patients) both *RB1* alleles are somatically inactivated in a single retinal progenitor cell (Aerts et al. 2006). But loss of function of *RB1* is insufficient to cause retinoblastoma by itself. Instead, biallelic loss of *RB1* only leads to formation of retinoma – "distinctive retinal lesions, highly associated with retinoblastoma but lacking malignant characteristics" (Gallie et al. 1982) – and causes genomic instability (Dimaras et al. 2008). However, due to this genomic instability caused by *RB1* loss, stable retinoma is not very common and leads in most cases to formation of retinoblastoma. A "third hit", a mutation or event additional to biallelic loss of *RB1*, is required for full-blown retinoblastoma formation (mutation M3 or event X in Figure 2.17). The event that leads to malignant proliferation is, however, not fully understood. One possible explanation might be genomic instability caused by loss of *RB1* which leads to changes in other genes (Corson and Gallie 2007) and therefore to initiation of the formation of retinoblastoma. Among others, several candidate genes responsible for full-blown retinoblastoma formation are *MDM4* (Laurie et al. 2006), *MDM2* (Laurie et al. 2006), and *MYCN* (Lee et al. 1984, Squire et al. 1986). Those oncogenes were reported to be overexpressed or gained in copy number. But also other mechanisms like gene loss (e.g. *RBL2*, *CDH11*) or even hypermethylation (e.g. *CASP8*, *MLH1*) can be responsible for the onset of retinoblastoma (Zhang et al. 2012, reviewed in Corson and Gallie 2007). As we later show in this study, overexpression of miRNAs – specifically the *miR-17~92* cluster – can also play an important role in retinoblastoma formation. Identification of such candidate lesions is of cardinal importance, as it can open up new possibilities in the treatment of retinoblastoma.

In the line with this, as demonstrated using mouse models (Zhang et al. 2004b, Laurie et al. 2006), additional inactivation of the *p53* tumor suppressor on *Rb1*/*p107*-deficient background dramatically accelerates retinoblastoma formation in mice. *p53* is therefore thought to be essential for apoptosis in *Rb1*-deficient cells which prevents or delays cancer formation (Sherr and McCormick 2002). Surprisingly, *TP53* (or *p53*) is usually not mutated in primary retinoblastoma. Mutations could only be found in metastatic retinoblastoma cells (Kato et al. 1996). p53 could even be activated in retinoblastoma cells to induce apoptosis (Nork et al. 1997), also showing that p53 is still functional in primary retinoblastomas. One suggested mechanism for *p53* inactivation in primary retinoblastoma is through overexpression of *Mdm2* and *Mdm4* (Laurie et al. 2006 and Figure 2.18), two negative

regulators of p53. An *in vitro* study also suggests nuclear exclusion of p53 as a possible mechanism of p53 inactivation even though the status of *p53* is *wild-type* (Schlamp et al. 1997).

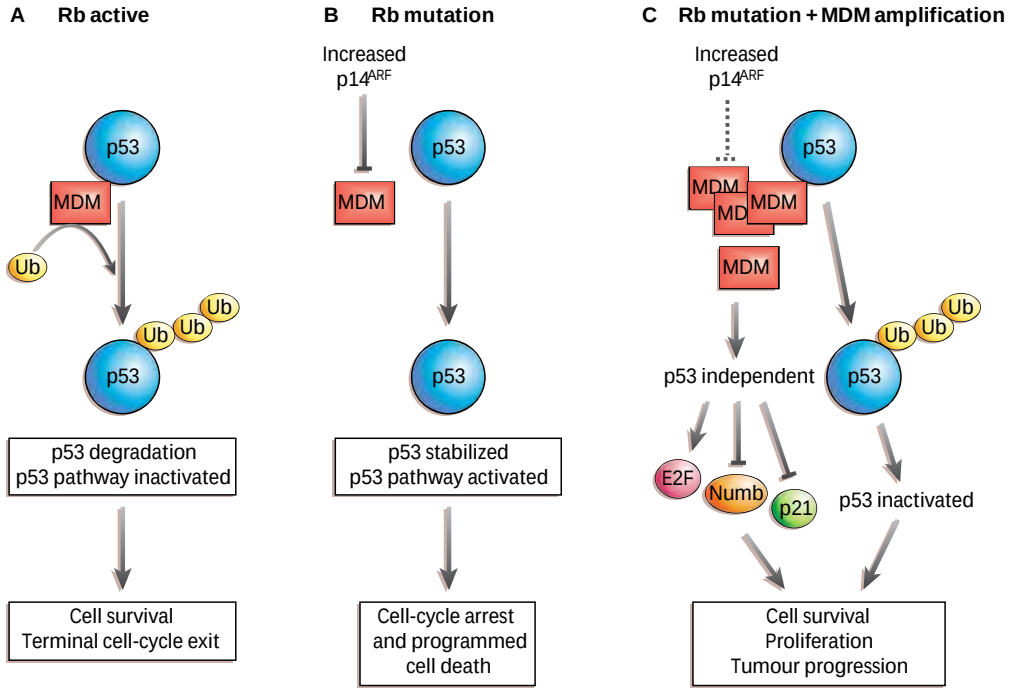

Figure 2.18: Role of Mdm2 and Mdm4 proteins in retinoblastoma.
(A) Under normal conditions – Rb1 is active – p53 protein levels are kept low by its negative regulator Mdm2 through ubiquitinylation and subsequent degradation. The gene-regulatory activity of p53 can additionally be inhibited by direct interaction with its other negative regulator Mdm4. (B) Upon mutation of the retinoblastoma gene (*Rb1*), $p14^{ARF}$ protein levels increase, leading to inactivation of *Mdm2* and promoting the activation of the p53 pathway. The results are usually cell-cycle arrest or cell death or sometimes facilitation of DNA repair. (C) Amplification of *Mdm2* or *Mdm4* in the absence of Rb1 blocks the activation of p53. Partly, because despite an increase of $p14^{ARF}$ protein levels, the high levels of Mdm2 or Mdm4 cannot be sufficiently decreased. Consequently, mutated cells survive, leading to enhanced proliferation and tumor progression. It is also speculated (Ganguli and Wasylyk 2003) that p53-independent interactions of Mdm2 with other proteins that regulate cell division, survival, or differentiation could additionally promote tumor progression (figure modified from Wallace 2006).

However, recent studies (Zhang et al. 2012) showed that upon loss of *RB1* the genome is in fact quite stable despite the previously reported genomic instability. *RB1* itself was actually the only known cancer gene which was mutated. More importantly, deregulation of different cancer pathways due to epigenetic changes was identified as a possible cause for the onset of retinoblastoma following biallelic loss of *RB1*.

Additionally, large deletions including *RB1* on chromosome 13q have been reported to result in fewer tumors than those with the common null mutations (DiCiommo et al. 2000, Albrecht et al. 2005). It is suggested that unknown adjacent genes that might be essential for the survival of the tumor cells could be deleted or partially deleted when large deletions of the

RB1 locus occur. Deletion of those adjacent genes might therefore partially block or delay tumor formation.

Mouse models of retinoblastoma

The first described genetically-engineered mouse model of spontaneous retinoblastoma was a transgenic mouse line in which cells of the retina expressed the oncogenic T antigen from the SV40 virus (Windle et al. 1990). T antigen was artificially introduced into the retinal cells since it inhibits the Rb1 protein which is responsible for retinoblastoma formation in human. But besides Rb1, T antigen also inhibits many other proteins, such as Rb1 family members p107 and p130. Even the p53 tumor suppressor is inhibited. This unspecific inhibition made it impossible to study the molecular mechanisms behind retinoblastoma. So different labs created a knockout mouse model where *Rb1* alone was specifically inactivated (Clarke et al. 1992, Lee et al. 1992, Jacks et al. 1992). These mice were lacking one copy of the *Rb1* gene, similar to the situation in humans. Surprisingly, these mice never developed retinoblastoma and even had perfectly normal retina. Further studies showed that the Rb1 family member p107 compensates loss of *Rb1* in mice during retinal development (Donovan et al. 2006) whereas loss of *RB1* is not tolerated in human retinal development. Indeed, mice lacking both *Rb1* and *p107* (Zhang et al. 2004b, Laurie et al. 2006) show unilateral retinoblastoma later in life. Additional loss of *Trp53* (or *p53*) in these *Rb1*/*p107*-deficient mice could further accelerate tumor formation and change the tumor spectrum from mostly unilateral retinoblastoma in *Rb1*/*p107*-deficient mice to mostly bilateral in *Rb1*/*p107*/*p53*-deficient mice. Consequently, the first knockout model of retinoblastoma (Zhang et al. 2004b, MacPherson 2004, Chen 2004) was created. Since *p53* is usually not lost in human retinoblastoma (Kato et al. 1996), it was later shown that overexpression of *Mdm4* could mimic *p53*-loss in *Rb1*/*p107*-deficient mice and therefore resemble the human molecular mechanisms involved in retinoblastoma formation more closely (Laurie et al. 2006, McEvoy et al. 2011). Instead of direct loss of *p53*, MDM4 can suppress p53-mediated cell death in *RB1*-deficient retinoblasts and therefore initiate tumor formation.

It is important to note that the knockout mouse model of retinoblastoma makes use of the retinal cell-specific *Chx10Cre*-transgene, which leads to the creation of mutant cells only in a subset of retinal cells (more about the mosaic expression of *Chx10Cre*, see chapter 4.1.1, page 45).

Current treatment strategies and clinical implications

Upon detection at an early stage, when the tumor is still contained within the eye, a vision-preserving treatment using systemic chemotherapeutics is preferred over enucleation, the removal of the eye. Upon first signs of leucocoria, retinoblastoma remains intraocular and is curable for about 3 to 6 months. With the usage of systemic chemotherapy in the 1990s, the 5-year survival rate is about 99% in the developed countries (Gombos and Chevez-Barrios 2007). But upon proptosis, the protrusion of the eye from the socket due to advanced spreading of tumor into the orbit (severe case in Figure 2.15 C), the only chance of cure is enucleation.

Recent studies, identifying *MDM2* and *MDM4* as possible targets for chemotherapy, should make it possible to specifically activate p53 to induce apoptosis in retinoblastoma cells. A small molecule inhibitor (nutlin-3a) of the interactions between p53 and both MDM2 and MDM4 was already shown to kill tumor cells (Laurie et al. 2005). A combination with a topoisomerase inhibitor (topotecan) which induces a p53-mediated DNA damage response could even enhance the effect (Brennan et al. 2011).

Better understanding of the molecular mechanisms of retinoblastoma may lead to identification of new pharmacological targets for the therapy against retinoblastoma. These new potential targets, such as miRNAs or even epigenetic modifications, could make it possible to very specifically target and kill the mutant cells without causing detrimental side effects that are common for chemotherapeutics available today.

3. Aims of the project

Several studies demonstrated that the overall levels of miRNAs are decreased in most human cancers (Chang et al. 2008, Thomson et al. 2006). This phenomenon could be explained by the known reduced stability and/or activity of proteins involved in the biogenesis of miRNAs, such as Dicer1, an RNAse III endonuclease (Hill et al. 2009, Karube et al. 2005, Thomson et al. 2006). At the same time, the absence of homozygous *DICER1* loss in human tumors and the fact that also in a number of mouse models homozygous loss of *Dicer1* was selected against (Kumar et al. 2009, Lambertz et al. 2010, Arrate et al. 2010), indicate that *Dicer1* is required for tumorigenesis.

To further investigate the molecular mechanism underlying the addiction to Dicer1 in human cancers, we studied its role in an established pre-clinical mouse model of retinoblastoma.

First, we tested whether *Dicer1*, and therefore a functional microRNA pathway, is required for normal retinal development in the mouse, both on *wild-type* and on a tumor susceptible background where the Rb1 pathway was compromised.

Then, *Dicer1*-deficient mice and appropriate control strains were regularly checked for retinoblastoma development to determine whether *Dicer1* would be required for tumor formation on different genetic backgrounds.

We found that simultaneous loss of *Dicer1* and *p53* is synthetic lethal on a tumor susceptible background. To shed light on the molecular mechanisms behind the synthetic lethal interaction and to identify a possible candidate microRNA responsible for the *Dicer1/p53* synthetic lethality, we performed various rounds of microRNA expression profiling on human and mouse tumors and control tissue.

Subsequently, we bred a conditional knockout mouse strain of the identified microRNA, namely *miR-17~92*, into our tumor susceptible mouse colony to determine the dependency of retinoblastoma formation on *miR-17~92*.

Upon realizing that both *Dicer1* and *miR-17~92* are synthetic lethal partners of *p53*, we tested a possible pharmacological application of downregulating different sets of

microRNAs of the *miR-17~92* cluster in established human retinoblastoma cell lines to specifically alter the growth of those cancer cell lines.

Ultimately, our finding of a set of microRNAs (miR-17/20a), of which downregulation could potentially kill retinoblastoma cells, should be explored as a highly selective therapeutic approach for the treatment of retinoblastoma or eventually even diseases with a compromised p53 pathway in general.

4. Results and conclusions

All experiments from the following sections were performed by the author (David N.) if not stated otherwise. All immunohistological stainings were done by Irina L. and Natacha R.

4.1 Mosaic inactivation of *Dicer1* in normal and *Rb1/p107*-deficient retinoblasts is tolerated during retinogenesis

In order to follow *Dicer1* deficient developing retinal progenitor cells (RPC), we crossed *Dicer1* conditional knockout mice (Murchison et al. 2005) with the retinal cell-specific *Chx10Cre* transgenic mouse line (Rowan and Cepko 2004) to conditionally inactivate *Dicer1* in the retina.

The BAC *Chx10Cre* transgenic construct (see also Figure 4.1) contains a sequence for a Cre-GFP fusion protein and an alkaline phosphatase (AP) reporter gene. Both can be used to specifically visualize the Cre-expressing retinal cells.

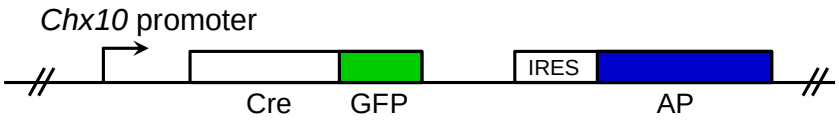

Figure 4.1: Schematic representation of the BAC *Chx10Cre* transgenic construct.
The GFP Cre-IRES-AP cassette of the modified BAC construct is integrated into the first exon of *Chx10* in the mouse genome (Rowan and Cepko 2004). Figure modified from Donovan and Dyer 2004 and Zhang et al. 2004b.

4.1.1 *Chx10Cre*-expression shows mosaicism in the retina

Expression of the BAC *Chx10Cre* construct can be visualized by AP staining of vibratome-cut 40µm sections of the mouse retina. We observed specific AP staining as early as of embryonic day 9.5 (E9.5) in the eye on sections from *wild-type* animals as shown in panel A in Figure 4.2. However, at day E9.5, only very few cells started to show a positive AP staining, which correlated with the expression of the Cre recombinase, while in the developing mouse, endogenous *Chx10* was expressed throughout the anterior optic vesicle and all neuroblasts of the optic cup. In the mature retina, the Chx10 protein is restricted to the inner nuclear layer (Liu et al. 1994). Therefore, starting at day E9.5, recombination of any floxed locus in the mouse genome may only occur in a fraction of progenitor cells.

Later on, at days E10.5 and E11.5 (panels B and C in Figure 4.2), more and more cells started to become AP stained. Importantly, even after retinal progenitor cells (RPCs) cease

proliferation by post-embryonic day P11 (Young 1985), AP staining – suggesting *Chx10Cre*-expression – remained mosaic. This notion is supported by anti-GFP immunohistochemical (IHC) stainings in Figure 4.3 which show that indeed only a fraction of Chx10-positive were GFP-positive as well.

Additionally, the grade of mosaicism can be highly variable between littermates. This mosaicism is probably due to the nature of the integration site or chromatin configuration of the BAC DNA (Rowan and Cepko 2004).

As a consequence of this mosaicism of Chx10Cre-expression in this mouse model, only a small subset of retinoblasts are mutant cells. The majority of the retinal cells remains *wild-type*.

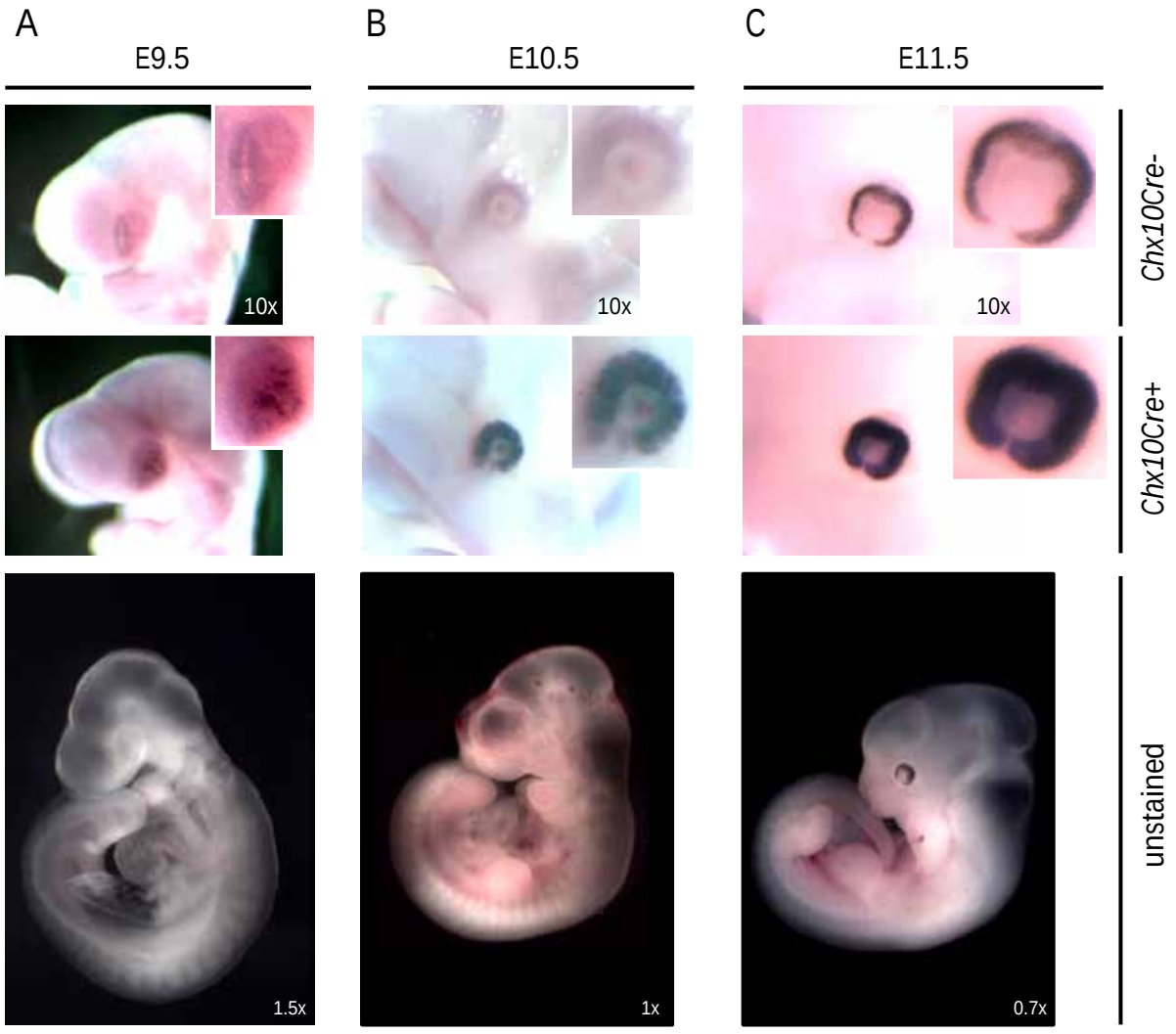

Figure 4.2: Expression of the *Chx10Cre* construct starts as early as of embryonic day 9.5.
The earliest time of *Chx10Cre* expression is at embryonic day 9.5 (E9.5). Chx10Cre-negative (*Chx10Cre-*) and Chx10Cre-positive (*Chx10Cre+*) embryos at embryonic days 9.5, 10.5, and 11.5 were whole-mount stained for AP reporter activity. AP activity can be observed in the developing eye as early as of E9.5 when single cells are visible. Later, at days E10.5 and E11.5, the AP reporter activity is visible in the whole retina.

4.1.2 *Dicer1* is dispensable for normal retinal development

Next, we performed IHC stainings on 5µm sections from paraffin-embedded tissues to highlight GFP expression in adult *wild-type* (*WT*) retina. GFP was detected in a subset of postmitotic bipolar and Müller cells which are located within the inner nuclear layer (INL) close to the outer plexiform layer (OPL) and the outer nuclear layer (ONL) (Figure 4.3).

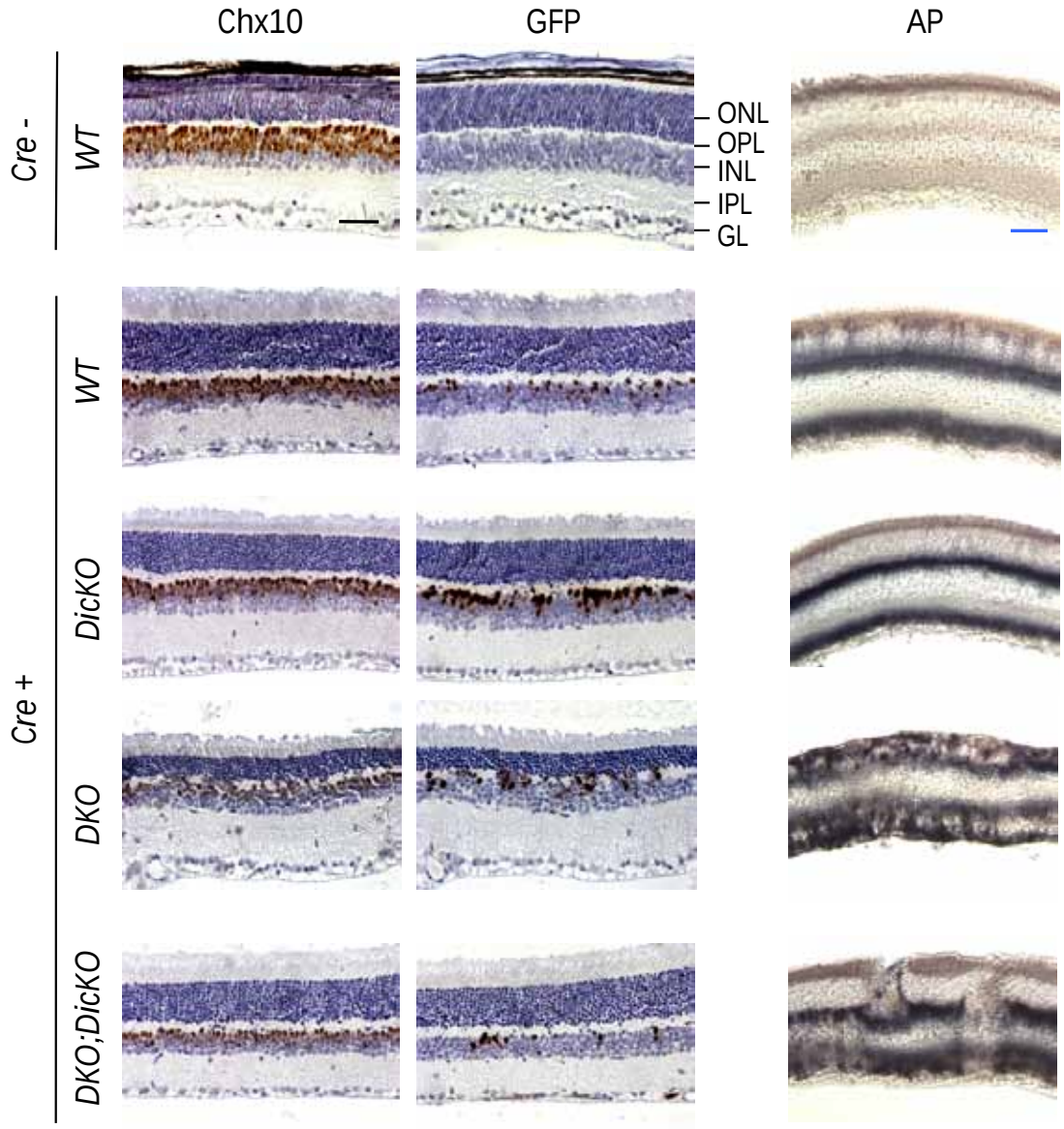

Figure 4.3: Mosaic inactivation of *Dicer1* in normal and *Rb1/p107*-deficient retinoblasts is tolerated during retinogenesis.

Chx10 and GFP immunostaining of adult (P21) *Chx10Cre; Dicer1*$^{+/+}$ (*WT*), *Chx10Cre*; *Dicer1*$^{lox/lox}$ (*DicKO*), *Chx10Cre; Rb1*$^{lox/lox}$*; p107*$^{-/-}$ (DKO) and *Chx10Cre; Rb1*$^{lox/lox}$*; p107*$^{-/-}$ *; Dicer1*$^{lox/lox}$ (DKO; DicKO) retinae. GFP-positive cells are detected in all mice (left panels). The three retinal nuclear layers (GL: ganglion layer; INL: inner nuclear layer; ONL: outer nuclear layer) and the two plexiform layers (OPL: outer plexiform layer; IPL: inner plexiform layer) are indicated. AP-stained transverse retinal sections are also shown (right panels). Regions of AP reporter activity are detected in all mice. Scale bars = 40µm. The IHC pictures were kindly provided by Irina Lambertz (CMG, UGent). The *WT* and *DicKO* IHC pictures were already used in the PhD thesis of Irina Lambertz (CMG, UGent) but are shown here for the sake of completeness.

GFP-positive cells could also be found in *Dicer1*-deficient *Chx10Cre*; *Dicer1*$^{lox/lox}$ retinae (further referred to as *DicKO*) suggesting that *Dicer1* is dispensable for normal retinal development. Importantly, also on an *Rb1/p107*-deficient background (*Chx10Cre; Rb1*$^{lox/lox}$*; p107*$^{-/-}$, further referred to as *DKO*), which ultimately leads to retinoblastoma development, was *Dicer1* deficiency still tolerated. Less GFP-positive cells could be found in *DKO; DicKO* retinae (histological sections in Figure 4.3 and quantification of FACS-sorted GFP-positive cells in Figure 4.4).

AP stainings on 40µm vibratome sections from adult retinae (P21) of the same set of genotypes could confirm the staining pattern of the IHC sections (Figure 4.3, right panel).

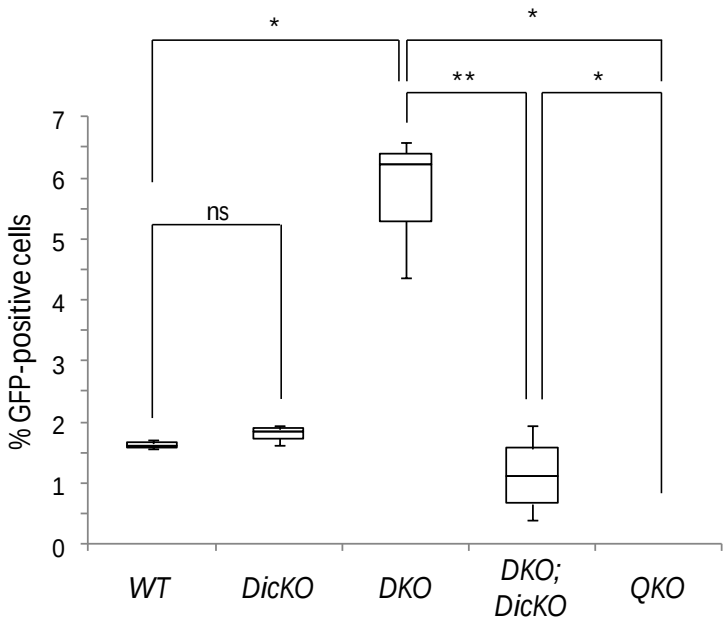

Figure 4.4: Percentage of Cre-GFP expression in the mouse retina at the age of P21 of various genotypes. Box plot diagram (bottom and top of the box showing the 25th and 75th percentile, respectively, band inside the box shows the median, and the end of the whiskers represent the minimum and maximum of the data) showing the percentage of GFP-positive cells in FACS-sorted mouse retinae at the postnatal age of P21 per genotype. For genotypes *WT*, *DicKO*, and *DKO* n=3, for *DKO; DicKO* n=4, and for *QKO* n=5. There is a clear significant difference between the *DKO* samples and either of the other samples (P-value of $P < 0.05$ (*) after an unpaired T-test with unequal variances between *WT* (or *DicKO*, or *QKO*) and *DKO* and $P < 0.01$ (**) between *DKO* and *DKO; DicKO*). Remark that in the *DKO; DicKO* samples GFP-positive cells are slightly less abundant than in the *WT* or *DicKO* retinae, however not significantly. Nonetheless, *DKO; DicKO* samples are significantly different from *QKO* samples ($P < 0.01$ (*)).

In *Chx10Cre* (*WT*) and *DicKO* mice only about 2% of the retinal cells showed GFP positivity (1.6 and 1.8%, respectively) whereas mice on a retinoblastoma-sensitized background (*DKO* mice) showed an increased percentage of GFP-positive cells (5.7% GFP-positive cells) (Figure 4.4). The latter is due to the fact, that with a compromised Rb1-pathway, retinal progenitor cells inappropriately exit the cycle and keep proliferating, thus

forming hyperproliferative lesions later in life, which develop into full-blown retinoblastoma (Zhang et al. 2004a, Zhang et al. 2004b). Importantly, *Dicer1* deficiency on a *Rb1*-compromised background (*Chx10Cre; Rb1$^{lox/lox}$; p107$^{-/-}$; Dicer1$^{lox/lox}$*, thereafter referred to as *DKO; DicKO* mice) slightly decreased the amount of GFP-positive cells (1.1% GFP-positive cells) compared to either *WT* mice or *Dicer1*-deficient mice on a background with functional Rb1 pathway (*DicKO* mice) (Figure 4.4).

Furthermore, IHC stainings for the two progenitor cell markers Chx10 and syntaxin, as well as for calretinin which is expressed in a subset of amacrine and ganglion cells, showed that *Dicer1* is dispensable for retinogenesis since both *WT* and *DicKO* retinae were normal and undistinguishable from each other (Figure 4.5).

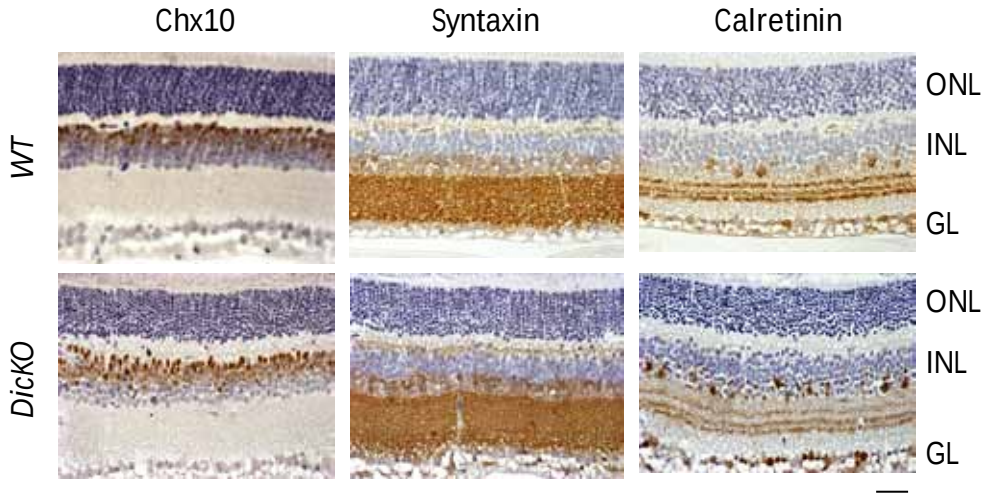

Figure 4.5: Retinogenesis is not affected in *DicKO* mice.
Chx10, Syntaxin, and Calretinin immunostaining of adult (P>21) *WT* and *DicKO* retinae. No difference in staining of the three retinal markers could be observed. The retinal structure in both *WT* and *DicKO* mice was normal. Therefore *Dicer1* deficiency did not negatively affect retinogenesis. Scale bar = 40µm (GL: ganglion layer; INL: inner nuclear layer; ONL: outer nuclear layer). Figure kindly provided by Irina Lambertz (CMG, UGent).

4.1.3 Expression of mature miRNAs is globally suppressed in *Dicer1*-deficient retinoblasts

The fact that retinogenesis was not compromised in *DicKO* and was even tolerated in *DKO; DicKO* mice, might be explained by incomplete recombination of the *Dicer1* locus and therefore remaining functional Dicer1 protein in those mutant cells. To exclude the possibility of incomplete recombination of the *Dicer1* allele, we FACS-sorted the GFP-positive cells of *Chx10Cre*, *DicKO*, *DKO*, and *DKO; DicKO* retinae at P21 (amount of GFP-positive cells in Figure 4.4) and genotyped the *Dicer1* locus (flow diagram for sample preparation in Figure

4.6 A). As expected, *DKO* cells only show a PCR product for the *wild-type* allele. Both *DicKO* and *DKO; DicKO* sorted mutant cells show a fully recombined *Dicer1* locus. No non-recombined allele was detectable, indicating that indeed these retinae were homozygously *Dicer1* deficient (Figure 4.6 B).

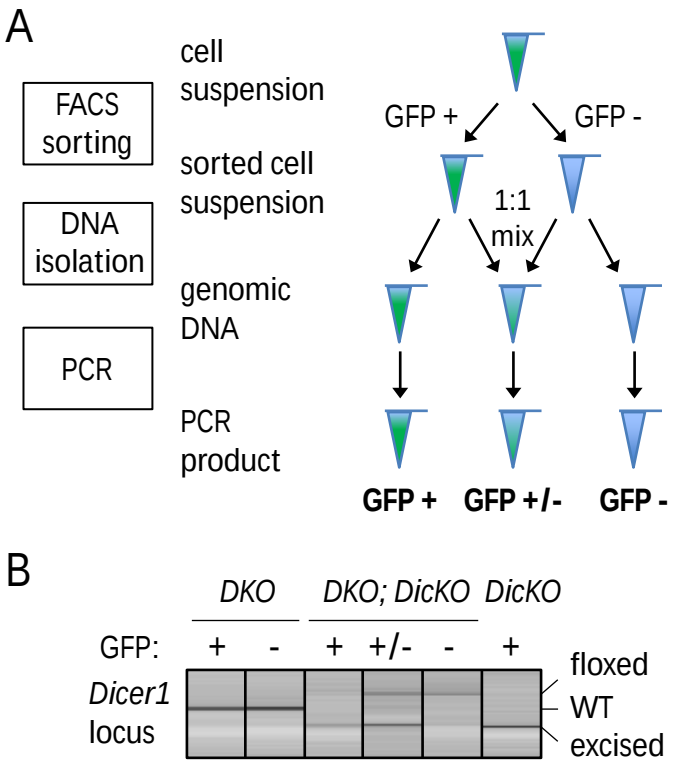

Figure 4.6: The *Dicer1* locus in Cre-positive *Dicer1*$^{lox/lox}$ cells is completely recombined.
(A) Flow diagram schematically showing the sample preparation for the recombination PCR in B. (B) Genotyping of FACS-sorted GFP-positive cells (GFP +) from adult retinas confirms complete recombination of the *Dicer1* locus in Cre-positive *Chx10Cre; Rb1*$^{lox/lox}$*; p107*$^{-/-}$ *; Dicer1*$^{lox/lox}$ (*DKO; DicKO*) and *Dicer1*$^{lox/lox}$ (*DicKO*) cells. A 1:1 mixture of GFP-positive and GFP-negative (GFP +/-) and GFP-negative cells (GFP -) were used as controls in the *DKO; DicKO* background. The possible product bands of the *Dicer1* recombination PCR are: floxed: floxed allele; WT: *wild-type* allele; excised: excised allele. The PCR products were visualized using the QIAxcel system (Qiagen).

To show that *Dicer1* deficiency also has functional consequences, we performed a microRNA expression profiling with the FACS sorted retina cells in collaboration with Pieter Mestdagh, Jo Vandesomple, and Frank Speleman (CMG, UGent). With the expression results of 509 murine miRNAs which were profiled, we could show that microRNA expression was dramatically and globally downregulated (10x downregulation) in either *DicKO* or *DKO; DicKO* cells compared to control retinae (Figure 4.7). Therefore we conclude that *Dicer1* is dispensable for retinogenesis by itself (Figure 4.5), and that, additionally, a severely downregulated miRNA pathway does not compromise normal retinal development.

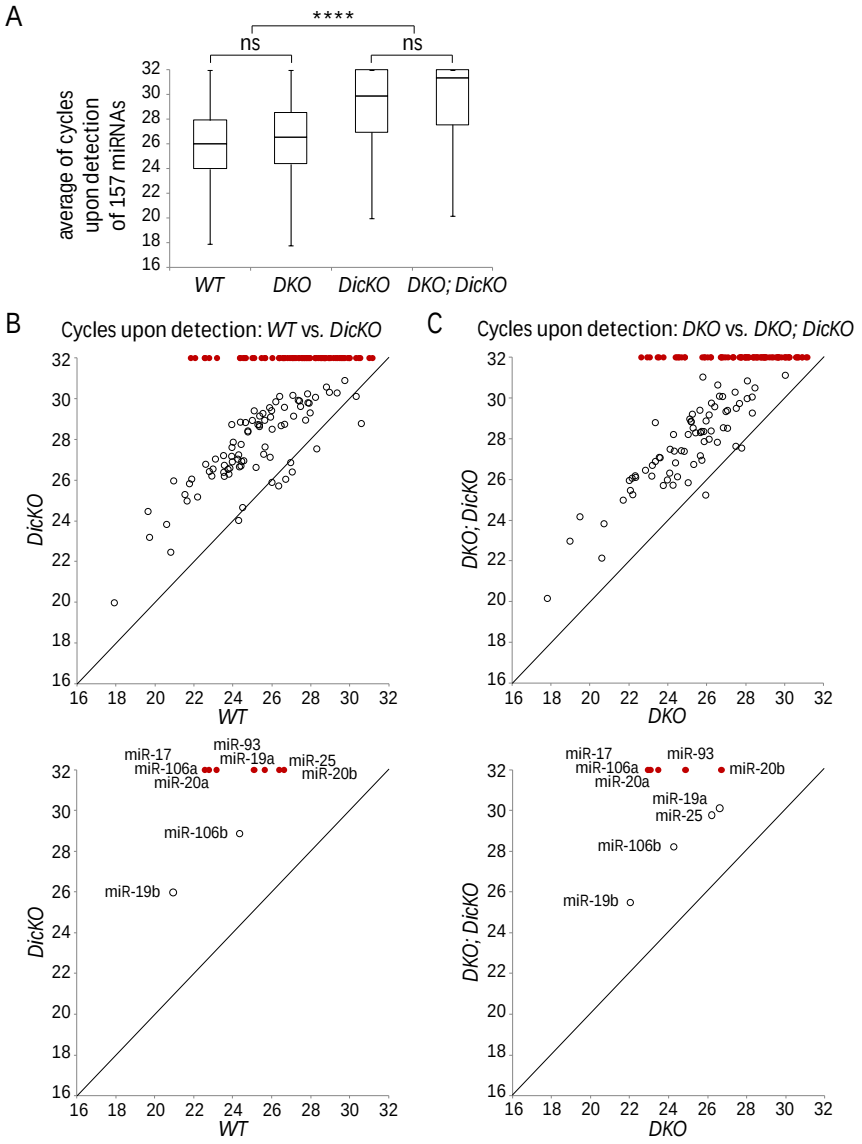

Figure 4.7: Expression of mature miRNAs is globally suppressed in FACS-sorted *Dicer1*-deficient retinoblasts.

Mature miRNAs expression levels in FACS-sorted GFP-positive cells from adult (P21) retinae of mice with the indicated genotypes show a global suppression of miRNA expression in *Dicer1*-deficient samples. (A) Box plot diagram (bottom and top of the box showing the 25th and 75th percentile, respectively, band inside the box shows the median, and the end of the whiskers represent the minimum and maximum of the data) showing the expression levels of mature miRNAs in FACS-sorted GFP-positive cells from adult retinae of mice (age is P21) with the indicated genotypes. For the *WT*, *DKO*, and *DicKO* genotypes n=3 and for *DKO; DicKO* n=4. *Dicer1*-deficient cells (*DicKO* and *DKO; DicKO*) show significantly lower miRNA expression levels (a higher average of cycles upon detection) as *Dicer1*-proficient cells (*WT* and *DKO*) ($P < 0.0001$ (****)). (B and C) Mature miRNAs expression levels in FACS-sorted GFP-positive cells from adult retinae of mice with the indicated genotypes. Data are presented as mean Ct values where high values represent low miRNA expression levels. More than half of the miRNAs expressed at detectable levels in normal and *Rb/p107*-deficient Chx10Cre-positive cells are no longer detectable in the purified *Dicer1*-deficient cells. The vast majority of the remaining miRNAs are expressed at levels that are >10-fold lower compared to the levels in *Dicer1*-proficient cells. miRNAs which were expressed in *WT* or *DKO* cells but which were not detectable in *DicKO* (*DKO; DicKO*, respectively) are marked in red and a value of 32 cycles upon detection was used for further calculations and representation in the graph. The upper panels of B and C show all expressed miRNAs, whereas the lower panels only depict the expressed members of the three *miR-17~92* and paralog clusters (*miR-17~92*, *miR-106a~363*, and *miR-106b~25*).

4.2 *Dicer1* is required for retinoblastoma formation

Retinal progenitor cells in *DKO* mice which have a compromised Rb1 pathway develop early hyperproliferative lesions due to failure to exit the cell cycle (Zhang et al. 2004b, Donovan et al. 2006) which leads to a slight disruption of the retinal laminar organization. As seen in Figure 4.8 B, the immature *Rb1/p107*-deficient cells (*DKO*) from the inner nuclear layer (INL) could protrude through the outer plexiform layer (OPL) and very few cells of the INL were even found in the inner plexiform layer (IPL). Those *DKO* mice only developed retinoblastoma with delayed and variable kinetics (Figure 4.8 A). As shown before in Figure 4.4, the knockout of *Dicer1* on this *Rb1*-deficient background (*DKO; DicKO*) decreased the number of mutant cells but was tolerated during retinogenesis (Figure 4.3). But, similar to retinae of *DKO* mice, *DKO; DicKO* retina also showed rosette formation and dysplasia (Figure 4.8 B). Surprisingly, even after 2 years, none of the 50 mice observed developed any form of retinoblastoma whereas 50% of all *DKO* mice developed retinoblastoma within about 300 days.

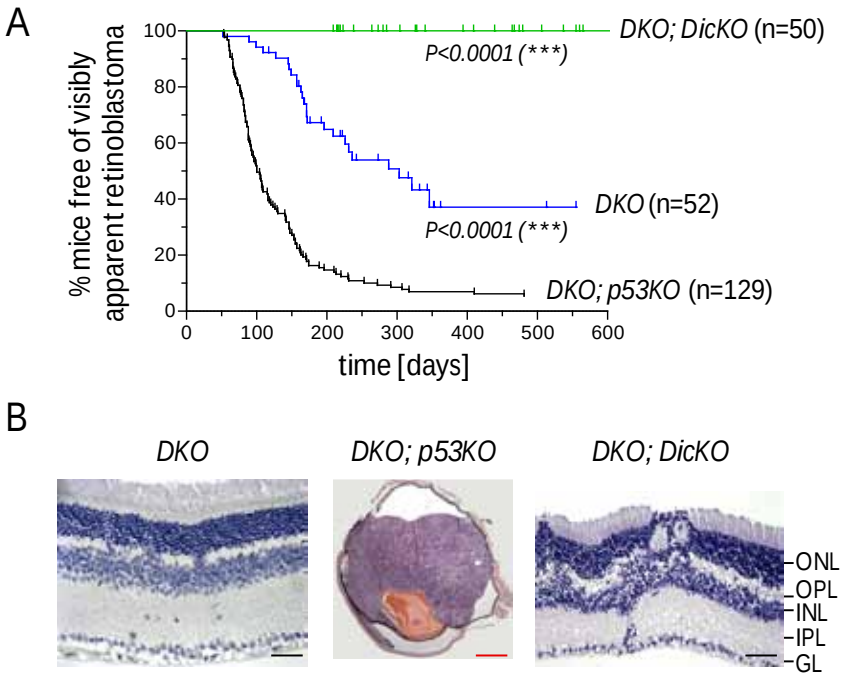

Figure 4.8: *Dicer1* is required for retinoblastoma formation.
(A) Kaplan-Meier curve showing the time to first observation of externally visible retinoblastoma. This time was markedly decreased in *Chx10Cre; Rb1$^{lox/lox}$; p107$^{-/-}$; p53$^{lox/lox}$* (*DKO; p53KO*) mice relative to *Chx10Cre; Rb1$^{lox/lox}$; p107$^{-/-}$* (*DKO*) littermates. *Chx10Cre; Rb1$^{lox/lox}$; p107$^{-/-}$; Dicer1$^{lox/lox}$* (*DKO; DicKO*) mice did not develop tumors (logrank Mantel-Cox test, *P*<0,0001) up to a observation period of 2 years (data shown up to 600 days). (B) Invasive tumors that fill the vitreous and the anterior chamber were found in *DKO; p53KO* mice as early as P60. Hematoxylin and eosin stain with the three retinal nuclear layers (GL: ganglion layer; INL: inner nuclear layer; ONL: outer nuclear layer) and the two plexiform layers (OPL: outer plexiform layer; IPL: inner plexiform layer) are indicated.. Black scale bars =40µm. Red scale bar = 400µm. The IHC pictures were kindly provided by Irina Lambertz (CMG, UGent).

The presence of GFP-positive cells in *Dicer1*-deficient retina on *WT* or *Rb1*-sensitized background as shown in Figure 4.4 demonstrates that protection against cancer in *DKO; DicKO* mice is not due to the death of tumor initiating cells. A possible explanation for the absence of tumor formation might be that, upon *Dicer1* inactivation, cells could still develop normally but are not able to proliferate at such high rates as *Rb1*-deficient cells (*DKO*). Since it was reported (Mudhasani et al. 2008) that loss of *Dicer1* can activate the p53 pathway, we speculated that p53-mediated cell cycle arrest and/or apoptosis might be the reason for the decreased number of GFP- and AP-positive mutant retinal cells and the absence of tumor formation in *DKO; DicKO* mice.

To address the question of whether p53-activation was responsible for the decreased fitness of retinal cells and the absence of retinoblastoma formation in *DKO; DicKO* mice, we introduced a conditional *p53* knockout allele into our *DKO* and *DKO; DicKO* mouse colonies. Additional loss of *p53* in *DKO* mice (*Chx10Cre; $Rb1^{lox/lox}$; $p107^{-/-}$; $p53^{lox/lox}$* thereafter called *DKO; p53KO*) accelerates tumor formation dramatically and is a well-accepted mouse tumor model (Zhang et al. 2004b, Zhang et al. 2004a, Laurie et al. 2006, McEvoy et al. 2011). More than 80% of the *DKO; p53KO* mice (106 out of 129) developed highly aggressive and invasive bilateral retinoblastoma with clear evidence of anterior chamber invasion (Figure 4.8 A and B). The median time for developing retinoblastoma for the *DKO; p53KO* mice was 100 days versus 303 days for *DKO* mice. Alternatively, instead of directly inactivating *p53* using a *p53*-knockout allele, also indirect downregulation of p53 via Mdmx-overexpression can be used to accelerate retinoblastoma formation (Laurie et al. 2006, McEvoy et al. 2011, Xiong et al. 2010).

4.3 *Dicer1* and *p53* act as synthetic lethal partners upon *Rb1/p107*-inactivation

4.3.1 *Chx10/Rb1/p107*-mutant cells are lost upon concomitant inactivation of *Dicer1* and *p53*

Next, we wanted to test whether *Dicer1* depletion on the *DKO; p53KO* background (*Chx10Cre; $Rb1^{lox/lox}$; $p107^{-/-}$; $p53^{lox/lox}$; $Dicer1^{lox/lox}$*, thereafter called *QKO*) could lead to retinoblastoma formation. Without p53-mediated cell cycle arrest or apoptosis due to loss of *Dicer1*, there might be a possibility that *QKO* mice could develop retinoblastoma similar to *DKO* or even *DKO; p53KO* mice. But unexpectedly, no GFP- or AP-positive cells could be

found in adult *QKO* retinae whereas adult *DKO; DicKO* retinae showed a normal pattern for GFP- and AP-stainings (Figure 4.9).

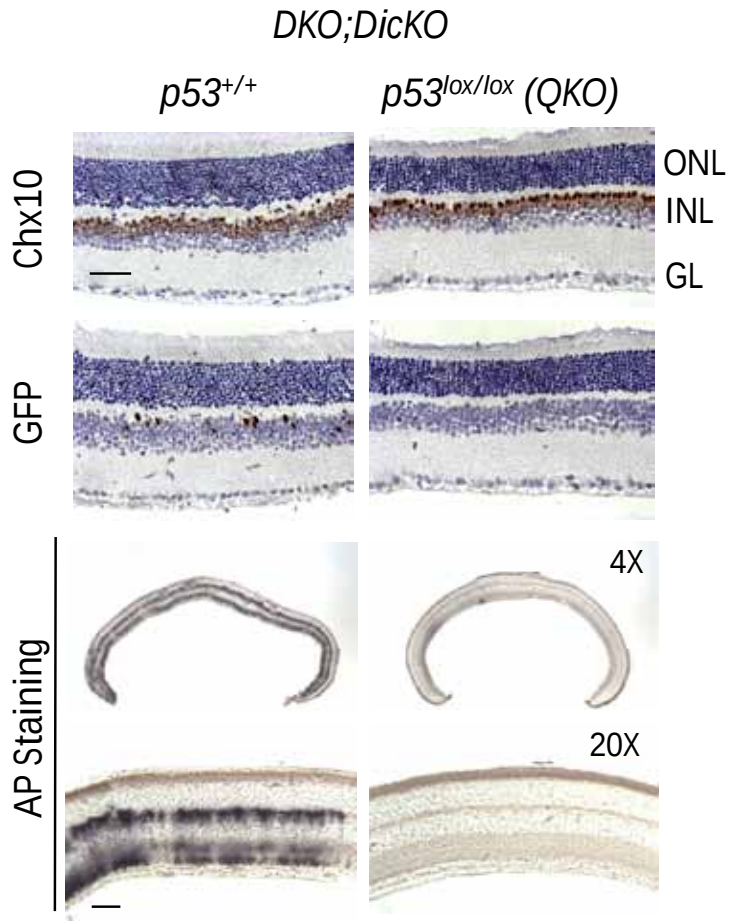

Figure 4.9: *Chx10/Rb1/p107*-mutant cells are lost upon concomitant inactivation of *Dicer1* and *p53*.
Chx10 and GFP immunostaining of *Chx10Cre; Rb1$^{lox/lox}$; p107$^{-/-}$; Dicer1$^{lox/lox}$; p53$^{+/+}$* (*DKO; DicKO; p53$^{+/+}$*) versus *Chx10Cre; Rb1$^{lox/lox}$; p107$^{-/-}$; p53$^{lox/lox}$; Dicer1$^{lox/lox}$* (*DKO; DicKO; p53$^{lox/lox}$* or *QKO*) retinae at P48. GFP-positive cells are only detected in p53 *wild-type* mice (upper panels). In AP-stained transverse retinal sections from adult mice with the indicated genotypes, regions of AP reporter activity were only detected in *p53 wild-type* mice (lower panels). The three retinal nuclear layers (GL: ganglion layer; INL: inner nuclear layer; ONL: outer nuclear layer) are indicated. Scale bars = 40µm. IHC stainings of the upper panel kindly provided by Irina Lambertz (CMG, UGent).

Additionally, the retinal architecture of adult *QKO* retinae was completely normal (Figure 4.10) and indistinguishable from *WT* retinae (to be compared with Figure 4.5) as Chx10, syntaxin, and calretinin stainings showed a normal disposition of the aforementioned cells. This opens the possibility that Chx10Cre/GFP-positive mutant cells were specifically eliminated or outcompeted during retinal development when *Dicer1* and *p53* were simultaneously inactivated. The mosaic expression level of the transgenic construct of the *Chx10Cre* transgenic mouse line could be the reason that the adult *QKO* retina in fact only consists of *WT* cells. Since only around 2% to 6% of all retinal cells expressed *Chx10Cre*

(Figure 4.4), an early elimination of these transgenic cells during retinal development might still be tolerated through compensation with the surrounding *WT* cells without compromising the morphology of the retina. To test this hypothesis we dissociated among others *DicKO*, *DKO; DicKO*; and *QKO* retinae and FACS-sorted the different cell suspensions for GFP positivity (Figure 4.4). Only in *DicKO* and *DKO; DicKO* (for both n = 3) GFP could be detected; this in around 2% of all cells analyzed. No GFP-positive cells could be found in *QKO* retinae (n = 5) at all.

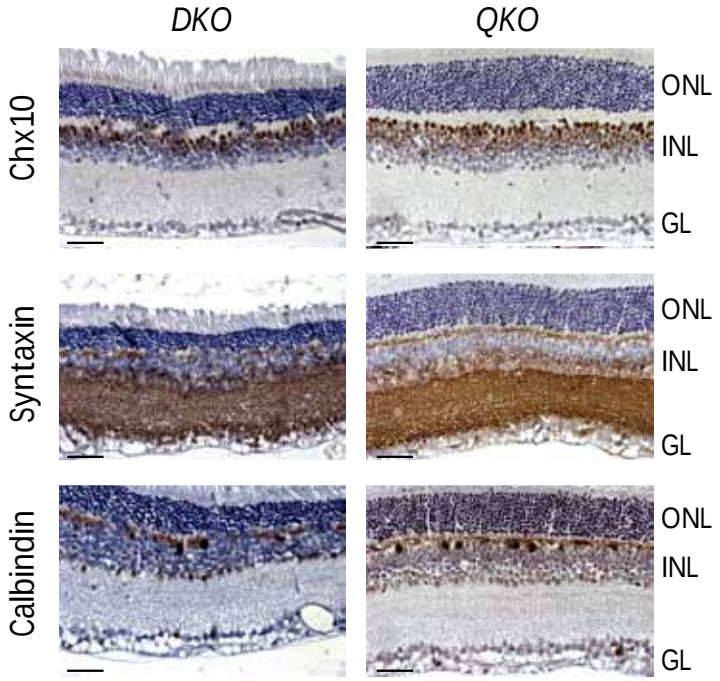

Figure 4.10: Retinogenesis is not affected in *QKO* mice.
Chx10, Syntaxin, and Calbindin immunostaining of *DKO* and *QKO* retinae at postnatal day 45 (P45). Scale bars = 40 µm (GL: ganglion layer; INL: inner nuclear layer; ONL: outer nuclear layer) Figure kindly provided by Irina Lambertz (CMG, UGent).

To prove that the retinae of *QKO* mice only consisted of *WT* cells, we analyzed the retina of *DKO; DicKO*, *DKO; p53KO*, and *QKO* mice for the recombination of the *Dicer1* and *p53* locus with the help of PCR-based genotyping (Figure 4.11). Consistent with our hypothesis we could neither detect the Cre-excised *Dicer1* nor *p53* locus in all *QKO* samples analyzed. Only the floxed locus of both genes was detectable. In contrast to the *QKO* samples the *DKO; DicKO* and *DKO; p53KO* samples clearly show PCR products of both the floxed and the excised *Dicer1* and *p53* genes. Due to the mosaicism in the *Chx10Cre* transgenic line and therefore presence of non-Cre-expressing cells, the non-excised (floxed) form of both *Dicer1* and *p53* genes was detected in *DKO; DicKO* and *DKO; p53KO*, respectively.

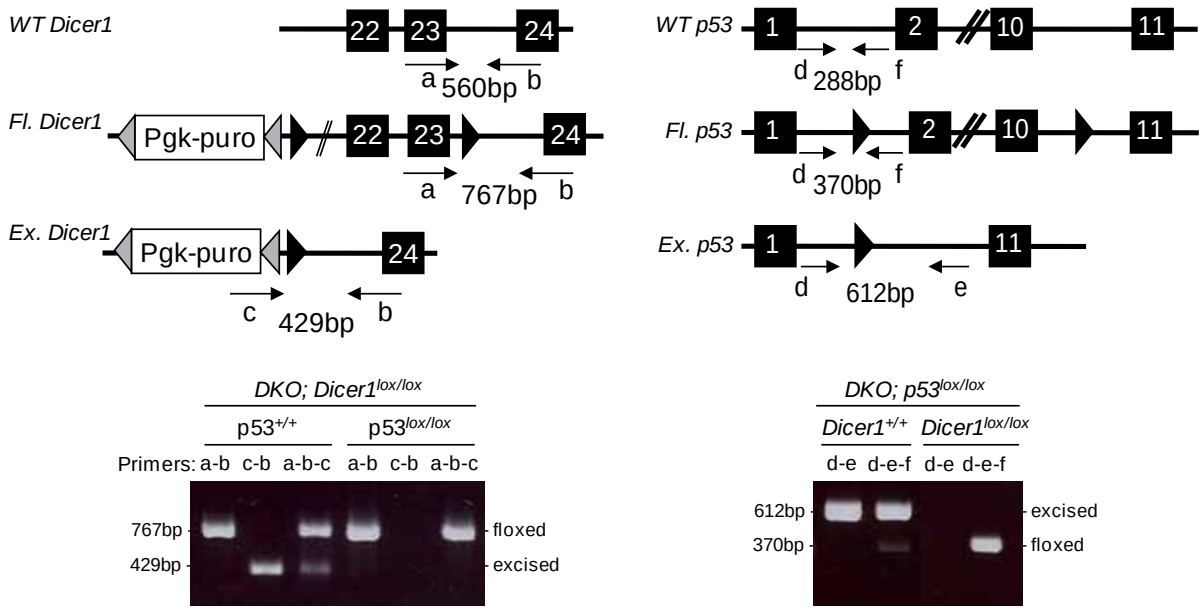

Figure 4.11: Depletion of the *Chx10Cre/Rb1/p107*-mutant cells in adult retinae upon co-inactivation of *p53* and *Dicer1*.

Schematic representation of the *Dicer1* and *p53 wild-type*, *floxed* and *Cre-excised* alleles (Top panels). DNA was prepared from P21 retinae of at least 5 mice with the indicated genotypes and examined by PCR using the primers depicted in the top panels. Representative PCRs are shown in the lower panels Figure kindly provided by Irina Lambertz (CMG, UGent).

This genotyping analysis therefore also excluded the possibility that *Chx10Cre; Rb1$^{lox/lox}$; p107$^{-/-}$; p53$^{lox/lox}$; Dicer1$^{lox/lox}$* mutant cells were present without expressing GFP or AP reporter genes at the age of P21.

4.3.2 *QKO* cells are still present during early retinogenesis

Another possible reason for the absence of mutant cells in *QKO* retinae might be a compromised Cre expression early during retinogenesis which would result in a lack of Cre-mediated recombination of each of the involved conditional knockout genes. Consequently, without recombination, the retina would only consist of *wild-type* cells.

To address this question we performed whole-mount AP stainings on QKO and control embryos of the age of around E12 (two left panels in Figure 4.12 A). As mentioned earlier, Chx10-positive retinal progenitor cells could be detected as early as day E9.5 (see Figure 4.2 and Rowan and Cepko 2004). Subsequently, the embryos were embedded in paraffin, 5µm sections were immunostained for GFP and analyzed with a confocal microscope (two right panels in Figure 4.12 A).

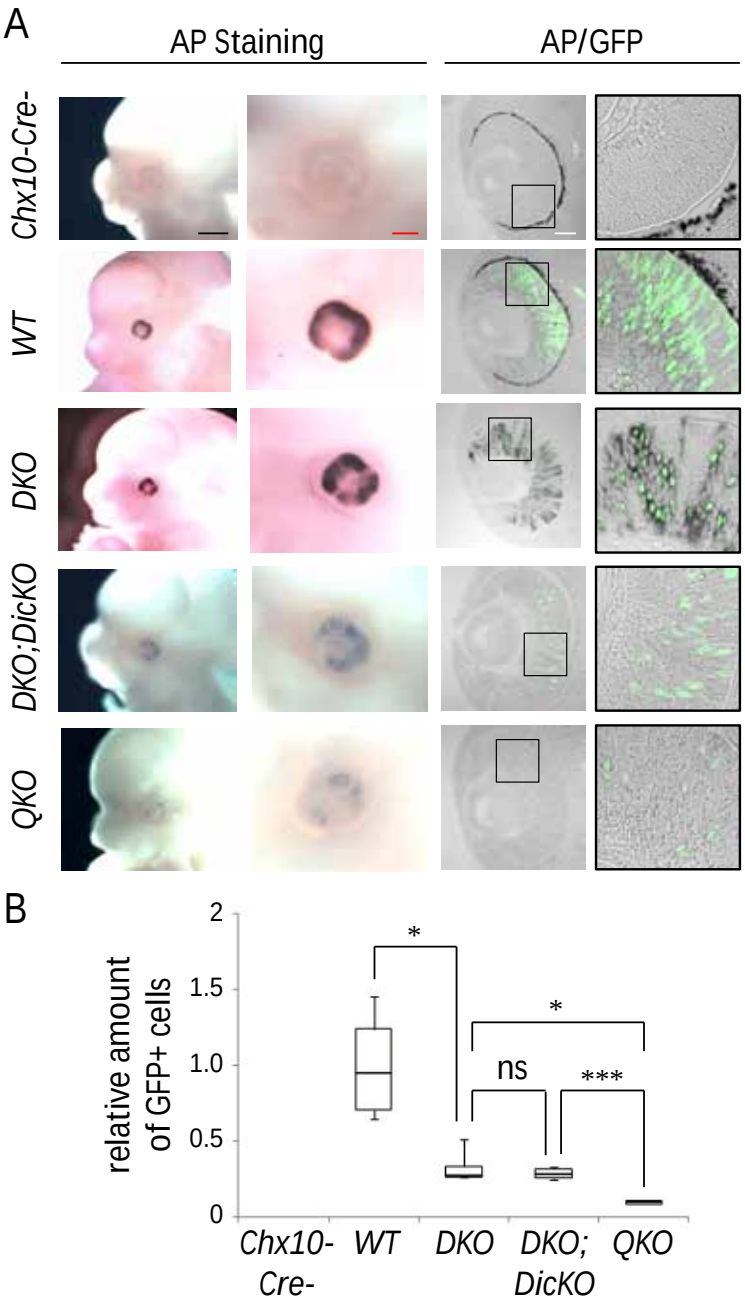

Figure 4.12: *QKO* cells are still present during early retinogenesis.

(A) *QKO* cells were detected during embryonic development. *Chx10Cre*-negative, *Chx10Cre*-positive *wild-type* (*WT*), *Chx10Cre; Rb1*$^{lox/lox}$*; p107*$^{-/-}$ (*DKO*), *Chx10Cre; Rb1*$^{lox/lox}$*; p107*$^{-/-}$*; Dicer1*$^{lox/lox}$; *p53*$^{+/+}$ (*DKO; DicKO*) and *Chx10Cre; Rb1*$^{lox/lox}$*; p107*$^{-/-}$*; Dicer1*$^{lox/lox}$; *p53*$^{lox/lox}$ (*QKO*) E12 embryos were whole-mount stained for AP reporter activity and subsequently sectioned for immunostaining against GFP. AP activity was observed in *QKO* embryos in distinct areas in the retina. Sections revealed these areas of AP reporter activity to be in retinal progenitor cells and not in retinal pigmented epithelium. GFP reporter expression, which was also detected, overlapped with areas of AP reporter activity in all but in *Chx10Cre-* embryos. Black scale bar = 1mm; red scale bar = 200µm; white scale bar = 10µm. (B) Box plot diagram showing the number of GFP-positive cells in E12 retinae from the experiment shown in A with indicated genotypes. The number of cells was evaluated by counting the number of GFP-positive cells in 5 microscopic fields of a comparable section from 3 different eyes of E12 embryos. *DKO* embryos showed significantly less GFP-positive cells in the retina compared to *WT* embryos (*P*-value from an unpaired two-tailed t-test < 0.05 (*)) but were not different when compared to *DKO; DicKO* embryos (ns). *QKO* embryos showed significantly less GFP-positive cells compared to *DKO* and *DKO; DicKO* embryos. *P*-values are < 0.05 (*) and < 0.001, (***) respectively.

We found that AP reporter activity could be detected in *WT*, *DKO*, *DKO; DicKO*, and *QKO* retina but, as expected, not in *Chx10Cre* negative embryos (two left panels in Figure 4.12 A). Also the immunofluorescence stainings against GFP revealed a similar staining pattern as the one of AP in all samples analyzed (two right panels in Figure 4.12 A), suggesting that both AP and GFP and therefore the recombinase Cre are expressed in *WT*, *DKO*, *DKO; DicKO*, and *QKO* retinae.

Thus, we can conclude that Cre expression by itself is not compromised in *QKO* retinae even during early retinogenesis and is therefore not the reason for the absence of GFP/AP staining in adult retinae.

Quantification of the GFP signal by counting the amount of GFP-positive cells per microscopic field revealed that the number of mutant cells in *QKO* retinae was significantly reduced compared to *DKO* (*P*-value < 0.05 (*), Figure 4.12 B) or *DKO; DicKO* retinae (*P*-value < 0.001 (***), Figure 4.12 B). This suggests that some of the *QKO* mutant cells might already have been counter-selected and/or removed in the time window between days E9.5 and E12.

4.3.3 Synergistic induction of apoptotic cell death by inactivation of *Dicer1* and *p53*

To explain the discrepancy of existing *QKO* mutant retinal cells at embryonic day E12 and the absence in adult *QKO* retinae, we looked for signs of apoptosis in the above-mentioned E12 embryos and two other embryonic stages (E13.5 and E14.5). More specifically, we performed an immunofluorescence co-staining for GFP and the activated form of caspase-3 (Casp-3*) as a marker for caspase-dependent apoptosis to visualize *QKO* mutant cells undergoing apoptosis (Figure 4.13). Casp-3* staining only overlapped with very few GFP-positive cells (~2%) in *QKO* retinae at the embryonic stage E12. Neither *Chx10Cre* negative, *WT*, nor *DKO; DicKO* retina showed any GFP/Casp-3*-double positive cells. Importantly, neither did the later embryonic stages E13.5 and E14.5 in all genotypes analyzed reveal any GFP/Casp-3*-double positive cells.

With these findings, we conclude that caspase-dependent apoptosis might be one mechanism via which the *QKO* mutant cells are eliminated shortly after the transgenic GFP-Cre protein is expressed in the retinal cells at the embryonic age of E9.5. Hence, *Dicer1* is required for the survival of *Rb1/p107*-deficient retinal progenitor cells in which *p53* is

additionally lost. Early elimination during retinogenesis would therefore be tolerated regarding the intact retinal architecture later in life.

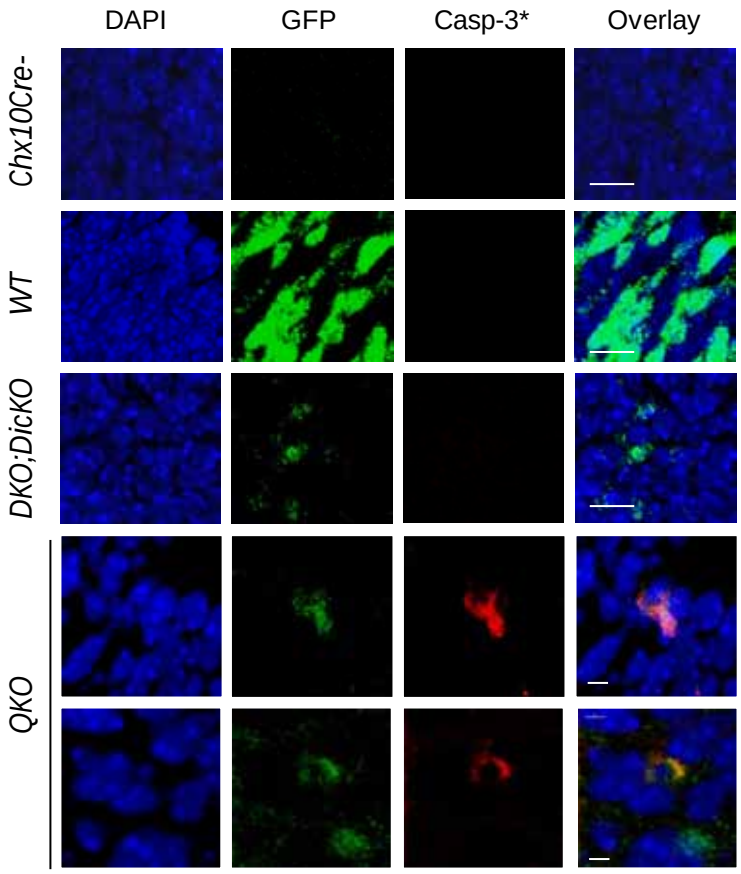

Figure 4.13: Synergistic induction of apoptotic cell death by co-inactivation of *Dicer1* and *p53*.
GFP-positive retinal progenitor cells (green) undergoing apoptosis (as detected by cleaved caspase-3-positivity (Casp-3*), red) were seen in E12 *QKO*, but not in *Chx10Cre-*, *Chx10Cre+* (*WT*), nor *DKO; DicKO* embryos. Scale bars = 2 µm.

4.3.4 Synthetic lethality of *Dicer1* and *p53* depends on *Rb1/p107*-deficiency

Next, we tested whether simultaneous inactivation of *Dicer1* and *p53* by itself could also lead to a loss of retinal cells. To do so, we performed an AP staining on retinae of adult *Chx10Cre; p53*$^{lox/lox}$*; Dicer1*$^{lox/lox}$ (*p53KO; DicKO*) mice (Figure 4.14 A). Positive AP stainings in the *p53KO; DicKO* mice suggest that the synthetic lethality of *Dicer1* and *p53* depends on *Rb1/p107*-deficiency. In other words, inactivation of *Dicer1* and *p53* are only synthetic lethal in cells which are subject to oncogenic stress.

To ensure complete recombination of both loci, *Dicer1* and *p53*, in the *Chx10Cre*-positive *p53KO; DicKO* retinal mutant cells, we FACS-sorted cell suspensions of dissociated *p53KO; DicKO* mouse retinae for GFP-positivity and performed recombination PCRs for

both loci on the sorted GFP-positive and control cells (Figure 4.14 B). Since we could exclusively detect the excised products of both *Dicer1* and *p53* loci in the GFP-positive cells, we can conclude that Cre-mediated recombination of both loci was complete and that all AP/GFP-positive retinal mutant cells in *p53KO; DicKO* mice were indeed *Dicer1* and *p53*-deficient.

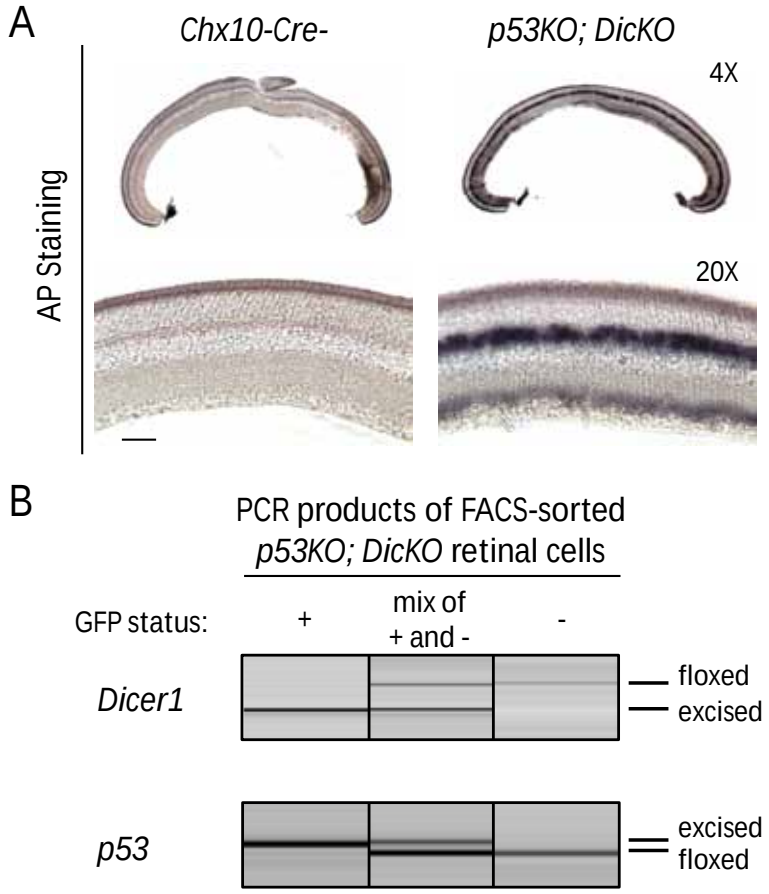

Figure 4.14: Inactivation of *Dicer1* and *p53* is only synthetic lethal in *Rb1/p107*-deficient cells.
(A) AP-stained transverse retinal sections from adult mice (P21) with the indicated genotypes. Regions of AP reporter activity are detected in *Chx10Cre; p53*$^{lox/lox}$; *Dicer1*$^{lox/lox}$ (*p53KO; DicKO*) and not in control *Chx10Cre*-negative retinae. Scale bar = 40µm. (B) Recombination PCRs for the *Dicer1* and *p53* locus show a complete recombination of both loci in retinae of *Chx10Cre; p53*$^{lox/lox}$*; Dicer1*$^{lox/lox}$ (*p53KO; DicKO*) mice. Only the excised PCR product of both loci is detectable in FACS-sorted GFP-positive (GFP +) *p53KO; DicKO* mutant cells, whereas both controls – a 1:1 mixture of GFP-positive and GFP-negative (GFP +/-) and GFP-negative cells (GFP -) – show either the floxed and the excised or only the floxed PCR products of both loci. FACS sorting and sample preparation was performed as schematically shown in Figure 4.6 A.

4.3.5 *QKO* mice do not develop retinoblastoma due to the synthetic lethal interaction between *Dicer1* and *p53*

Taking together the above mentioned data, *QKO* mice should not develop any retinoblastoma, since the simultaneous inactivation of *Dicer1 and p53* in retinal progenitor cells on *Rb1/p107*-deficient background (*QKO*) leads to loss of those mutant cells, as shown in the previous sections. Hence, without mutant cells, the resulting adult retinae of those mice would completely consist of *wild-type* cells (except for the *p107* gene which will be null, even without Cre-expression, since it is a direct knockout allele and no conditional floxed allele, as in all other transgenic mouse lines used in this study), which would not allow formation of retinoblastoma.

As expected, none of the 78 *QKO* mice observed developed visible retinoblastoma after more than 2 years (Figure 4.15) whereas *DKO; p53KO* mice showed a very aggressive and nearly 100% penetrant phenotype with hyperproliferative lesions which ultimately lead to retinoblastoma formation within an average time frame of 100 days (Figure 4.8 and Figure 4.15). Such dysplastic lesions were also observed in retinae of *DKO; DicKO* mice which did not develop retinoblastoma. The important difference between the absence of retinoblastoma formation in *QKO* and *DKO; DicKO* mice is, that the pool of *Rb1/p107*-mutant retinoblasts was completely eliminated in *QKO* mice whereas it was still present in *DKO; DicKO* mice. Eventually, there might be a theoretical chance that those *Rb1/p107*-mutant cells present in *DKO; DicKO* mice give rise to severely delayed retinoblastoma (further discussed in section 5.1).

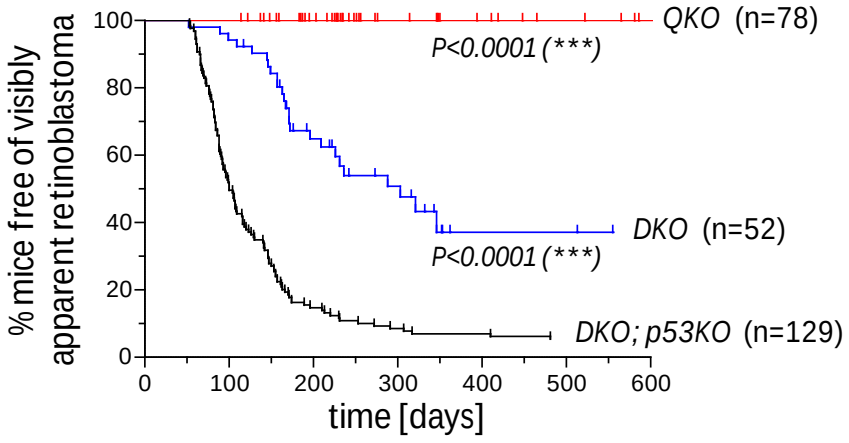

Figure 4.15: *Dicer1* is required for retinoblastoma formation.
Kaplan-Meier curve showing the time to first observation of externally visible retinoblastoma. This time was markedly decreased in *Chx10Cre; Rb1$^{lox/lox}$; p107$^{-/-}$; p53$^{lox/lox}$* (*DKO; p53KO*) mice relative to *Chx10Cre; Rb1$^{lox/lox}$; p107$^{-/-}$* (*DKO*) littermates. *Chx10Cre; Rb1$^{lox/lox}$; p107$^{-/-}$; p53$^{lox/lox}$; Dicer1$^{lox/lox}$* (*QKO*) mice did not develop tumors (logrank Mantel-Cox test, P<0.0001) up to a observation period of 2 years (data shown up to 600 days).

4.4 The *miR-17~92* cluster is overexpressed in retinoblastoma

The miRNA screenings and their analysis shown in the following section were performed by Pieter M. All human retinoblastoma samples and controls for this miRNA analysis were prepared by Johannes S. and Alexander S. The aCGH analysis was performed by Candy K.

Based on our data so far, *Dicer1* might look like a promising pharmacological target to specifically eradicate *p53*-deficient tumor cells, while leaving *p53 wild-type* cells unharmed. But as our lab previously showed (Lambertz et al. 2010), partial inactivation of *Dicer1* leads to more rapid and more aggressive tumor formation as compared to *Dicer1 wild-type* tumor cells. We therefore concluded that *Dicer1* functions as a haploinsufficient tumor suppressor. Targeting *Dicer1* through chemotherapy or other approaches of downregulating its enzymatic activity might therefore even worsen the tumor phenotype instead of eliminating the tumor cells. Thus, another approach might be necessary to find "drugable" synthetic lethal interactors of p53 for cell-specific elimination of tumor cells.

Instead of targeting *Dicer1* directly, a set of miRNAs of which processing depends on Dicer1, and are therefore downstream of Dicer1, might be a better and more specific pharmacological target to remove tumor cells with an impaired p53 pathway. To find such a set of miRNAs, we profiled miRNA expression in P21 retinae from *Chx10Cre*-negative (*WT*) and *DKO* mice and compared it to the profiling results of tumor tissue from *DKO; p53KO* mice – in collaboration with the labs of Frank Speleman (CMG, UGent), Johannes Schulte and Alexander Schramm (both UK Essen, Germany). A set of 102 miRNAs could be identified as significantly upregulated in the *DKO; p53KO* tumors compared to retinae samples of *WT* mice (Figure 4.16 A and Table S 1).

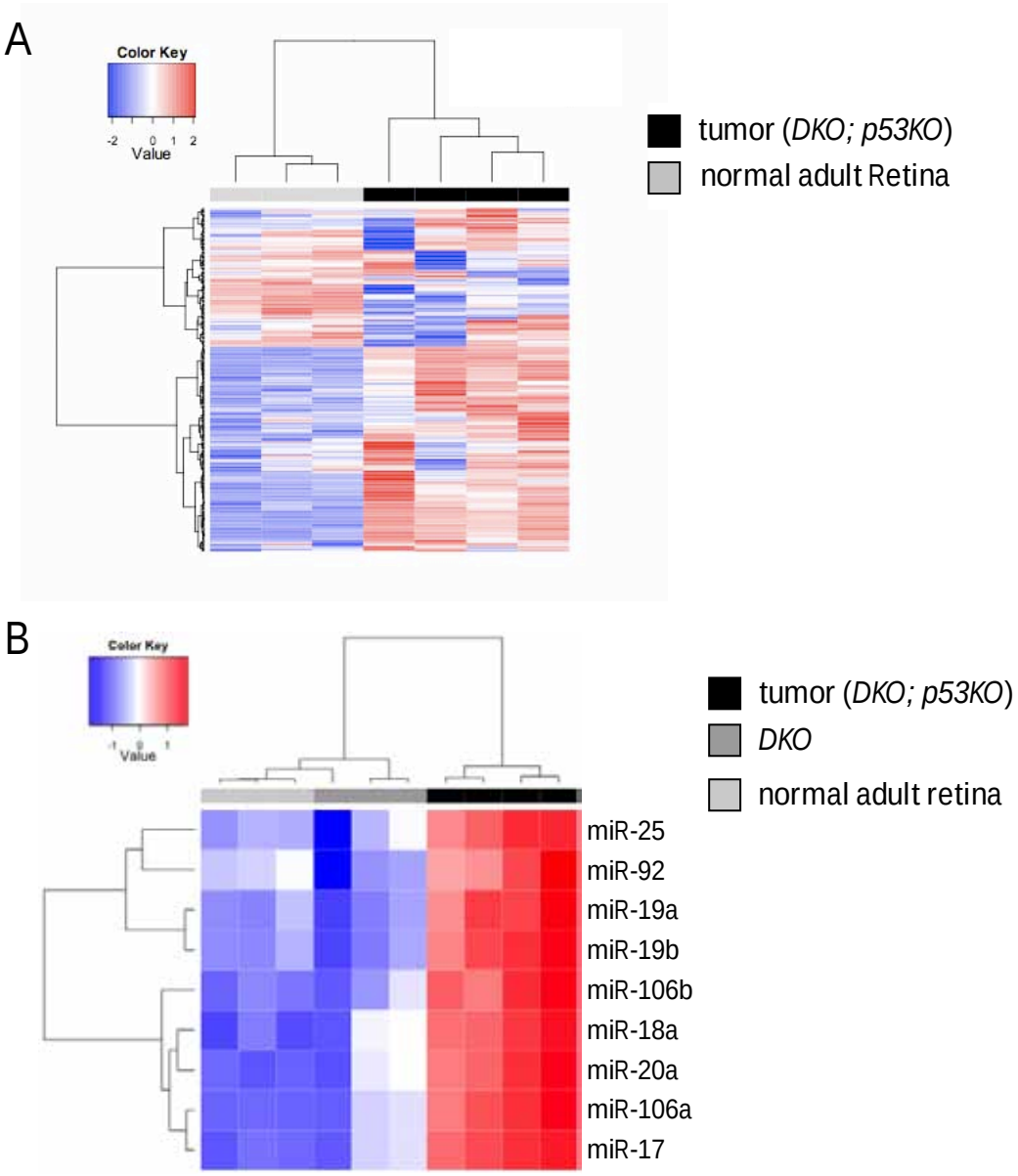

Figure 4.16: miRNA profiling of mouse *DKO; p53KO* tumors.
(A) Heat map of differentially expressed miRNAs in 3 normal adult mouse retinae (*Chx10Cre*-negative mice, light grey) and 4 mouse *DKO; p53KO* tumors (black). (B) Heat map of the *miR-17~92* and paralog clusters in 3 normal mouse retinae (*Chx10Cre*-negative mice, light grey), in 3 retinae from *DKO* mice (dark grey), and 4 tumors from *DKO; p53KO* mice (black). Figure kindly provided by Pieter Mestdagh (CMG, UGent).

To narrow down the list of putative 102 miRNAs which were upregulated in mouse tumors, we also profiled the miRNA expression in 29 different human primary retinoblastomas to be able to correlate the human data with the previously mentioned mouse data set. When comparing the 29 human retinoblastoma samples with 6 normal human retinae, we found 68 miRNAs which were significantly upregulated in the human retinoblastoma samples (Figure 4.17 A, Table S 2)

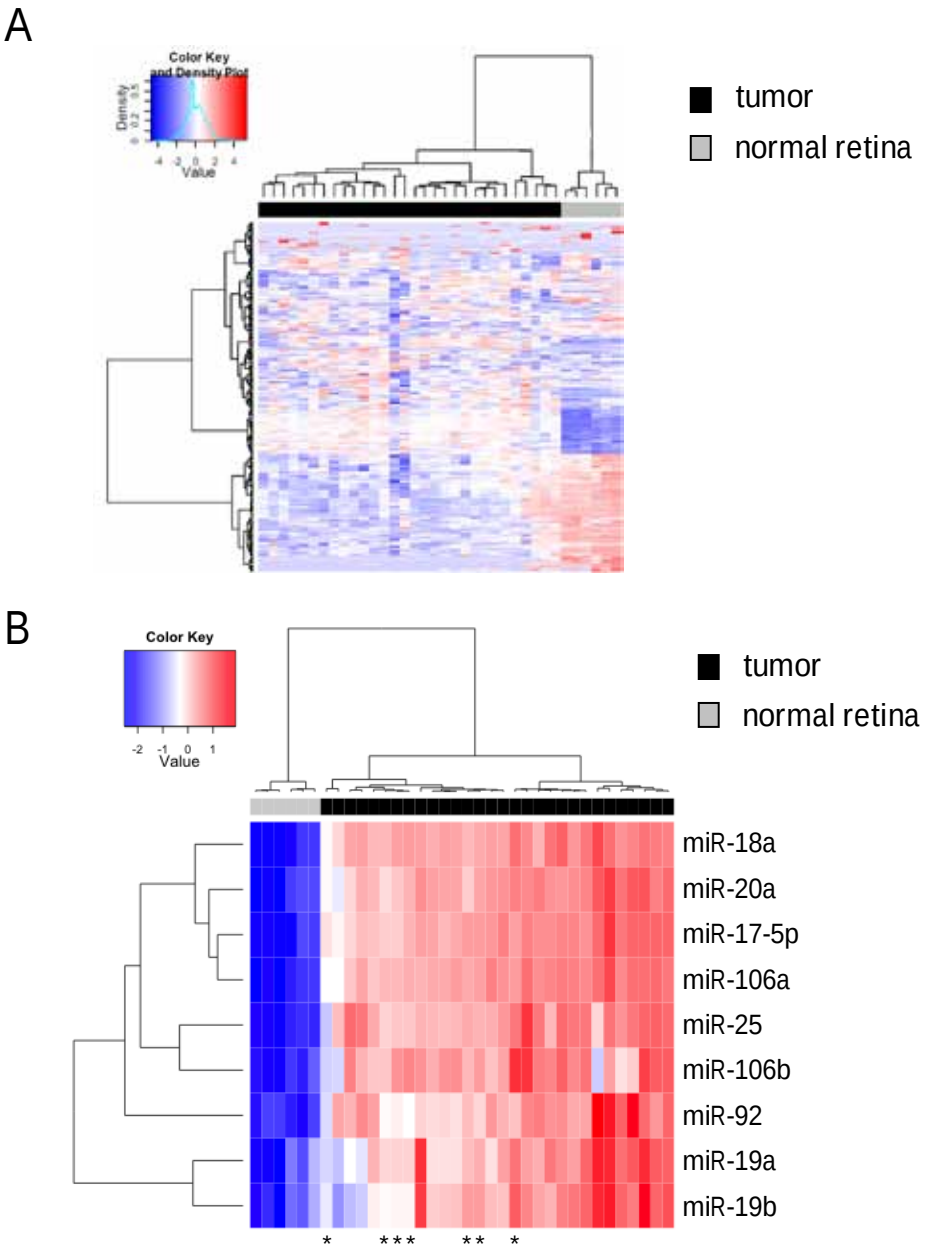

Figure 4.17: miRNA profiling of human tumors.
(A) Heat map of differentially expressed miRNAs in 6 normal adult retinae (light grey) and 29 primary tumors (black). (B) Heat map of the *miR-17~92* and paralog clusters in 6 normal adult retinae (light grey) and 29 primary tumors (black). (*) indicates patients with *Rb1* germline mutations. Figure kindly provided by Pieter Mestdagh (CMG, UGent).

Comparing the miRNA expression profile across the two species, we could identify 25 miRNAs that were upregulated in both mouse and human tumors (Table 4.1 and Table S 3).

Table 4.1: List of miRNAs that are upregulated both in mouse and human tumors.

From a list of 102 in tumors upregulated miRNAs in mice and 68 miRNAs in human, a list of 25 miRNAs commonly upregulated in both species was compiled. miRNAs in red belong to the *miR-17~92* or the two paralogue clusters.

miRNAs	Murine tumor vs. normal retina	Human tumor vs. normal retina
miR-449b	128.99	16.70
miR-449	102.68	155.43
miR-18a	72.28	79.08
miR-106a	51.89	22.47
miR-17-5p	47.58	26.31
miR-20b	45.10	14.16
miR-20a	36.49	26.48
miR-93	30.59	23.38
miR-19b	10.95	4.49
miR-19a	9.93	6.89
miR-186	7.49	1.85
miR-18a*	7.46	63.91
miR-34b	7.06	2.18
miR-17*	7.05	2.95
miR-106b	6.48	10.64
miR-155	5.93	2.13
miR-34c	5.71	11.48
miR-15b	5.45	26.18
miR-301	4.17	7.43
miR-195	3.36	2.86
miR-25	3.30	15.64
miR-16	3.03	7.01
miR-92	2.94	6.41
miR-532	2.12	3.49
miR-130a	1.71	2.25

Interestingly, 12 of the commonly upregulated miRNAs were members of the oncogenic *miR-17~92* and *miR-106b~25/miR-106a~363* paralog clusters (van Haaften and Agami 2010).

Consistent with the discovery of the putative important role of the *miR-17~92* and paralog clusters in retinoblastoma, hierarchical clustering of all retinoblastoma samples and normal retinae based on miRNA expression also identified 9 of the highly upregulated miRNAs in all mouse and human tumor samples analyzed as members of these clusters (Figure 4.16 B, Figure 4.17 B, Figure 4.18).

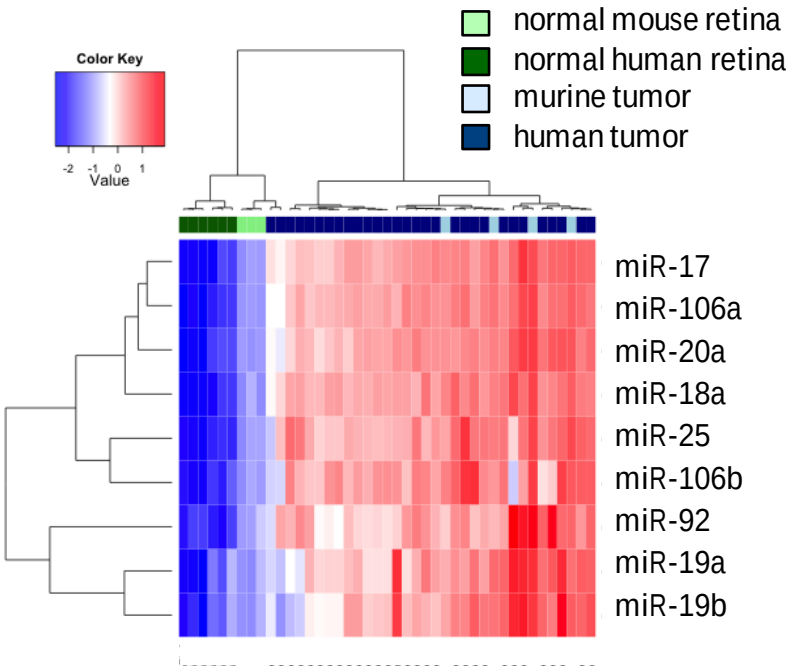

Figure 4.18: The *miR-17~92* cluster is overexpressed in retinoblastoma.
Heat map showing the overexpression of the *miR-17~92* and paralog clusters in 4 mouse *DKO; p53KO* tumors (light blue), and 30 different primary human retinoblastoma (dark blue) when compared to normal mouse retina (*Chx10Cre*-negative mice, light green) and normal human retina (dark green). Figure kindly provided by Pieter Mestdagh (CMG, UGent).

To explore the potential causes of miRNA deregulation in human retinoblastoma, we looked for genomic aberrations using a 44K oligonucleotide array which had been specifically designed to include regions harboring miRNA genes. In addition to identifying previously reported retinoblastoma-associated genomic aberrations (1q gain and 6p22 gain were frequently seen in our cohort), we found copy number gains, including the *miR-17~92* locus, which lies on chromosome 13, as well as whole or partial chromosome 13 gains (Figure 4.19). *miR-17~92* copy number gains, which importantly did not include the closely linked *RB1* locus, were seen in 17% of the patients (5 out of 29 cases analyzed). There was evidence of focal amplification in 1 out of 29 cases analyzed (16.450 +/- 1.322 copies per cell). Moreover, while the *RB1* locus was deleted in 21% of cases (6/29), this deletion never included the closely linked *miR-17~92* locus. This analysis therefore indicates that upregulation of the *miR-17~92* cluster is, at least in a subset of retinoblastomas, a direct consequence of increased gene copy number. Since transcription of *miR-17~92* is positively regulated by the E2Fs (Aguda et al. 2008), which are themselves upregulated upon *Rb1* loss, and negatively regulated by p53 (Yan et al. 2009), deregulation of their transcriptional activities may also account for *miR-17~92* overexpression.

Regardless of the underlying mechanism, our data demonstrate that the *miR-17~92* cluster is overexpressed in 100% of retinoblastomas analyzed. These findings are consistent with the recent demonstration that enforced *miR-17~92* overexpression in mice cooperates with *Rb1* pathway mutations to promote retinoblastoma (Conkrite et al. 2011).

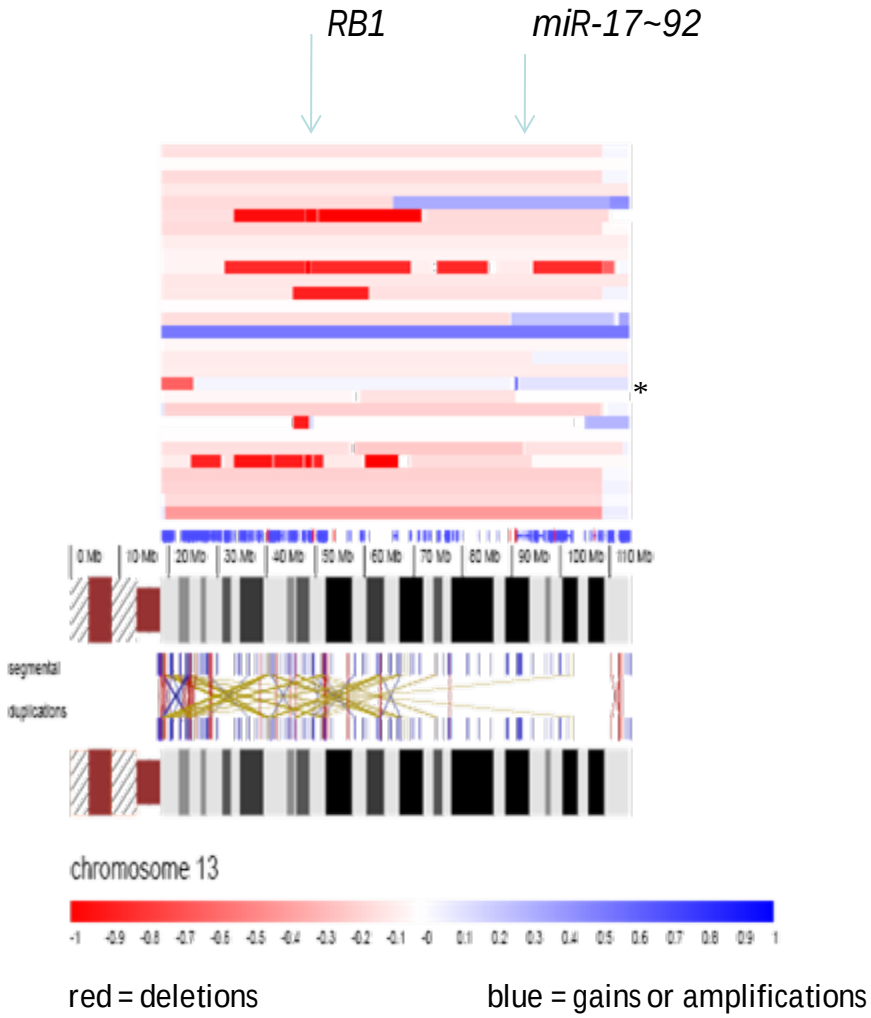

Figure 4.19: CGH Analysis of 30 human retinoblastomas.
Copy number status of the *RB1* and *miR-17~92* locus on chromosome 13 for 30 retinoblastoma tumor samples. Deletions are marked in red, amplifications and gains in blue. * marks one tumor sample exhibiting a focal amplification of the *miR-17~92* locus (16,450 +/- 1,322 copies per cell as validated and determined by quantitative PCR analysis). Figure kindly provided by Candy Kumps (CMG, UGent).

4.5 *miR-17~92* phenocopies *Dicer1 as* synthetic lethal partner of *p53*

The cell culture work with the Y79 retinoblastoma cell lines shown in the following section was performed by Frederic C. The miRNA expression analysis in different human retinoblastoma cell lines and controls was done by Alexander S. and Johannes S. Western blot analysis of these cell lines was done by Aart G. J.

4.5.1 *miR-17~92* deficiency restricts retinoblastoma development in mice

Once we discovered the importance of the *miR-17~92* cluster in retinoblastoma due to overexpression in 100% of all cases analyzed, we wanted to test the relevance of a conditional loss of *miR-17~92* in *DKO; p53KO* mice which are prone to develop rapid and aggressive retinoblastoma. The synthetic lethality between *Dicer1* and *p53* could be, at least partly, mediated by *miR-17~92*.

Therefore we crossed the already described conditional *miR-17~92*$^{lox/lox}$ knockout mice (Ventura et al. 2008) into the tumor prone *Chx10Cre; Rb1*$^{lox/lox}$*; p107*$^{-/-}$*; p53*$^{lox/lox}$ (*DKO; p53KO*) background to generate *Chx10Cre; Rb1*$^{lox/lox}$*; p107*$^{-/-}$*; p53*$^{lox/lox}$*; miR-17~92*$^{lox/lox}$ (*DKO; p53KO; miR-17~92KO*) mice. Subsequently, we assessed the appearance of retinoblastoma formation in those mice every week. Strikingly, none of the *DKO; p53KO; miR-17~92KO* mice (*DKO; p53KO; miR-17~92*$^{lox/lox}$ in the graph) (19 out of 19) developed retinoblastoma in an observation period of up to 300 days. In contrast, 88% of the *DKO; p53KO* (*DKO; p53KO; miR-17~92*$^{+/+}$ in the graph) mice (15 out of 17) developed retinoblastoma by 125 days of age (Figure 4.20). Altogether, the median age of visibly apparent retinoblastoma of the *DKO; p53KO* mice was 77 days.

While homozygous loss of *miR-17~92* in *DKO; p53KO* mice completely blocked tumor formation, loss of one allele of *miR-17~92* on a *DKO; p53KO* background delayed tumor formation significantly (Figure 4.20 A) compared to *DKO; p53KO* mice. 12 out of 20 (60%) *Chx10Cre; Rb1*$^{lox/lox}$*; p107*$^{-/-}$*; p53*$^{lox/lox}$*; miR-17~92*$^{lox/+}$ (*DKO; p53KO; miR*$^{lox/+}$) mice developed either uni- or bilateral retinoblastoma with a median time of tumor onset of 124 days of age (n=20) (Figure 4.20 C). Additionally, heterozygous loss of *miR-17~92* also reduced the aggressiveness of retinoblastoma development compared to *DKO; p53KO* mice. Whereas 87% of tumor-bearing *DKO; p53KO* mice developed bilateral retinoblastoma, only 42% of *DKO; p53KO; miR*$^{lox/+}$ mice (Figure 4.20 B) did so.

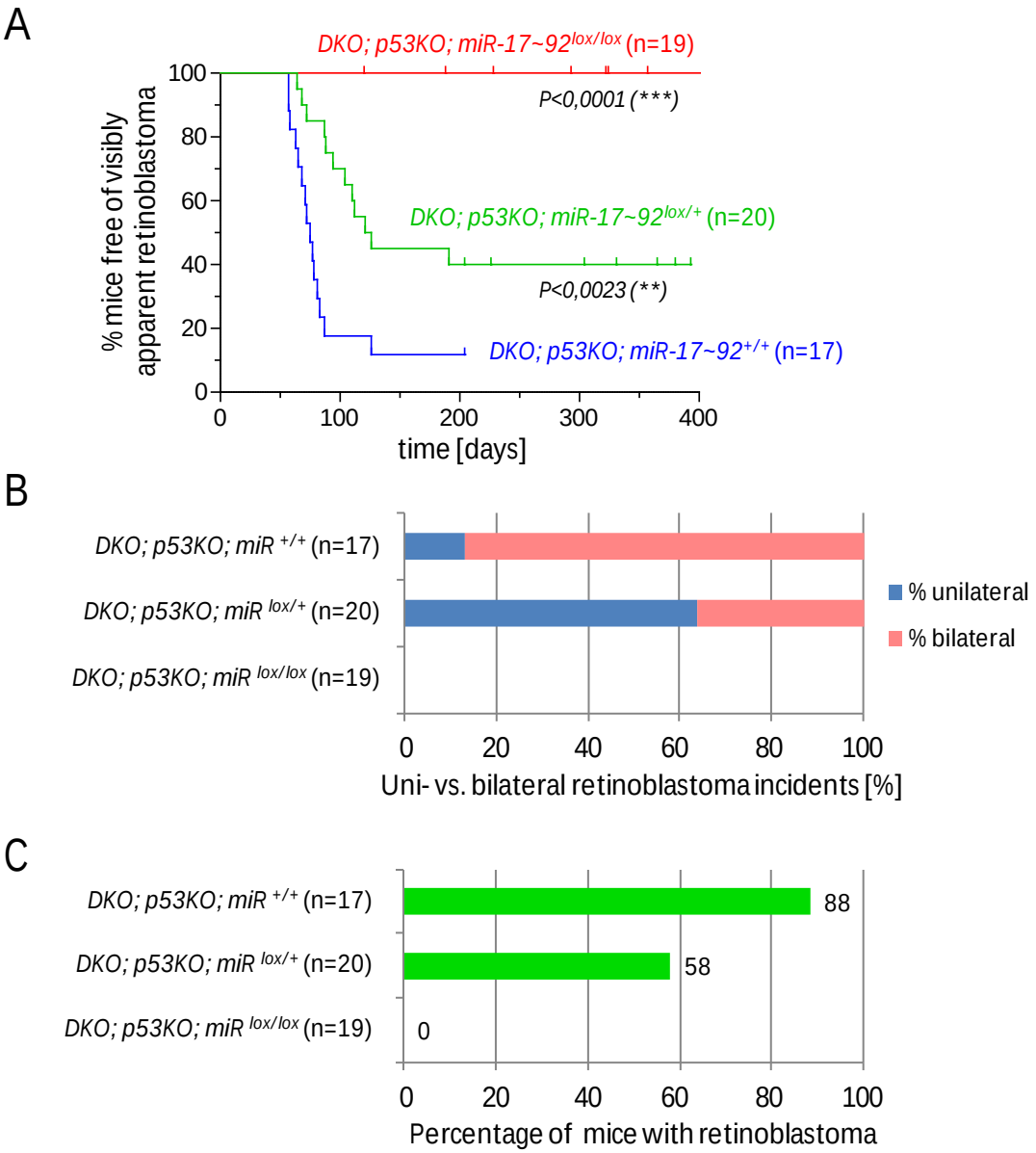

Figure 4.20: *miR-17~92* deficiency prevents retinoblastoma development in mice.
(A) Kaplan-Meier plot analysis of the time to first observation of externally visible retinoblastoma. 13 out of 17 (87%) *Chx10Cre; Rb1$^{lox/lox}$; p107$^{-/-}$; p53$^{lox/lox}$; miR-17~92$^{+/+}$* (*DKO; p53KO; miR$^{+/+}$*) mice developed aggressive and invasive bilateral retinoblastoma with a median time of tumor onset of 75 days of age (n=17). 2 out of these 16 mice develop unilateral retinoblastoma. None out of 19 *Chx10Cre; Rb1$^{lox/lox}$; p107$^{-/-}$; p53$^{lox/lox}$; miR-17~92$^{lox/lox}$* (*DKO; p53KO; miR$^{lox/lox}$*) mice developed retinoblastoma up to a 400-days observation period. 12 out of 20 (60%) *Chx10Cre; Rb1$^{lox/lox}$; p107$^{-/-}$; p53$^{lox/lox}$; miR-17~92$^{lox/+}$* (*DKO; p53KO; miR$^{lox/+}$*) mice developed either uni- or bilateral retinoblastoma with a median time of tumor onset of 124 days of age (n=20). The Kaplan-Meier curve of latter mice is significantly different from the two other curves, *DKO; p53KO; miR$^{+/+}$* and *DKO; p53KO; miR$^{lox/lox}$*.(P < 0.0001 (***) and P = 0.0023 (**) respectively, determined with a logrank Mantel-Cox test). (B) Distribution of uni- and bilateral retinoblastoma in *DKO; p53KO* mice with different *miR-17~92* status. (C) Percentage of tumor bearing mice with the genotype *DKO; p53KO* with different *miR-17~92* status.

4.5.2 Simultaneous loss of *miR-17~92* and *p53* on a *Rb1/p107*-deficient background is synthetic lethal

To be able to explain the absence of tumor formation in the *DKO; p53KO; miR-17~92KO* mice, we stained adult retinae of various genotypes for AP reporter activity. Positive AP staining could be detected in retinae of *Chx10Cre; miR-17~92$^{lox/lox}$* (*miR-17~92KO*) and *Chx10Cre; Rb1$^{lox/lox}$; p107$^{-/-}$; miR-17~92$^{lox/lox}$* (*DKO; miR-17~92KO*) mice, but not in retinae of *DKO; p53KO; miR-17~92KO* mice (Figure 4.21).

We therefore conclude, that the absence of retinoblastoma formation in the *DKO; p53KO; miR-17~92KO* mice is due to the synthetic lethal interaction between *miR-17~92* and *p53*. Hence, loss of *miR-17~92* phenocopies the loss of *Dicer1*. Furthermore, as with *Dicer1*, simultaneous loss of *miR-17~92* and *p53* is only synthetic lethal on a *Rb1/p107*-deficient background, since AP positive mutant retinal cells can also be detected in *Chx10Cre; p53$^{lox/lox}$*; *miR-17~92$^{lox/lox}$* (*p53KO; miR-17~92KO*) adult retinae (Figure 4.21).

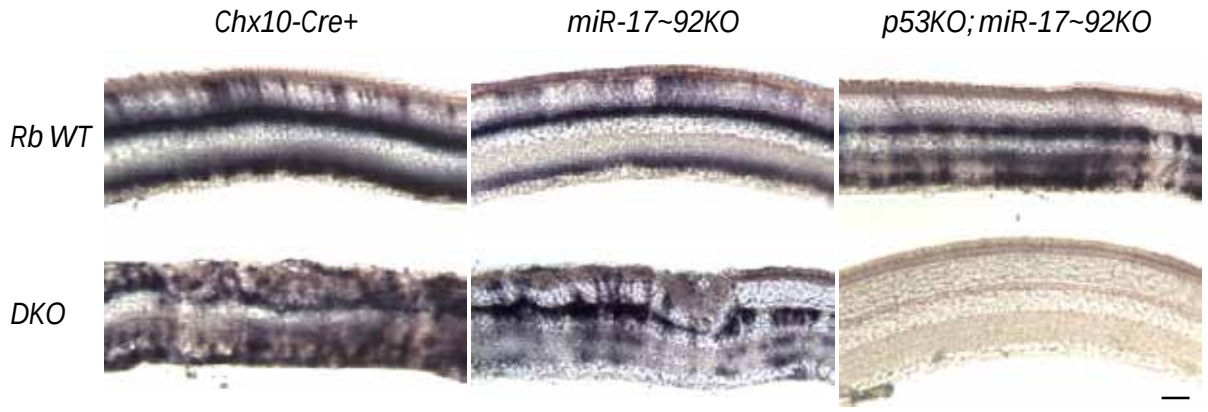

Figure 4.21: Simultaneous loss of *miR-17~92* and *p53* on a *Rb1/p107*-deficient background leads to synthetic lethality in the mutant cells.

AP-stained transverse retinal sections (40µm) from adult mice with the indicated genotypes. Regions of AP reporter activity are only detected in *Chx10Cre* (*Chx10-Cre+*), *Chx10Cre; miR-17~92$^{lox/lox}$* (*miR-17~92KO*), *Chx10Cre; p53$^{lox/lox}$*; *miR-17~92$^{lox/lox}$* (*p53KO; miR-17~92KO*), *Chx10Cre; Rb1$^{lox/lox}$; p107$^{-/-}$* (*DKO*), and *Chx10Cre; Rb$^{lox/lox}$; p107$^{-/-}$; miR-17~92$^{lox/lox}$* (*DKO; miR-17~92KO*) but not in *Chx10Cre; Rb1$^{lox/lox}$; p107$^{-/-}$; p53$^{lox/lox}$; miR-17~92$^{lox/lox}$* (*DKO; p53KO; miR-17~92KO*) retinae. Scale bar = 40µm.

Ultimately, our data suggests, that *miR-17~92*, as is the case with *Dicer1*, is dispensable for normal retinogenesis but is required for aggressive and invasive retinoblastoma development in *Rb1/p107/p53*-deficient retinae, since loss of *miR-17~92* on this background leads to synthetic lethality with *p53*.

4.5.3 The synthetic lethal interaction between *p53* and *miR-17~92* depends on the genetic background

In order to generate *DKO; p53KO; miR-17~92KO* mice, a total of 16 breeding pairs were set up. Of the 16 breeding pairs, 9 gave offspring to at least one *DKO; p53KO; miR-17~92KO* mouse per breeding pair. In total, 19 mice were monitored for visibly apparent retinoblastoma over an observation period of up to 400 days (red lined curve in Figure 4.22 A). As previously described (section 4.5.1, page 68 and Figure 4.20 A), none of the mice of this group developed retinoblastoma. We explained the phenotype with our findings that simultaneous loss of p53 and *miR-17~92* on a *Rb1/p107*-deficient background leads to synthetic lethality and therefore eradication of all mutant cells (section 4.5.2, page 70). Further on, this group will be referred to as the cancer-resistant group.

Surprisingly, 7 out of 16 breeding pairs gave birth to a group of 36 mice of which 23 mice (64%, Figure 4.22 C) developed either uni- or bilateral retinoblastoma with a median time of tumor onset of 137 days of age (curve with red dashed line in Figure 4.22). A majority of 18 retinoblastoma incidents (78%) were unilateral and only 5 (22%) were bilateral (Figure 4.22 B). From now, this group will be referred to as the non cancer-resistant group.

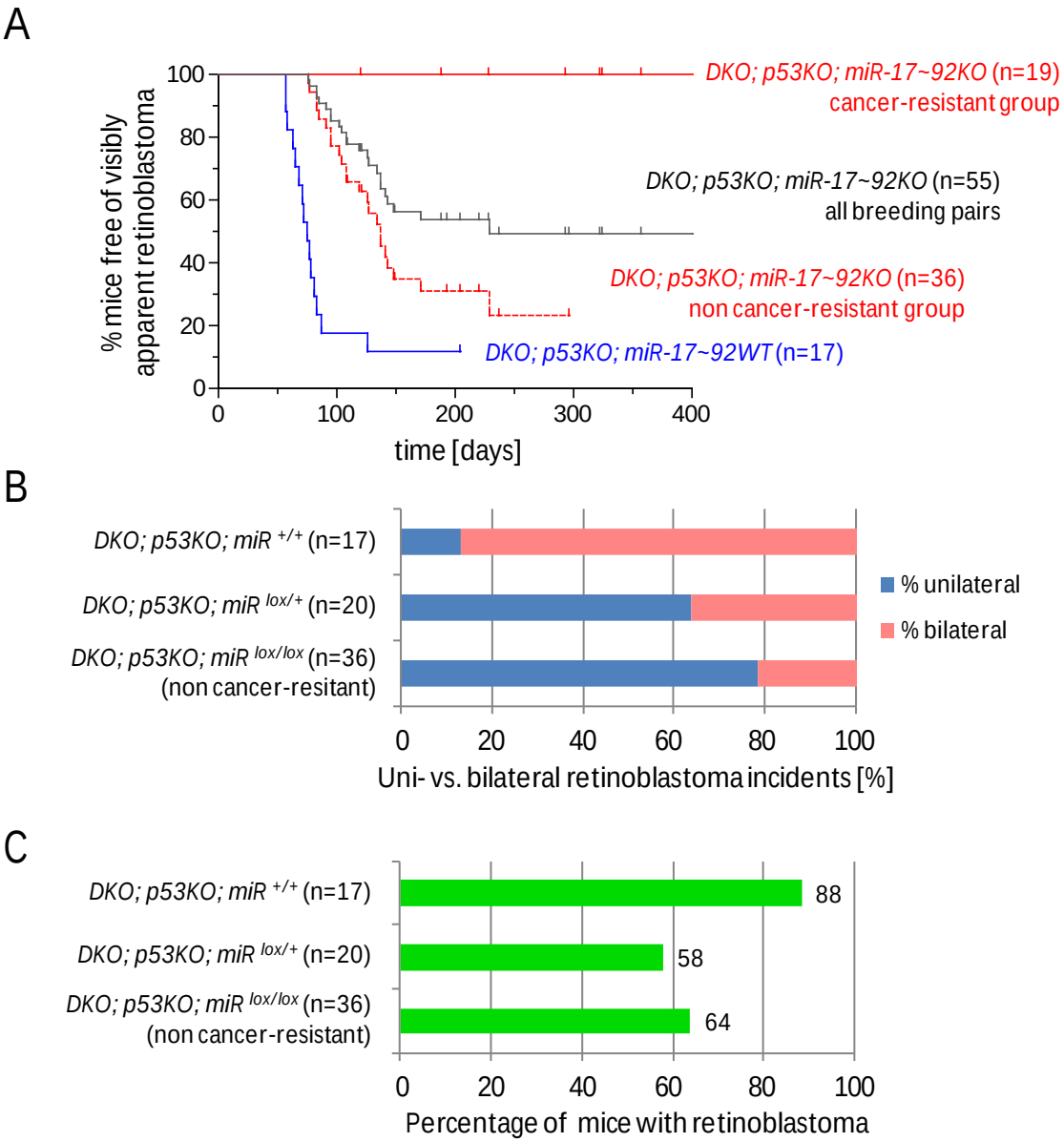

Figure 4.22: A sub-population of *DKO; p53KO; miR-17~92KO* mice developed retinoblastoma.
(A) Kaplan-Meier plot analysis of the time to first observation of externally visible retinoblastoma. In a sub-population of *Chx10Cre; Rb1$^{lox/lox}$; p107$^{-/-}$; p53$^{lox/lox}$; miR-17~92$^{lox/lox}$* (*DKO; p53KO; miR-17~92KO*) mice, 23 out of 36 (64%) developed either uni- or bilateral retinoblastoma with a median time of tumor onset of 137 days of age (n=36). In another subpopulation of *DKO; p53KO; miR-17~92KO* mice of a different group of breeding pairs, none out of 19 mice developed retinoblastoma up to a 400-days observation period. When only considering the genotype itself and disregarding the differences in group-related tumor phenotype, 23 of all 55 mice got either uni- or bilateral retinoblastoma (42%) with a median time of tumor onset of 229 days of age. The Kaplan-Meier curve for *Chx10Cre; Rb1$^{lox/lox}$; p107$^{-/-}$; p53$^{lox/lox}$; miR-17~92$^{+/+}$* (*DKO; p53KO; miR-17~92WT*) mice is shown for comparison and is further described in Figure 4.20 A. (B) Distribution of uni- and bilateral retinoblastoma in *DKO; p53KO* mice with different *miR-17~92* status. (C) Percentage of tumor bearing mice of genotype *DKO; p53KO* with different *miR-17~92* status.

To further investigate the differences in tumor occurrences in both groups we performed AP stainings on young adult (P23) and old adult (P95 and P324) retinae. Consistent with the tumor incidences, all retinae analyzed from the cancer-resistant group

showed no or occasionally very little AP staining (Figure 4.23 A and B), suggesting an eradication of most, if not all, mutant cells. However, all retinae analyzed from the non cancer-resistant group always showed an intense AP staining covering the whole surface of the retina and both the outer nuclear layer (ONL) and the inner plexiform layer (IPL). Some of those surviving *DKO; p53KO; miR-17~92KO* mutant cells will eventually give rise to retinoblastoma as visible in the white tumor tissue covering part of the retina in Figure 4.23 A (right panel).

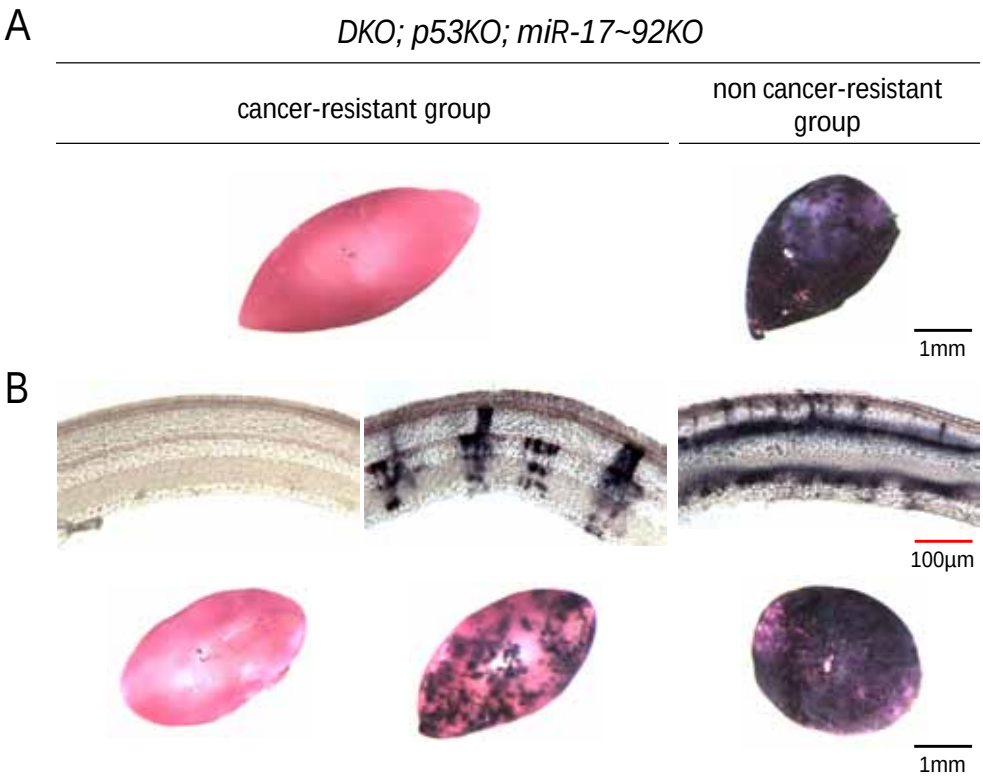

Figure 4.23: The synthetic lethal interaction between *p53* and *miR-17~92* depends on the genetic background.
(A) Retina of old adult (P324 and P95, respectively) *Chx10Cre; Rb1$^{lox/lox}$; p107$^{-/-}$; p53$^{lox/lox}$; miR-17~92$^{lox/lox}$* (*DKO; p53KO; miR-17~92KO*) mice stained for AP activity. Whereas the retina of the cancer-resistant group shows no AP activity suggesting an eradication of all mutant cells, the retina of the non cancer-resistant group is intensely stained for AP activity. White tumor tissue is covering part of the retina which was not visible before dissection. (B) The upper panel shows AP-stained transverse retinal sections (40µm) from young adult (P23) *DKO; p53KO; miR-17~92KO* mice of both the cancer-resistant and non cancer-resistant group. The lower panel shows AP-stained retinae of the same genotypes indicated before sectioning. The two littermate retinae of the cancer-resistant group show little or no AP-positivity. The retina from the non cancer-resistant group shows an intense AP staining covering both the outer nuclear layer (ONL) and the inner plexiform layer (IPL) of the whole retina. Black scale bars = 1mm, red scale bar = 100µm.

Together, these data suggest that the synthetic lethal interaction between *p53* and *miR-17~92* could depend on a modifier gene or a yet unknown factor, such as a single nucleotide polymorphism (SNP) or a polymorphism involving an amino acid change. Serendipitously,

through maintaining different breeding pairs on completely mixed backgrounds, we could identify those two genetic groups which gave rise to either mice developing retinoblastoma or being completely cancer-free due to the synthetic lethality between *p53* and *miR-17~92*.

4.5.4 *miR-17~92* knockdown impairs growth of established human retinoblastoma cells

To test the pharmacological and clinical relevance of the synthetic lethal interaction between *miR-17~92* and *p53* and therefore the survival function of *miR-17~92*, we used the established human retinoblastoma cell lines RBL15, WERI-Rb1 and Y79 to manipulate the levels of the various miRNAs of the *miR-17~92* cluster, as well as p53 levels itself.

We first looked for the expression levels of miR-17, miR-18a, miR-19a, miR-20a, miR-19b, and miR-92 as part of the *miR-17~92* cluster in those retinoblastoma cell lines compared to two normal retinae (in collaboration with the labs of Alexander Schramm and Johannes Schulte (UK Essen, Germany)). Consistent with our miRNA expression analysis in mouse and human retinoblastoma tumors, we found that the *miR-17~92* cluster was expressed at very high levels in the retinoblastoma cell lines (Figure 4.24 A). In Y79 cells, expression of the *miR-17~92* cluster was around 10 times higher than in normal retinae and in RBL15 and WERI-Rb1 cells, expression was even around 100 times higher.

Subsequently, we inhibited individual members of the *miR-17~92* cluster and assessed cell growth with a cell titer glow assay. Whereas individual inhibition did not result in decreased cell growth, transfection of a mixture of miR-17/20a inhibitors (anti-miR-17/20a) into the Y79 cell line showed a reproducible and significant decrease of cell growth at days 7 and 9 post-transfection (*P*-values are < 0.05 (*) for day 7 and day 9, sh-ctrl anti-miR-ctrl vs. sh-ctrl anti-miR-17/20a in Figure 4.24 B). A similar effect in growth inhibition was also observed in WERI-Rb1 cells.

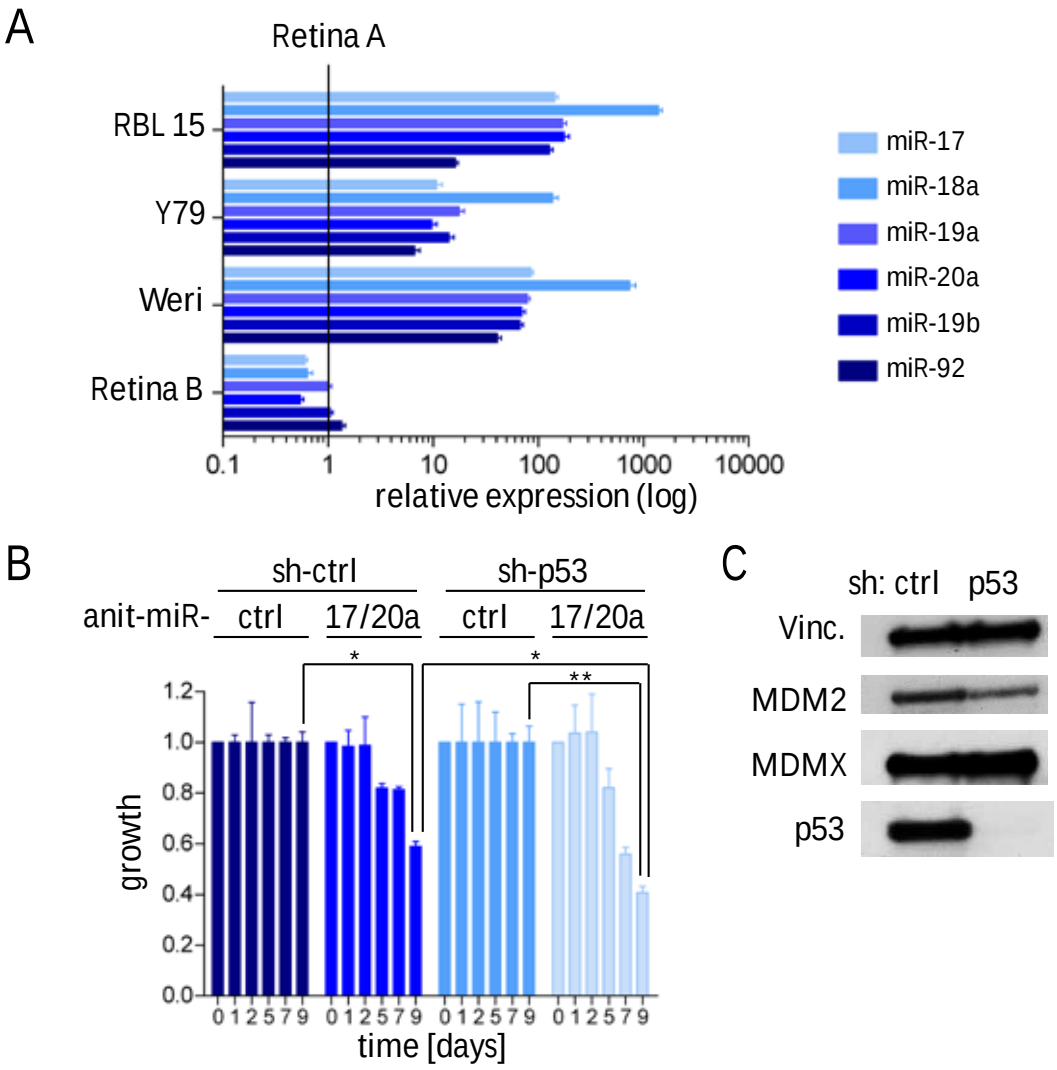

Figure 4.24: *miR-17~92* knockdown impairs growth of established human retinoblastoma cells.
(A) Expression analysis by RT-qPCR of miR-17, miR-18a, miR-19a, miR-20a, miR-19b, and miR-92 in normal human retina and the established retinoblastoma cell lines WERI-Rb1, Y79 and RBL15. Data represents the mean of three independent experiments ±SE. (B) Transfection of a 1:1 mixture of anti-miR17 and anti-miR20a into Y79-derived cell lines expressing either shRNAs control (sh-ctrl) or shRNAs directed against human p53 (sh-p53). Cell growth was assessed using cell titer-glow assays up to 9 days post-transfection. Data represent the mean of two independent experiments (±SD) and are presented as the relative growth of anti-miR-17/20a-transfected cells (anit-miR-17/20a) compared to the growth of cells transfected with a control antagomiR (anti-miR-ctrl), which was set to 1. *P*-values from an unpaired two-tailed *t*-test between sh-control cells transfected with the anti-miR17/20a mixture (sh-ctrl anti-miR-17/20a) and transfected with a control antagomiR (sh-ctrl anti-miR-17/20a) are <0.05 (*) for day 7 and day 9. *P*-values from an unpaired two-tailed *t*-test between sh-p53 cells transfected with the anti-miR17/20a mixture (sh-p53 anti-miR-17/20a) and transfected with a control antagomiR (sh-p53 anti-miR-ctrl) are <0.01 (**) for day 7 and <0.05 (*) for day 9. Importantly, transfection of the anti-miR17/20a mixture into sh-p53 cells (sh-p53 anti-miR-17/20a) resulted in significant decreased cell growth at both days 7 and 9 when compared to sh-control cells transfected with the anti-miR17/20a mixture (sh-ctrl anti-miR-17/20a). *P*-values are <0.05 (*) for day 7 and day 9. (C) Western blot analysis of total protein extracts from Y79 cells stably expressing scramble (sh-ctr) or p53-directed (sh-p53) shRNAs. Vinculin (Vinc.) is used as a loading control. Data for Figure part A kindly provided by Alexander Schramm and Johannes Schulte (University Hospital of Essen, Essen, Germany). Data for Figure part B kindly provided by Frederic Clermont (LMCB, VIB-KULeuven, Belgium). Figure part C kindly provided by Aart G. Jochemsen (Leiden University Medical Center; Leiden, The Netherlands).

It is important to note, that the p53 tumor suppressor pathway is compromised in retinoblastoma through overexpression of negative regulators of p53 such as *Mdm2* (Xu et al. 2009) and *Mdm4* (Laurie et al. 2006) but that p53 can still be activated (Kondo et al. 1997). Such a compromised p53 pathway in Y79 cells, combined with a knockdown of members of the *miR-17~92* cluster, might explain why we can observe growth inhibition – an indication for a possible conservation of the synthetic lethality between *p53* and the *miR-17~92* cluster in pre-formed retinoblastoma – even without additionally altering p53 levels. But since p53 can still be activated in Y79 cells (Kondo et al. 1997) we wanted to test our finding that the survival function of the *miR-17~92* cluster is strongly *p53*-dependent by further artificially downregulating p53 levels in Y79 cells. That is why we (in collaboration with the Jochemsen lab, Leiden) created a *p53*-knockdown cell line by stably transfecting an shRNA targeting p53 vector into the Y79 cell line to decrease the levels of p53 (sh-p53 in Figure 4.24 B and C). As shown by a western blot, the protein levels of p53 are virtually undetectable in the sh-p53 Y79 cell line (sh-p53) whereas levels of Mdm4 (also known as Mdmx) and Mdm2 are similar to the transfection control (sh-ctrl) (Figure 4.24 C). Consistent with our finding that the survival function of the *miR-17~92* cluster in mice is *p53*-dependent, we also found a decrease in cell growth, when transfecting those human sh-p53 Y79 cells with a mixture of miR-17/20a inhibitors (sh-p53 anti-miR-17/20a vs. sh-p53 anti-miR-ctrl). Importantly, there even was a significantly stronger decrease in cell growth when comparing the anti-miR-17/20a transfection results of the sh-p53 Y79 cell line (sh-p53 anti-miR-17/20a in Figure 4.24 B) to its parental or sh-control Y79 cell line (sh-ctrl anti-miR-17/20a in Figure 4.24 B). *P*-values are < 0.05 (*) for day 7 and day 9 as indicated in the graph in Figure 4.24 B.

In summary, these transfection experiments in human retinoblastoma cell lines suggest that high expression levels of miR-17 and miR-20a are required for survival in human retinoblastoma. Low levels of these miRNAs result in a synthetic lethal interaction with *p53* and are therefore not tolerated by the tumor cells. These findings make the *miR-17~92* cluster, and miR-17 and miR-20a specifically, an interesting target for a new pharmacologic and therapeutic approach to selectively remove cancer cells in the context of retinoblastoma treatment.

5. Discussion, conclusions, and future perspectives

Cancer is the second leading cause of death in European countries, closely following diseases of the circulatory system (Niederlaender 2006). Worldwide it is one of the most prominent health problems on earth. When extrapolating those trends to the upcoming years, cancer incidents will still rise, mainly due to aging of the population. Genetic mutations accumulate – turn healthy cells into tumor cells – and are therefore much more likely to occur in an advanced age.

Among one of the genes identified as relevant player in carcinogenesis, is the tumor suppressor protein p53. It is mutated or compromised in virtually all kind of cancers, either by direct mutation or by harboring a genetic defect upstream or downstream in the p53 pathway. Identification of genes which show synthetic lethal interactions with p53, could therefore represent a promising therapeutic approach of treating tumors with an impaired p53 pathway. Being able to target and inhibit those new synthetic lethal partners of *p53* with drugs, would on the one hand allow a tumor-specific treatment while circumventing attacks on the healthy tissue, and on the other hand allow treatment of a broad spectrum of cancer types, since *p53* is widely inactivated across different tumor types.

miRNAs are small non-coding RNAs which post-transcriptionally regulate gene expression by either targeting messenger RNAs (mRNAs) for translational repression or induce mRNA degradation. There is growing evidence suggesting an important role of miRNAs in human diseases, especially cancer (Calin and Croce 2006). Differential expression of miRNAs is well-documented in many types of cancer (Calin et al. 2002, Lu et al. 2005, He et al. 2005) and therefore puts inhibition or reconstitution of miRNAs in the focus of many therapeutic approaches (see also Figure 2.4).

Studies to reveal characteristic miRNA signatures in human cancers showed that miRNAs can either act as tumor suppressors or as oncogenes – being down- or upregulated in human cancers (Esquela-Kerscher and Slack 2006). Interestingly, similar studies also demonstrated that, despite several upregulated miRNAs, the overall levels of miRNAs are decreased in cancer cells (Chang et al. 2008, Thomson et al. 2006). It is suggested that levels of proteins involved in the biogenesis of miRNAs, such as Dicer1, are often low in cancer cells (Thomson et al. 2006). This lead us and others (Lambertz et al. 2010, Kumar et al. 2009) to subsequent experiments in mice where downregulation of *Dicer1* could promote tumorigenesis. Whereas downregulation or loss of one allele of *Dicer1* is found in human tumors (Hill et al. 2009), biallelic loss could never be observed (Karube et al. 2005,

Pampalakis et al. 2010). In previous studies we already showed some initial data suggesting that complete *Dicer1* loss prevents mice from getting retinoblastoma in an otherwise tumor prone background (Lambertz et al. 2010). This suggested that although low levels of Dicer1 or miRNAs are connected with enhanced tumorigenesis, *Dicer1* itself or miRNAs processed by Dicer1 are required for tumor formation. The reason for the necessity of *Dicer1* or specific miRNAs for tumor development was, however, not clear.

Here, we identified *Dicer1* as well as the miRNA cluster *miR-17~92* as synthetic lethal partners of *p53* in a *Rb1/p107*-deficient background. In a mouse model of retinoblastoma we showed that simultaneous loss of either of the two, *Dicer1* or *miR-17~92*, together with *p53* lead to loss of tumorigenesis due to the synthetic lethal interaction. This not only opens the field of miRNAs to new possibilities of cancer treatments but also provides a mechanistic explanation for the addiction of cancer cells to *Dicer1*.

5.1 The *Dicer1*/*p53* synthetic lethality protects mice from retinoblastoma

To investigate the consequences of *Dicer1* disruption in retinoblastoma development, we chose a conditional mouse model expressing Cre under the control of a retina-specific promoter in combination with a mouse line prone to develop retinoblastoma.

Since germline inactivation of *Dicer1* results in early embryonic lethality in mice (Bernstein et al. 2003), we used mice with a conditional floxed allele of *Dicer1* (Murchison et al. 2005) and specifically inactivated *Dicer1* in retinoblasts by combining this *Dicer1* allele with the retinal *Chx10Cre* transgenic line (Rowan and Cepko 2004). Chx10 is a transcription factor critical for progenitor cell proliferation and bipolar cell determination in the developing retina and is exclusively expressed in these cell populations. It is important to note that, due to the nature of the integration site or chromatin configuration of the transgenic construct, Chx10Cre-expression is mosaic in the retina (Rowan and Cepko 2004). As a consequence, only a small subset of retinoblasts express Chx10Cre and are therefore mutant cells. The majority of the retinal cells remains *wild-type*.

The conditional floxed allele of *Dicer1* (Murchison et al. 2005), which we used to inactivated *Dicer1*, is design in such a way that no functional Dicer1 protein can be expressed. Murchison and colleagues were not even able to detect protein domains of Dicer1, which were not affected by the Cre-mediated excision, suggesting that there is no expression of full length or truncated forms of Dicer1 at all. Additionally, since both loxP sites reside in both

RNase III domains, Cre-mediated recombination would result in a completely non-functional form of a theoretical truncated Dicer1 protein after translation of the recombined *Dicer1*-transcript. This design of the floxed allele of *Dicer1* would also exclude a functional form of t-Dicer, a recently identified splice variant of DICER1 in humans, which lacks the dsRNA binding domain and is defective in one active center of one RNase III domain (Potenza et al. 2010).

In order to induce retinoblastoma development, two additional mouse lines were introduced – the *Rb1*$^{lox/lox}$ and the *p107*-null line. On the one hand, conditional inactivation of the Rb1 pathway leads to an inappropriate exit from the cell cycle of retinal progenitor cells and a block in rod maturation (Zhang et al. 2004a). But on the other hand, development of retinoblastoma in mice (but not in humans) is inhibited by the compensatory effects of *p107*, another Rb1 family member (Donovan et al. 2006). Consequently, inactivation of both Rb1 family members (*Chx10Cre; Rb1*$^{lox/lox}$*; p107*$^{-/-}$, or *DKO mice*) in the retina leads to the formation of early hyperproliferative lesions (Zhang et al. 2004a), often referred to as retinomas (DiCiommo et al. 2000). Aggressive and invasive tumors are, however, rarely found in this background.

Upon additional inactivation of the p53 pathway on the *DKO* background, mice develop highly aggressive and invasive retinoblastoma within a shortened time of tumor onset compared to *DKO* mice. To obtain this exacerbated phenotype, inactivation of the p53 pathway can either be achieved by direct inactivation of the *p53* locus itself with the help of a floxed *p53* mouse line (Marino et al. 2000, Jonkers et al. 2001) or by transgenic conditional overexpression of *Mdm4* (Xiong et al. 2010), a negative regulator of p53. Both mouse lines, *Chx10Cre; Rb1*$^{lox/lox}$*; p107*$^{-/-}$*; p53*$^{lox/lox}$ (referred to as *DKO; p53KO*) (Zhang et al. 2004b, Laurie et al. 2006) and *Chx10Cre; Rb1*$^{lox/lox}$*; p107*$^{-/-}$*; Mdm4*^{Tg} (referred to as *DKO; Mdm4Tg*) (McEvoy et al. 2011) have a median time of tumor onset at around 100 days compared to 303 days of the *DKO* mice. It is important to note, that although the tumor spectrum and kinetics of *DKO; p53KO* and *DKO; Mdm4Tg* mice are very similar (Zhang et al. 2004b, McEvoy et al. 2011), *p53* loss has never been found in human tumors (Kato et al. 1996) whereas *Mdm4* overexpression is a common trait in virtually all cases of retinoblastoma (Laurie et al. 2006, McEvoy et al. 2011). For all our experiments described in this thesis, *DKO; p53KO* mice were used. Crosses with *DKO; Mdm4Tg* mice to confirm our findings on a background closer to the human situation are presently in progress.

In this work we show that, upon simultaneous inactivation of *Dicer1* and *p53* on a *Rb1/p107*-deficient background (referred to as *QKO* mice), mutant retinoblasts are lost, probably due to an apoptotic cell death. As a consequence of eradication of all mutant cells, *QKO* mice do not develop retinoblastoma. Although loss of *Dicer1* in *DKO* mice (*DKO; DicKO*) also appears to protect against retinoblastoma (Figure 4.8 A), the reason for the absence of tumorigenesis is completely different. Whereas *QKO* mice have a *wild-type* (*WT*) retina due to death of the mutant cells, *DKO; DicKO* mice still retain mutant cells and even show hyperproliferative lesions and rosette formations in adult retina (Figure 4.3). In an observation period of up to two years, *DKO; DicKO* mice however have not developed retinoblastoma, despite retinal defects.

The fact that these mice do not develop retinoblastoma could be explained in two different ways. First, *DKO; DicKO* mice have a reduced number of mutant cells compared to *DKO* or *WT* mice, both at the embryonic (Figure 4.12) and adult stage (Figure 4.4). With less mutant cells capable of initiating retinoblastoma development, the chances for tumor initiation are lower. Given the fact that *DKO* mice develop retinoblastoma with a median time of tumor onset of around 300 days with a penetrance of only 50%, reduction of the amount of mutant cells through additional inactivation of *Dicer1* might delay tumor formation beyond the lifespan of the mice. To test this hypothesis, $Rb1^{lox/lox}$; $p107^{-/-}$; $Dicer1^{lox/lox}$ mice could be crossed with another transgenic Cre line, such as *Pax6-Cre*, in which the whole peripheral neuroretina expresses *Cre* (Marquardt et al. 2001) – instead of using the transgenic *Chx10Cre* line which shows mosaic *Cre* expression of around 2% of all retinal cells (Rowan and Cepko 2004 and Figure 4.4). If the hypothesis would be correct, *Pax6-Cre;* $Rb1^{lox/lox}$; $p107^{-/-}$; $Dicer1^{lox/lox}$ should develop retinoblastoma, probably with delayed kinetics compared to *Pax6-Cre;* $Rb1^{lox/lox}$; $p107^{-/-}$ mice.

Secondly, and more importantly, the synthetic lethality between *Dicer1* and *p53* could also explain the absence of retinoblastoma in *DKO; DicKO* mice. Considering that inactivation of *p53* is such a prevalent oncogenic event during retinoblastoma formation, *Rb1/p107/Dicer1*-deficient retinal cells which survive into adulthood might be killed off as soon as p53 function becomes compromised through alterations of the *p53* locus itself or by alterations of loci of p53 regulators such as *Mdm4*. As a consequence of the *Dicer1/p53* synthetic lethality, all tumor initiating events, otherwise resulting in retinoblastoma formation, would therefore lead to cell death and removal of any cells capable of forming aggressive and invasive tumors. Since the Rb1 and p53 pathways are inactivated in most human cancers,

Dicer1/p53 synthetic lethality might also explain why homozygous loss of *Dicer1* is not seen in other human cancers (Karube et al. 2005, Pampalakis et al. 2010).

5.2 The *miR-17~92* cluster might represent a better drug target than *Dicer1*

Identification and targeting of synthetic lethal interaction partners of *p53* might lead to novel cancer cell-specific therapeutic modalities. Although we discovered the *Dicer1/p53* synthetic lethal interaction in context of oncogenic stress, our previous data and that of others (Lambertz et al. 2010, Kumar et al. 2009) – showing that partial inactivation of *Dicer1* exacerbates tumorigenesis – argue against direct targeting of *Dicer1* for therapeutic purposes. Additionally, *Dicer1* is required for the correct development and homeostasis of several cell types and tissues such as skin (Yi et al. 2006), cardiac and skeletal muscles (Singh et al. 2011, O'Rourke et al. 2007), white adipose tissue (Mudhasani et al. 2010, Mudhasani et al. 2011), neural crest cells (Zehir et al. 2010), male and female mouse reproductive organs (Maatouk et al. 2008, Gonzalez and Behringer 2009, Korhonen et al. 2011), and the retina (Georgi and Reh 2010, Pinter and Hindges 2010, Georgi and Reh 2011). Thus, by systemically targeting *Dicer1*, one would not only risk to enhance tumorigenesis but also to cause toxicity in normal cells. It is important to mention, that the defects in retinal development in *Dicer1*-deficient retinae as observed by others (Georgi and Reh 2010) is not seen in our mouse lines – most likely because we use a *Cre*-expressing transgenic construct which is only expressed in a small subset of retinal cells (for mosaic expression of *Chx10Cre* refer to Rowan and Cepko 2004 and section 4.1.1, page 45) instead of the whole peripheral neuroretina (*Pax6Cre* in Georgi and Reh 2010).

Therefore, the ideal therapeutic target would be a specific miRNA or set of miRNAs downstream of *Dicer1* which could mediate its pro-survival function to avoid the overall downregulation of miRNA processing caused by homozygous loss of *Dicer1* and the associated side effects. Here, we show that the *miR-17~92* cluster could be a promising candidate for a drug target since genetic inactivation of *miR-17~92* phenocopies loss of *Dicer1* and causes synthetic lethality when simultaneously lost with *p53* on an oncogenic background. Similar to *QKO* mice, *DKO; p53KO; miR-17~92KO* mice do not develop retinoblastoma due to the eradication of the mutant cell pool. In contrast to *Dicer1*, whose non-mosaic inactivation in the retina leads to several differentiation defects (Pinter and Hindges 2010, Georgi and Reh 2010), absence of *miR-17~92* in the retina is tolerated even in a non-mosaic fashion (Conkrite et al. 2011).

Together, these data suggest *miR-17~92* as a promising cancer cell-specific target for the treatment of retinoblastoma.

5.3 Data from preclinical mouse models have to be further validated

In the preclinical mouse model for retinoblastoma we based our experiments on the findings, that direct loss of *p53* would be required to cause synthetic lethality with either *Dicer1* or *miR-17~92*. As mentioned before, in human retinoblastoma, it is not the direct loss of *p53* which can be observed (Kato et al. 1996) but rather the overexpression of its negative regulator *Mdm4* (Laurie et al. 2006, McEvoy et al. 2011). Therefore, it is important to test whether the synthetic lethality, already observed between *miR-17~92* and *p53* in *DKO; p53KO; miR-17~92KO* mice, can also be reconstructed in *DKO; Mdm4Tg* or other transgenic mice in which the p53 function is indirectly altered.

5.4 The temporal context of the synthetic lethal interactions has to be investigated more closely

As shown by AP stainings during early embryonic development (Figure 4.12), the synthetic lethal event in retinoblasts has to take place very early during retinogenesis. We argue that probably only very early removal of mutant cells could be tolerated and compensated during tightly regulated retinogenesis as we can observe in our experiments. The retina of *QKO* and *DKO; p53KO; miR-17~92KO* mice is indistinguishable from *WT* retina, both in size and morphology, suggesting that correct retinogenesis is not affected by an early induced cell death due to the synthetic lethal interactions. In this context, the used transgenic Cre line *Chx10Cre* might be crucial for the correct and functional development of the retina, since expression of transgenic *Cre* is only mosaic and limited to 2 - 5 % of cells in the retina (Figure 4.4). Any broader expression levels of *Cre* throughout the retina might result in developmental defects due to massive cell death caused by the synthetic lethality. It would therefore be interesting to test the loss of *Dicer1* or *miR-17~92* in $Rb1^{lox/lox}$; $p107^{-/-}$; $p53^{lox/lox}$ mice in combination with different transgenic Cre lines, such as *Pax6-Cre* or *Nestin-Cre*, where Cre is more broadly expressed throughout the retina. In *Pax6-Cre* mice, *Cre* is expressed in the peripheral neuroretina but not in central progenitor cells (Marquardt et al. 2001). *Nestin-Cre* expression is even broader expressed since it can be detected throughout the developing nervous system and in neuronal and glial cell precursors (MacPherson et al. 2003, Tronche et al. 1999).

Furthermore, it is important to know – both for the therapeutic relevance and also to understand the molecular mechanism of the synthetic lethal interactions involving *Dicer1/p53* and *miR-17~92/p53* – whether the synthetic lethality is only confined to retinal progenitor cells as in our mouse models or whether it is also applicable to pre-formed retinoblastoma cells. To begin to address this question we used human retinoblastoma cell lines harboring p53 pathway alterations as preclinical model system and showed that pharmacological inactivation of miR-17/20a, two members of the *miR-17~92* cluster, leads to decreased cell growth. More experiments are still required to get a deeper understanding of which miRNAs – or which combination of miRNAs – of the *miR-17~92* cluster would result in the most efficient growth defect upon miRNA inactivation.

Additionally, the question should be addressed, whether the *wild type* cells surrounding the mutant cells in the mouse retina are involved in the induction of synthetic lethality. This involvement could explain to some part the differences in the extent of induced cell death/growth suppression in the mouse model compared to the experiments in the human Y79 retinoblastoma cell lines, which purely consist of cancer cells and are not influenced by *wild type* cells as it could be in the case of the *in vivo* mouse experiments.

5.5 The precise mechanism behind the synthetic lethal interaction remains unclear

As we could show, the *Dicer1/p53* and *miR-17~92/p53* synthetic lethal interactions both depend on the presence of oncogenic stress in form of *Rb1/p107*-deficiency (Figure 4.14 A and Figure 4.21). However, the precise mechanism explaining the synthetic lethal effect in both scenarios remains to be addressed.

DNA damage could contribute to the synthetic lethal phenotype

One possible explanation for the necessity of oncogenic stress might include the involvement of DNA damage. As previous reports show, loss of *Dicer1* causes DNA damage and induces p53 pathway activation (Mudhasani et al. 2008, Tang et al. 2008). Additionally, both oncogenic stress (Bartkova et al. 2005) as well as loss of *Rb1* (Seoane et al. 2008, Shamma et al. 2009) induce DNA damage. As a consequence, the extent of DNA damage caused by loss of *Dicer1* in combination with oncogene-induced DNA replication stress and DNA damage due to *Rb1* loss might be too high for cells with a disrupted p53 pathway to cope with, and therefore cells might die by mitotic catastrophe (Fragkos and Beard 2011). Interestingly, *in vitro* studies suggest that this form of mitotic cell death is independent of

apoptosis and autophagy and rather induced by mechanical damage (Fragkos and Beard 2011). This phenomenon is also in line with the difficulties we had to show a significant number of apoptotic cells during retinogenesis at embryonic day 12 (Figure 4.13 and Figure 4.12). Besides caspase-dependent apoptosis, cell death by mitotic catastrophe might therefore be another explanation for the synthetic lethal interaction of *Dicer1* and *p53*. Interestingly, another caspase-independent form of retinal cell death was recently identified and connected to a receptor interaction protein (RIP) kinase, RIP3 (Trichonas et al. 2010). It was shown that RIP3-mediated programmed necrosis is another key mechanism in photoreceptor cell death besides the well-studied mechanism of caspase-dependent apoptosis. This RIP3-dependent but caspase-independent form of cell death could therefore be yet another mechanistic explanation of the *Dicer1/p53* synthetic lethal interaction.

Another major cause for DNA damage and genetic instability are reactive oxygen species (ROS) (Sablina et al. 2005). Recent studies in small-cell lung cancer cells (SCLC) showed that loss of *RB1* induces ROS accumulation and DNA damage (Ebi et al. 2009). Importantly, this increase in ROS levels as well as increased DNA damage, which should inhibit growth and induce apoptosis in normal healthy cells, was counterbalanced in these cancer cells by high levels of *miR-17~92* to prevent apoptosis and growth inhibition. As these studies demonstrated in non-small cell lung cancer (NSCLC) cells, artificial overexpression of *miR-20a*, a component of the *miR-17~92* cluster, could abrogate *RB1* knockdown-induced apoptosis, ROS generation and induction of DNA damage. Therefore, elevated ROS levels and induction of DNA damage due to loss of *miR-20a* might ultimately be the trigger for cell death and could be one possible explanation for the synthetic lethal interaction between *miR-17~92* and *p53*. These findings would be in line with the assumptions that DNA damage might be a possible cause for the synthetic lethal interaction in *Dicer1* deficient cells as described before.

Ebi et al. also showed in the same study, that not only *miR-20a* overexpression could reduce DNA damage in NSCLC cells but that also treatment with *N*-Acetyl-L-cysteine (NAC) had the same effect. NAC is a ROS inhibitor which was shown to protect the genome from oxidation by ROS and can protect mice from tumor development upon loss of *p53* (Sablina et al. 2005). To test the involvement of DNA damage response in our mouse model and to answer the question for a possible mechanism of the synthetic lethal interactions, we treated *QKO* mice with 50 mM NAC as described by Sablina et al. (Sablina et al. 2005). Subsequently, we analyzed adult retinae for AP activity at P21. We hypothesized that, due to the NAC treatment, ROS levels should be reduced, thus leading to lower levels of DNA

damage in the retina and consequently preventing cell death caused by the *Dicer1/p53* synthetic lethal interaction. Unfortunately, none of the retinae analyzed showed any positive staining for AP activity (data not shown) suggesting that either manipulation of ROS levels via NAC treatment might not lower levels of DNA damage to a non-lethal stage or that there might be other factors – independent of the DNA damage response – contributing to the synthetic lethality.

Small molecules targeting components of the pathway involved in the stress response to ROS were already shown to selectively kill cancer cells with elevated transformation-induced oxidative stress levels (Raj et al. 2011). Combining application of these small molecules with inhibitors of *miR-17~92* might therefore even be more specific in killing cancer cells and could result in less toxic side effects through combinatory therapy.

Genetic modifiers are likely to contribute to the synthetic lethal interactions

The fact that the *miR-17~92/p53* synthetic lethal interaction depends on the genetic background (Figure 4.22 and Figure 4.23), opens up more questions about the molecular basis and mechanism of this synthetic lethality.

A possible explanation for the dependency of the synthetic lethal interaction seen in *DKO; p53KO; miR-17~92KO* mice on the genetic background, might be the involvement of genetic modifiers, such as single nucleotide polymorphisms (SNPs), a polymorphism involving an amino acid change, or variants of enhancer regions in the different breeding pairs. Potentially, those modifiers might contribute to the synthetic lethal phenotype by influencing pathways involved in the synthetic lethality, such as the p53 or Rb1 pathway. However, the precise mechanism of their involvement remains unclear.

A possible model for the synthetic lethal phenotype involves accumulation of various stress levels

Taken together our data, we suggest a possible model where intra- and extracellular stress levels contribute to the synthetic lethal phenotype. Stress in form of oncogenic stress, DNA damage, and ROS accumulation might gradually increase stress levels up to a point where additional loss of *p53* can no longer be tolerated by the cell, leading to cell death. Genetic modifiers are thereby likely to play an important role in defining the lethal threshold of the stress gradient leading to the synthetic lethal phenotype we could observe in the context of loss of either *Dicer1/p53* and *miR-17~92/p53* (Figure 5.1).

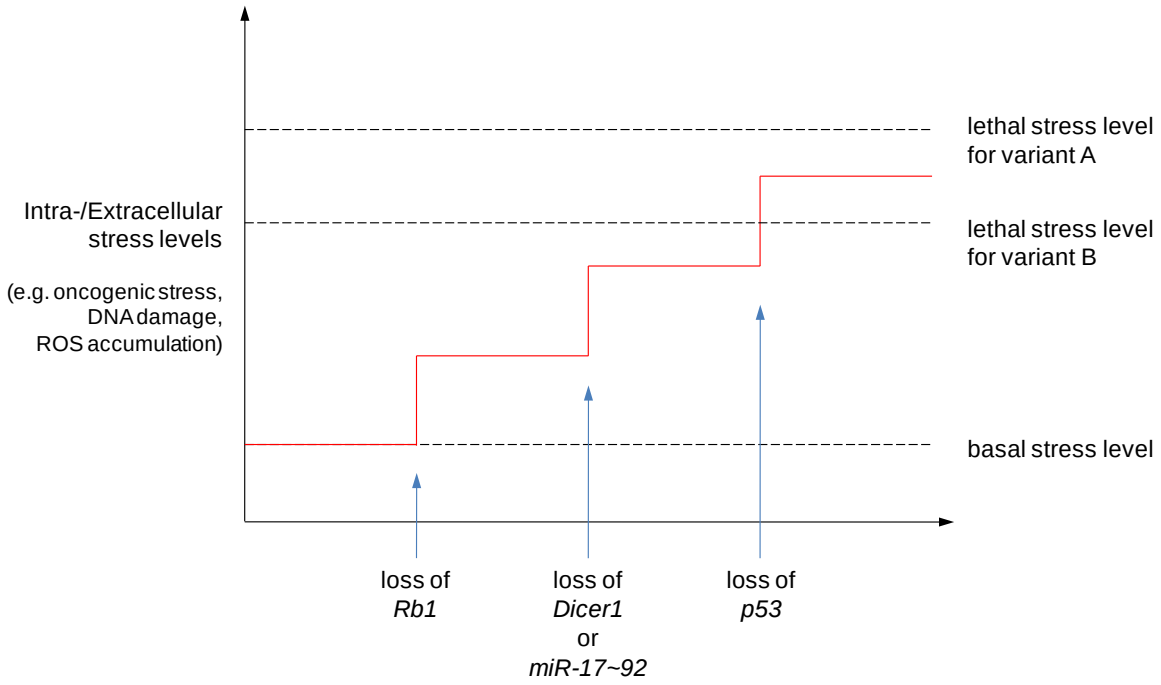

Figure 5.1: Model proposition for contribution of various stress levels to the synthetic lethal phenotype. Various forms of intra- and extracellular stress such as oncogenic stress, DNA damage, and ROS accumulation might gradually contribute to a level of stress which is not tolerable by the cell anymore upon additional loss of *p53*. Additionally, genetic modifiers are likely to play an important role in modifying the lethal threshold of the stress gradient (lethal stress level for variant A vs. variant B) and might be another trigger to initiate the synthetic lethal effect. Whereas variant B of the genetic modifier might have a lethal effect in the context of simultaneous loss of *Rb1*, *Dicer1* (or *miR-17~92*), and *p53*, variant A might increase the stress threshold to tolerable, non-lethal levels and mutant cells might still survive.

5.6 Clinical relevance and future perspectives

Collectively, our findings provide new insights into the important role of *Dicer1* and the miRNA pathway in tumorigenesis. We show that inhibition of miR-17/20a could be explored as a highly selective therapeutic target for retinoblastoma treatment and suggest further development and optimization of miR-17/20a inhibitors. Although further studies have to validate whether the *Dicer1/p53* synthetic lethal interaction also occurs in other cancer types, our study raises the possibility that targeting miRNAs that function as synthetic lethal partners with *p53* may represent a new avenue of research in cancer prevention and therapy.

Inhibition of miRNAs as therapeutic intervention was already shown to be very valuable and efficient in treating diseases. One example is the well-studied and highly abundant miRNA miR-122, of which *in vivo* inhibition was evaluated in mice and in non-human primates (Krutzfeldt et al. 2005, Elmen et al. 2008). In mice, an inhibitor against miR-122 was successfully administered by intravenous injection in form of an "antagomiR" –

a chemically modified, cholesterol-conjugated single-stranded RNA analogue complementary to a specific miRNA. The levels of miR-122 were not only undetectable after injection, but the inhibition was also long lasting since no miR-122 was detectable for as long as 23 days after injection. Additionally it was shown, that these inhibitors were also miRNA specific and that even prolonged treatment showed no apparent toxic side effects as measured by alterations in body weight or serum markers of liver toxicity. Most importantly, inhibition of miR-122, which target genes play an important role in cholesterol biosynthesis, also had a functional effect in mice treated with this inhibitor, as cholesterol levels in those mice were decreased for at least two weeks (Krutzfeldt et al. 2005). An inhibitor against miR-122 is already in Phase II of clinical trials (Santaris Pharma A/S).

In the case of retinoblastoma, sub-conjunctival injection of molecules that inhibit miRNAs could be used for treatment. By avoiding systemic exposure to those miRNA inhibitors, potential side effects of such a treatment in other tissue or organs should further be minimized.

6. Materials and Methods

6.1 Mouse strains and genotyping

All animal experiments were performed in accordance with the guidelines of the University of Leuven Animal Care and Use Ethical Committee. All mouse strains were maintained on a mixed genetic background.

6.1.1 Genotyping

Table 6.1: Genotyping strategies.

Transgene	***Chx10Cre***	***Dicer1 lox***	***miR-17~92 lox***	***p107 KO***	***p53 lox***	***Rb1 lox***
Primer sequence 1	GGGCACCTGGGACCAACTTCACGA	ATTGTTACCAGCGCTTAGAATTCC	TCGAGTATCTGACAATGTGG	TGTCCTGAGCATGAACAGAC	AAGGGGTATGAGGGACAAGG	GGCGTGTGCCATCAATG
Primer sequence 2	CGGCGGCGGTCACGAACTCC	GGGAGGAGGTGTACGTCTACAATT	TAGCCAGAAGTTCCAAATTGG	TCGCTGGCAGTCTGAGTCAG	GAAGACAGAAAAGGGGAGGG	AACTCAAGGGAGACCTG
Primer sequence 3	-	TCGGAATAGGAACTTCGTTTAAAC	-	ACGAGACTAGTGAGACGTGC	CACAAAAACAGGTTAAACCCAG	-
Amount of DNA [µl]	1.5	1.5	1.5	2	0.5	1.5
5µl of 5M betaine	yes	no	no	yes	yes	yes
PCR program:						
Temperature 1 [°C]	94	94	94	94	94	94
Time 1 [sec]	240	300	180	120	240	120
Temperature 2 [°C]	94	94	94	92	94	92
Time 2 [sec]	60	60	30	60	60	60
Temperature 3 [°C]	60	60	53	60	60	60
Time 3 [sec]	60	60	30	120	60	120
Temperature 4 [°C]	72	72	72	72	72	72
Time 4 [sec]	60	60	60	120	60	120
Number of cycles for steps 2-4	32	35	35	30	32	30
Temperature 5 [°C]	-	-	72	-	-	-
Time 5 [sec]	-	-	120	-	-	-
Size *WT* band [bp]	-	560	255	300	430	650
Size mutant band [bp]	800	760	289	370	580	720
Size excised band [bp]	-	430	-	-	610	-
Mouse described in	Rowan and Cepko 2004	Murchison et al. 2005	Ventura et al. 2008	Zhang et al. 2004b	Jonkers et al. 2001	Zhang et al. 2004b

Genomic DNA was isolated by lysing 1 or 2 toes of the mouse subjected to genotyping in 100µl DirectPCR Tail Lysis reagent (Viagen Biotech, #101-T) containing 0.2mg/ml Proteinase K. If possible, toes were collected between P5 and P15. Lysis was done by incubating the samples for 13h at 55 °C in a PCR heating block. Samples were heat-inactivated for 45 min at 85 °C. The PCR reactions were carried out using a Taq PCR core kit (Qiagen, #201225) and contained:

Volume of DNA as specified in Table 6.1
2.5µl 10x PCR buffer
Volume of 5M betaine as specified in Table 6.1
0.5µl dNTPs (10mM each)
0.5µl primer 1 (100µM)
0.5µl primer 2 (100µM), if primer 3 was also used, volume was 0.25µl
0.25µl primer 3 (100µM), if necessary
0.125µl Taq DNA polymerase (5 U/µl)
DNase/RNase free destilled water to 25µl final volume

The resulting PCR products were visualized using a QIAxcel multicapillary electrophoresis system (Qiagen). Sizes of the individual PCR products are indicated in Table 6.1.

6.2 Mouse handling

6.2.1 Tumor monitoring

All mice presented in a Kaplan-Meier curve were weekly screened for appearance of visible retinoblastoma in both eyes. As soon as a white cluster of tumor cells was apparent with the unaided eye in the anterior chamber of the eye, the mouse was classified as tumor-bearing animal (see also Figure 6.1 for representative examples of different retinoblastoma stages). In rare cases of tumor incidents, white spots of tumor cells were absent in the anterior chamber. Instead, the vitreous cavity behind the lens was visibly filled with white tumor tissue and the eyes had a swollen appearance.

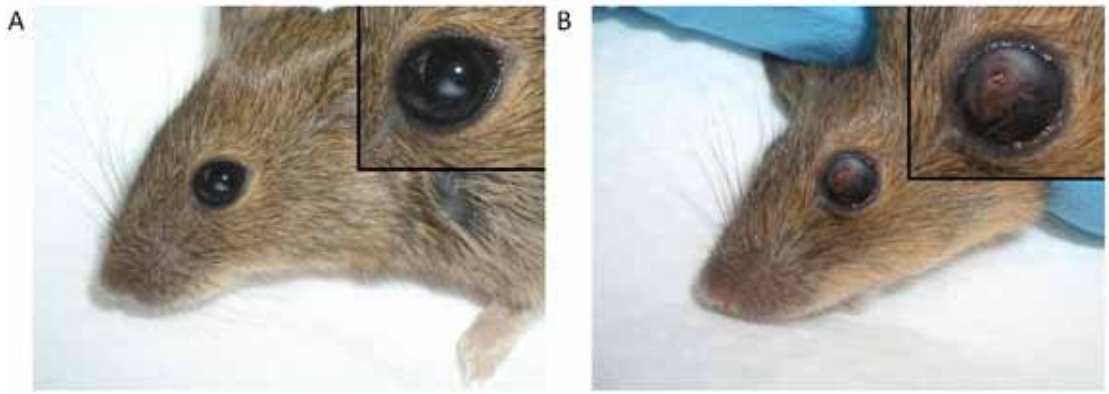

Figure 6.1: Tumor appearance in two representative *DKO; p53KO* littermate mice.
Two *Chx10Cre; Rb1*$^{lox/lox}$*; p107*$^{-/-}$*; p53*$^{lox/lox}$ (*DKO; p53KO*) littermate mice at the age of P81 at different stages of retinoblastoma. (A) Early stage of retinoblastoma 9 days after tumor detection. A white cluster of tumor cells is clearly visible underneath the cornea in the anterior chamber. (B) Late stage of retinoblastoma 24 days after tumor detection. Tumor cells invaded most of the anterior chamber and the overall size of the eye is therefore increased as well. At this stage blood vessel formation is necessary for the tumor to grow (red tissue in the middle of the eye).

6.2.2 BrdU injections

Mice were injected intraperitoneally with BrdU (100 µg/g of body weight) 1 hour prior to sacrifice.

6.3 Histology

6.3.1 Immunohistochemistry

After enucleation, the eyes were fixed overnight in 4% paraformaldehyde/PBS, dehydrated (1 h incubation in each 70% EtOH, 90% EtOH, and 100% EtOH) and immersed in 1-Butanol for 2x 1 h (all steps at room temperature) and 3 - 3.5 h in liquid paraffin at 65 °C. Eyes were paraffin embedded with the optic nerve parallel to the sectioning plane and stored at +4 °C overnight prior to sectioning. 5 µm sections were either used for Haematoxylin & Eosin (H&E) or further deparaffinized with xylene (2x 5 min) and stepwise rehydrated with 100%, 95%, 70%, and 30% EtOH. Each step was performed 2x for 3 min each. Samples were then rinsed in tap water, incubated in PBS (pH 7.4) for 5 min, and rinsed in ddH_2O. The antigens were unmasked by cooking for 20 min in R-buffer A (PickCell Laboratories) using a 2100 Retriever (PickCell Laboratories) and cooled down for 100 min. Sections were incubated twice for 5 min in PBS before they were either used for immunoperoxidase staining or immunofluorescence.

Immunoperoxidase staining

For blocking the endogenous peroxidase activity, sections were incubated in DAKO REAL Peroxidase-blocking solution (DAKO, S2023) for 20 min. Additionally, the samples were blocked for 30 min with 5% goat serum in DAKO antibody diluent (DAKO, S2022). For overnight incubation in a humidified chamber at +4 °C, each antibody was diluted to the appropriate concentration with the blocking solution (see Table 6.3). After washing the specimen twice with PBS for 5 min, each secondary antibody was used in the appropriate dilution in DAKO antibody diluent for an incubation of 1 h at RT. To increase the sensitivity of detection of the Chx10, GFP, and Ki67 antigens, the slides were additionally incubated with the R.T.U. Vectastain Elite ABC Kit (Vector Laboratories, PK-7200). For detection, the DAB Substrate kit (BD Pharmingen, 550880) was used. To visualize the nuclei, the sections were briefly counterstained with haematoxylin solution, dehydrated, mounted and finally pictures were taken as described for the H&E staining.

Table 6.2: Antibodies and their dilutions used for immunoperoxidase stainings.

Antigen	**Primary antibody**		**Secondary antibody**	
	Company (catalog ID)	**Dilution**	**Company (catalog ID)**	**Dilution**
BrdU	BD Pharmingen (550803)	1/10	BD Pharmingen (550803)	according to manual
Ki67	DAKO Cytomation (M7249)	1/30	DAKO Cytomation (E0468)	1/300
Chx10	Exalpha biologicals (X1180P)	1/300	Calbiochem (JA1310)	1/500
GFP	Santa Cruz (9996)	1/300	DAKO Cytomation (E0433)	1/500
Syntaxin	Sigma (S0664)	1/20 000	DAKO Cytomation (K4000)	according to manual
Calretinin	Millipore (MAB1568)	1/700	DAKO Cytomation (K4000)	according to manual
Calbindin	Abcam (9481-500)	1/100	DAKO Cytomation (K4000)	according to manual
Cleaved Caspase-3	Cell Signalling (9664)	1/100	DAKO Cytomation (K4002)	according to manual

Immunofluorescence

Sections were blocked for 30 min with 5% goat serum in DAKO antibody diluent (DAKO, S2022). For overnight incubation in a humidified chamber at +4 °C, each antibody was diluted to the appropriate concentration with the blocking solution (see Table 6.3). After washing the specimen twice with PBS for 5 min, each secondary antibody was used in the appropriate dilution in DAKO antibody diluent for an incubation of 45 min at RT in the dark. The secondary antibodies were removed by washing 3x with PBS. Sections were then mounted with mounting medium containing DAPI staining solution (Vectashield) and stored at -20 °C until pictures were taken with the Nikon A1 confocal microscope.

Table 6.3: Antibodies and their dilutions used for immunofluorescence.

Antigen	Primary antibody		Secondary antibody	
	Company (catalog ID)	Dilution	Reactivity and fluorochrome (company)	Dilution
GFP	Santa Cruz (9996)	1/300	anti-mouse Alexa Fluor-555 (Invitrogen)	1/1000
Cleaved Caspase-3	Cell Signalling (9664)	1/100	anti-mouse Alexa Fluor-488 (Invitrogen)	1/1000

Haematoxylin & Eosin (H&E) staining

The 5 µm sections were deparaffinized with xylene (2x 5 min) and stepwise rehydrated with 100%, 90%, 70% EtOH, and distilled water. Each step was performed 2x for 1 min each. The tissues were then stained with haematoxylin solution for 8 min, rinsed with water and stained with Eosin for 2 min. To remove all the water from the tissue, sections were stepwise dehydrated in each 70% EtOH, 90% EtOH, 100% EtOH, and xylene. Each step was performed 2x for 1 min. After mounting with DPX (Fluka Biochemica, 44581) pictures were acquired using an Olympus BX51 microscope.

6.3.2 Alkaline phosphatase (AP) staining

Dissected retinae (method described in Donovan and Dyer 2006) were fixed for 1h in 4% paraformaldehyde/PBS on ice or at +4 °C. To heat-inactivate the intrinsic, non-specific alkaline phosphatase activity, retinae were incubated at 65 °C for 30 min in PBS. After cooling down samples were rinsed once in AP detection buffer (100 mM Tris pH 9.5, 50 mM $MgCl_2$, 100 mM NaCl) before developing in 4-Nitro blue tetrazolium chloride/5-Bromo-4-

chloro-3-indolyl-phosphate (NBT/BCIP Ready-to-Use tablets, Roche) for 4h. Stained retinae were embedded in 4% agarose/PBS and 40µm sections were analyzed.

When performing whole mount AP staining on mouse embryos at different embryonic stages, the above mentioned protocol was used up to the development in NBT/BCIP solution. Instead of 4 h, the embryos were stained overnight in NBT/BCIP solution, rinsed twice in PBS and directly analyzed by light microscopy or further treated for immunofluorescence analysis as described in 6.3.1. For immunofluorescence stainings of the embryos, the whole embryo (more specifically the upper half, the lower half was used for genotyping) was used for fixation, dehydration, and paraffin-embedding instead of enucleation of the eyes.

6.4 Cell sorting and FACS analysis

Freshly dissected retinae were washed with prewarmed PBS (without Ca^{2+} and without Mg^{2+}) and resuspended in 200µl PBS. After adding 20µl of 100x trypsin stock (10 mg/ml in 1x PBS, Sigma), cells were incubated for 5 min at 37 °C and several times carefully inverted in an eppendorf tube. After the incubation, the tubes were carefully flicked to dissociate the cells more easily. After another incubation time of 2-4 minutes at 37 °C, cells were again carefully flicked in the eppendorf tubes to generate a single cell suspension. To stop the digestion process and remove DNA agglutination, 20 µl of 100x soybean trypsin inhibitor stock (10 mg/ml in 1x PBS, Sigma) and 20µl of 100x DNaseI stock (2 mg/ml in 1x PBS, Sigma), respectively, were added to the cell suspension and the tubes were carefully flicked. After 5 min incubation at 37 °C, 500µl of 1x PBS were added and the suspension was filtered using a 70µm cell strainer (BD Biosciences). The filtered flowthrough was put on ice and the resulting retinal cell suspensions were directly analyzed using a BD FACSCanto II flow cytometer (BD Biosciences) or sorted for GFP-positivity using a FACSVantage cytometer (BD Biosciences).

6.5 Recombination analysis

DNA was isolated from dissected retinae and isolated tumors using DNeasy Blood & Tissue Kit (Qiagen). *Dicer1* recombination was analyzed by PCR using the following primers: (a) 5'-ATTGTTACCAGCGCTTAGAATTCC; (c) 5'-TCGGAAT AGGAACTTCGTTTAAAC and the reverse (b) primer 5'-GGGAGGTGTACGTCTACAATT. *Tp53* recombination was analyzed by PCR using the

following primers: (d) 5'-CACAAAAACAGGTTAAACCCAG and the reverse primers (f) 5'-AGCACATAGGAGGCAGAGAC and (e) 5'-GAAGACAGAAAAGGGGAGGG. PCR conditions were as follow: 1x precycle at 94°C for 3min and 30cycles of 94°C, 30sec; 60°C, 30sec; 72°C, 45sec.

6.6 Retinoblastoma tumor samples and RNA isolation

Immediately following enucleation, dissected retinae or tumor samples were removed from the mouse eyes under the binocular using forceps. The specimens were placed on ice and immediately processed for RNA or DNA isolation. Before tumor samples were collected from human retinoblastoma samples, serial cryosections where obtained from all tumors. The first and last cryosection of each series were H & E stained for tumor cell content verification. 3 - 5 mm^3 samples were placed on ice and immediately processed for RNA and DNA isolation. Total RNA and genomic DNA were isolated using the miRNeasy kit (Qiagen) and the QIAmp mini kit (Qiagen), respectively, according to manufacturer's instructions. Written informed consent was obtained from patients and/or their parents. All procedures have been approved by the Institutional Review Board of the Children's University Hospital of Essen.

6.7 microRNA expression analyses

For human samples, miRNA expression profiling was performed as described in Mestdagh et al. 2008. For murine samples, 60 ng of total RNA was reverse transcribed using the murine stem-loop megaplex pool A and B followed by limited cycle pre-amplification (Applied Biosystems). Expression of 430 human and 509 murine miRNAs was profiled using Taqman miRNA assays on a 7900HT detection system (Applied Biosystems). Data were normalized using the global mean (Mestdagh et al. 2009). miRNA expression data are available as RDML-files upon request (Lefever et al. 2009). Differentially expressed miRNAs were identified using the Mann-Whitney test followed by multiple testing correction according to the Benjamini-Hochberg algorithm. Hierarchical clustering was performed using method Ward and distance Manhattan. All statistical analyses were performed using R Bioconductor software.

6.8 Array-comparative genomic hybridization (array CGH)

Samples were profiled on a custom designed 44K/60K array (Agilent Technologies) enriched for miRNA and T-UCR regions and regions around cancer gene census genes. Utilizing random prime labeling (BioPrime ArrayCGH Genomic Labeling System, Invitrogen), 150 ng of test and control DNA (DNA from an EBV cell line if cell lines were tested or male control DNA, Promega if tumor samples were tested) was labeled with Cy3 and Cy5 dyes (GE healthcare). Slides were scanned using an Agilent scanner (Agilent Technologies) and an in-house developed visualization software program called arrayCGHbase (http://medgen.ugent.be/arrayCGHbase) was used for analysis (Menten et al. 2005). Array CGH profiles were evaluated by using the circular binary segmentation (CBS) algorithm.

6.9 Cell culture and inhibition of miRNAs

Retinoblastoma cell lines Weri and Y79 were authenticated by DNA fingerprinting (DMSZ, Braunschweig, Germany). Cells were cultured in suspension in Dulbecco's Modified Eagles Medium (DMEM) (Invitrogen), containing 15% FCS, Penicillin/Streptomycin, 4 mM L-Glutamin, 50 µM ß-Mercaptoethanol and 0.1% Insulin (all from Invitrogen). 1,5x 10^4 Weri and Y79 cells/well were seeded on 24-well plates and transfected with 25 pmol of specific antagomiRNAs or scrambled Cy3-labelled control oligos (Ambion) using siPORT NeoFX Transfection Agent (Ambion) according to the manufacturers recommendations. CellTiter-Glo Luminescence Cell Viability Assay was adapted from manufacturer's recommendation. Briefly, 30 µl of cell culture medium containing cells were transferred in an opaque-walled 96-well plate and equilibrated at room temperature for 30 min. An equivalent amount (30 µl) of CellTiter-Glo reagent was added to each well, mixed and incubated for 10 min before reading luminescence.

7. References

Abramson, D. H., K. Beaverson, et al. (2003). "Screening for retinoblastoma: presenting signs as prognosticators of patient and ocular survival." *Pediatrics* **112**: 1248-55.

Abramson, D. H., C. M. Frank, et al. (1998). "Presenting signs of retinoblastoma." *The Journal of pediatrics* **132**: 505-8.

Aerts, I., L. Lumbroso-Le Rouic, et al. (2006). "Retinoblastoma." *Orphanet J Rare Dis* **1**: 31.

Aguda, B. D., Y. Kim, et al. (2008). "MicroRNA regulation of a cancer network: consequences of the feedback loops involving miR-17-92, E2F, and Myc." *Proceedings of the National Academy of Sciences of the United States of America* **105**: 19678-83.

Albrecht, P., B. Ansperger-Rescher, et al. (2005). "Spectrum of gross deletions and insertions in the RB1 gene in patients with retinoblastoma and association with phenotypic expression." *Human mutation* **26**: 437-45.

Alexander, R. P., G. Fang, et al. (2010). "Annotating non-coding regions of the genome." *Nat Rev Genet* **11**(8): 559-71.

Anand, S., B. K. Majeti, et al. (2010). "MicroRNA-132-mediated loss of p120RasGAP activates the endothelium to facilitate pathological angiogenesis." *Nature medicine* **16**: 909-14.

Arrate, M. P., T. Vincent, et al. (2010). "MicroRNA Biogenesis Is Required for Myc-Induced B-Cell Lymphoma Development and Survival." *Cancer research*: 1-10.

Babiarz, J. E., J. G. Ruby, et al. (2008). "Mouse ES cells express endogenous shRNAs, siRNAs, and other Microprocessor-independent, Dicer-dependent small RNAs." *Genes & development* **22**: 2773-85.

Bader, J. L., a. T. Meadows, et al. (1982). "Bilateral retinoblastoma with ectopic intracranial retinoblastoma: trilateral retinoblastoma." *Cancer genetics and cytogenetics* **5**: 203-13.

Bader, J. L., R. W. Miller, et al. (1980). "Trilateral retinoblastoma." *Lancet* **2**: 582-3.

Bartkova, J., Z. Horejsi, et al. (2005). "DNA damage response as a candidate anti-cancer barrier in early human tumorigenesis." *Nature* **434**(7035): 864-70.

Bender, A. and J. R. Pringle (1991). "Use of a screen for synthetic lethal and multicopy suppressee mutants to identify two new genes involved in morphogenesis in Saccharomyces cerevisiae." *Mol Cell Biol* **11**(3): 1295-305.

Berezikov, E., W.-J. Chung, et al. (2007). "Mammalian mirtron genes." *Molecular cell* **28**: 328-36.

Berger, A. H., A. G. Knudson, et al. (2011). "A continuum model for tumour suppression." *Nature* **476**: 163-9.

Bernstein, E., S. Y. Kim, et al. (2003). "Dicer is essential for mouse development." *Nat Genet* **35**(3): 215-7.

Bommer, G. T., I. Gerin, et al. (2007). "p53-mediated activation of miRNA34 candidate tumor-suppressor genes." *Current biology : CB* **17**: 1298-307.

Bonci, D., V. Coppola, et al. (2008). "The miR-15a-miR-16-1 cluster controls prostate cancer by targeting multiple oncogenic activities." *Nat Med* **14**(11): 1271-7.

Boominathan, L. (2010a). "The guardians of the genome (p53, TA-p73, and TA-p63) are regulators of tumor suppressor miRNAs network." *Cancer Metastasis Rev* **29**(4): 613-39.

Boominathan, L. (2010b). "The tumor suppressors p53, p63, and p73 are regulators of microRNA processing complex." *PloS one* **5**: e10615.

Bowman, R. J. C., M. Mafwiri, et al. (2008). "Outcome of retinoblastoma in east Africa." *Pediatric blood & cancer* **50**: 160-2.

Braun, C. J., X. Zhang, et al. (2008). "p53-Responsive micrornas 192 and 215 are capable of inducing cell cycle arrest." *Cancer Res* **68**: 10094-10104.

Brennan, R. C., S. Federico, et al. (2011). "Targeting the p53 pathway in retinoblastoma with subconjunctival Nutlin-3a." *Cancer research* **71**: 4205-13.

Broaddus, E., A. Topham, et al. (2009). "Incidence of retinoblastoma in the USA: 1975-2004." *The British journal of ophthalmology* **93**: 21-3.

Burkhart, D. L. and J. Sage (2008). "Cellular mechanisms of tumour suppression by the retinoblastoma gene." *Nature reviews. Cancer* **8**: 671-82.

Calin, G. a. and C. M. Croce (2006). "MicroRNA signatures in human cancers." *Nature reviews. Cancer* **6**: 857-66.

Calin, G. A., C. D. Dumitru, et al. (2002). "Frequent deletions and down-regulation of micro-RNA genes miR15 and miR16 at 13q14 in chronic lymphocytic leukemia." *Proceedings of the National Academy of Sciences of the United States of America* **99**: 15524-9.

Canadian-Retinoblastoma-Society (2009). "National Retinoblastoma Strategy Canadian Guidelines for Care: Stratégie thérapeutique du rétinoblastome guide clinique canadien." *Canadian journal of ophthalmology. Journal canadien d'ophtalmologie* **44 Suppl 2**: S1-88.

Canturk, S., I. Qaddoumi, et al. (2010). "Survival of retinoblastoma in less-developed countries impact of socioeconomic and health-related indicators." *The British journal of ophthalmology* **94**: 1432-6.

Cao, Q., R.-S. Mani, et al. (2011). "Coordinated regulation of polycomb group complexes through microRNAs in cancer." *Cancer cell* **20**: 187-99.

Celli, J., H. van Bokhoven, et al. (2003). "Feingold syndrome: clinical review and genetic mapping." *Am J Med Genet A* **122A**(4): 294-300.

Chang, T.-C., E. A. Wentzel, et al. (2007). "Transactivation of miR-34a by p53 broadly influences gene expression and promotes apoptosis." *Molecular cell* **26**: 745-52.

Chang, T.-C., D. Yu, et al. (2008). "Widespread microRNA repression by Myc contributes to tumorigenesis." *Nature genetics* **40**: 43-50.

Cheloufi, S., C. O. Dos Santos, et al. (2010). "A dicer-independent miRNA biogenesis pathway that requires Ago catalysis." *Nature* **465**: 584-9.

Chipuk, J. E., T. Kuwana, et al. (2004). "Direct activation of Bax by p53 mediates mitochondrial membrane permeabilization and apoptosis." *Science* **303**(5660): 1010-4.

Cifuentes, D., H. Xue, et al. (2010). "A novel miRNA processing pathway independent of Dicer requires Argonaute2 catalytic activity." *Science (New York, N.Y.)* **328**: 1694-8.

Clarke, A. R., E. R. Maandag, et al. (1992). "Requirement for a functional Rb-1 gene in murine development." *Nature* **359**: 328-30.

Cole, K. A., E. F. Attiyeh, et al. (2008). "A functional screen identifies miR-34a as a candidate neuroblastoma tumor suppressor gene." *Molecular cancer research : MCR* **6**: 735-42.

Comings, D. E. (1973). "A general theory of carcinogenesis." *Proceedings of the National Academy of Sciences of the United States of America* **70**: 3324-8.

Conkrite, K., M. Sundby, et al. (2011). "miR-17~92 cooperates with RB pathway mutations to promote retinoblastoma." *Genes & development*.

Corney, D. C., A. Flesken-Nikitin, et al. (2007). "MicroRNA-34b and MicroRNA-34c are targets of p53 and cooperate in control of cell proliferation and adhesion-independent growth." *Cancer Res* **67**(18): 8433-8.

Corson, T. W. and B. L. Gallie (2007). "One hit, two hits, three hits, more? Genomic changes in the development of retinoblastoma." *Genes, chromosomes & cancer* **46**: 617-34.

Danovi, D., E. Meulmeester, et al. (2004). "Amplification of Mdmx (or Mdm4) directly contributes to tumor formation by inhibiting p53 tumor suppressor activity." *Mol Cell Biol* **24**: 5835-5843.

de Pontual, L., E. Yao, et al. (2011). "Germline deletion of the miR-17~92 cluster causes skeletal and growth defects in humans." *Nature genetics*.

Dews, M., A. Homayouni, et al. (2006). "Augmentation of tumor angiogenesis by a Myc-activated microRNA cluster." *Nature genetics* **38**: 1060-5.

DiCiommo, D., B. L. Gallie, et al. (2000). "Retinoblastoma: the disease, gene and protein provide critical leads to understand cancer." *Seminars in cancer biology* **10**: 255-69.

Diederichs, S. and D. A. Haber (2006). "Sequence variations of microRNAs in human cancer: alterations in predicted secondary structure do not affect processing." *Cancer research* **66**: 6097-104.

Dimaras, H., V. Khetan, et al. (2008). "Loss of RB1 induces non-proliferative retinoma: increasing genomic instability correlates with progression to retinoblastoma." *Human molecular genetics* **17**: 1363-72.

Dimaras, H., K. Kimani, et al. (2012). "Retinoblastoma." *Lancet*.

Dobzhansky, T. (1946). "Genetics of natural populations; recombination and variability in populations of Drosophila pseudoobscura." *Genetics* **31**: 269-90.

Donovan, S. L. and M. a. Dyer (2004). "Developmental defects in Rb-deficient retinae." *Vision research* **44**: 3323-33.

Donovan, S. L. and M. a. Dyer (2006). "Preparation and square wave electroporation of retinal explant cultures." *Nature protocols* **1**: 2710-8.

Donovan, S. L., B. Schweers, et al. (2006). "Compensation by tumor suppressor genes during retinal development in mice and humans." *BMC biology* **4**: 14.

Dryja, T. P., S. Friend, et al. (1986). "Genetic sequences that predispose to retinoblastoma and osteosarcoma." *Symposium on Fundamental Cancer Research* **39**: 115-9.

Dworakowska, D., E. Jassem, et al. (2004). "MDM2 gene amplification: a new independent factor of adverse prognosis in non-small cell lung cancer (NSCLC)." *Lung Cancer* **43**: 285-295.

Dyer, M. A. and R. Bremner (2005). "The search for the retinoblastoma cell of origin." *Nature reviews. Cancer* **5**: 91-101.

Ebi, H., T. Sato, et al. (2009). "Counterbalance between RB inactivation and miR-17-92 overexpression in reactive oxygen species and DNA damage induction in lung cancers." *Oncogene* **28**: 3371-9.

Elmen, J., M. Lindow, et al. (2008). "LNA-mediated microRNA silencing in non-human primates." *Nature* **452**(7189): 896-9.

Ender, C., A. Krek, et al. (2008). "A human snoRNA with microRNA-like functions." *Mol Cell* **32**(4): 519-28.

Esquela-Kerscher, A. and F. J. Slack (2006). "Oncomirs - microRNAs with a role in cancer." *Nature reviews. Cancer* **6**: 259-69.

Esteller, M. (2011). "Non-coding RNAs in human disease." *Nature reviews. Genetics* **12**: 861-74.

Fabbri, M., R. Garzon, et al. (2007). "MicroRNA-29 family reverts aberrant methylation in lung cancer by targeting DNA methyltransferases 3A and 3B." *Proceedings of the National Academy of Sciences of the United States of America* **104**: 15805-10.

Feingold, M., B. D. Hall, et al. (1997). "Syndrome of microcephaly, facial and hand abnormalities, tracheoesophageal fistula, duodenal atresia, and developmental delay." *Am J Med Genet* **69**(3): 245-9.

Feng, Z., C. Zhang, et al. (2011). "Tumor suppressor p53 meets microRNAs." *Journal of molecular cell biology* **3**: 44-50.

Ferrari, E., C. Lucca, et al. (2010). "A lethal combination for cancer cells: synthetic lethality screenings for drug discovery." *Eur J Cancer* **46**(16): 2889-95.

Fragkos, M. and P. Beard (2011). "Mitotic catastrophe occurs in the absence of apoptosis in p53-null cells with a defective G1 checkpoint." *PLoS ONE* **6**(8): e22946.

Francoz, S., P. Froment, et al. (2006). "Mdm4 and Mdm2 cooperate to inhibit p53 activity in proliferating and quiescent cells in vivo." *Proc Natl Acad Sci U S A* **103**: 3232-3237.

Friend, S. H., R. Bernards, et al. (1986). "A human DNA segment with properties of the gene that predisposes to retinoblastoma and osteosarcoma." *Nature* **323**: 643-6.

Gallie, B. L., R. M. Ellsworth, et al. (1982). "Retinoma: spontaneous regression of retinoblastoma or benign manifestation of the mutation?" *British journal of cancer* **45**: 513-21.

Ganguli, G. and B. Wasylyk (2003). "p53-independent functions of MDM2." *Mol Cancer Res* **1**(14): 1027-35.

Garcia, D., M. R. Warr, et al. (2011). "Validation of MdmX as a therapeutic target for reactivating p53 in tumors." *Genes & development* **25**: 1746-57.

Garzon, R., G. Marcucci, et al. (2010). "Targeting microRNAs in cancer: rationale, strategies and challenges." *Nature reviews. Drug discovery* **9**: 775-89.

Gebeshuber, C. A., K. Zatloukal, et al. (2009). "miR-29a suppresses tristetraprolin, which is a regulator of epithelial polarity and metastasis." *EMBO reports* **10**: 400-5.

Georges, S. A., M. C. Biery, et al. (2008). "Coordinated regulation of cell cycle transcripts by p53-Inducible microRNAs, miR-192 and miR-215." *Cancer Res* **68**(24): 10105-12.

Georgi, S. A. and T. A. Reh (2010). "Dicer is required for the transition from early to late progenitor state in the developing mouse retina." *Journal of Neuroscience* **30**: 4048.

Georgi, S. a. and T. A. Reh (2011). "Dicer is required for the maintenance of Notch signaling and gliogenic competence during mouse retinal development." *Developmental neurobiology*.

Goddard, a. G., J. E. Kingston, et al. (1999). "Delay in diagnosis of retinoblastoma: risk factors and treatment outcome." *The British journal of ophthalmology* **83**: 1320-3.

Gombos, D. S. and A. P. Chevez-Barrios (2007). "Current treatment and management of retinoblastoma." *Current oncology reports* **9**: 453-8.

Gonzalez, G. and R. R. Behringer (2009). "Dicer is required for female reproductive tract development and fertility in the mouse." *Mol Reprod Dev* **76**(7): 678-88.

Hainaut, P. and M. Hollstein (2000). "p53 and human cancer: the first ten thousand mutations." *Adv Cancer Res* **77**: 81-137.

Han, X., G. Garcia-Manero, et al. (2007). "HDM4 (HDMX) is widely expressed in adult pre-B acute lymphoblastic leukemia and is a potential therapeutic target." *Mod Pathol* **20**(1): 54-62.

Hanahan, D. and R. A. Weinberg (2000). "The hallmarks of cancer." *Cell* **100**: 57-70.

Hanahan, D. and R. A. Weinberg (2011). "Hallmarks of cancer: the next generation." *Cell* **144**: 646-74.

Harbour, J. W., S. L. Lai, et al. (1988). "Abnormalities in structure and expression of the human retinoblastoma gene in SCLC." *Science* **241**(4863): 353-7.

Hartman, J. L. t., B. Garvik, et al. (2001). "Principles for the buffering of genetic variation." *Science* **291**(5506): 1001-4.

Haupt, Y., R. Maya, et al. (1997). "Mdm2 promotes the rapid degradation of p53." *Nature* **387**: 296-299.

Hayashita, Y., H. Osada, et al. (2005). "A polycistronic microRNA cluster, miR-17-92, is overexpressed in human lung cancers and enhances cell proliferation." *Cancer research* **65**: 9628-32.

He, L., X. He, et al. (2007). "A microRNA component of the p53 tumour suppressor network." *Nature* **447**(7148): 1130-4.

He, L., J. M. Thomson, et al. (2005). "A microRNA polycistron as a potential human oncogene." *Nature* **435**: 828-33.

Hermeking, H. (2009). "The miR-34 family in cancer and apoptosis." *Cell Death Differ* **17**(2): 193-9.

Hill, D. A., J. Ivanovich, et al. (2009). "DICER1 mutations in familial pleuropulmonary blastoma." *Science (New York, N.Y.)* **325**: 965.

Hood, J. D., M. Bednarski, et al. (2002). "Tumor regression by targeted gene delivery to the neovasculature." *Science* **296**(5577): 2404-7.

Hu, W., C. S. Chan, et al. (2010). "Negative regulation of tumor suppressor p53 by microRNA miR-504." *Mol Cell* **38**(5): 689-99.

Isaac, C. E., S. M. Francis, et al. (2006). "The retinoblastoma protein regulates pericentric heterochromatin." *Molecular and cellular biology* **26**: 3659-71.

Ivanovska, I., A. S. Ball, et al. (2008). "MicroRNAs in the miR-106b family regulate p21/CDKN1A and promote cell cycle progression." *Mol Cell Biol* **28**(7): 2167-74.

Jacks, T., A. Fazeli, et al. (1992). "Effects of an Rb mutation in the mouse." *Nature* **359**(6393): 295-300.

Jonkers, J., R. Meuwissen, et al. (2001). "Synergistic tumor suppressor activity of BRCA2 and p53 in a conditional mouse model for breast cancer." *Nat Genet* **29**(4): 418-25.

Karube, Y., H. Tanaka, et al. (2005). "Reduced expression of Dicer associated with poor prognosis in lung cancer patients." *Cancer science* **96**: 111-5.

Kato, M. V., T. Shimizu, et al. (1996). "Loss of heterozygosity on chromosome 17 and mutation of the p53 gene in retinoblastoma." *Cancer letters* **106**: 75-82.

Kivelä, T. (2009). "The epidemiological challenge of the most frequent eye cancer: retinoblastoma, an issue of birth and death." *The British journal of ophthalmology* **93**: 1129-31.

Knudson, a. G. (1971). "Mutation and cancer: statistical study of retinoblastoma." *Proceedings of the National Academy of Sciences of the United States of America* **68**: 820-3.

Knudson, a. G. (2001). "Two genetic hits (more or less) to cancer." *Nature reviews. Cancer* **1**: 157-62.

Kohl, N. E., N. Kanda, et al. (1983). "Transposition and amplification of oncogene-related sequences in human neuroblastomas." *Cell* **35**(2 Pt 1): 359-67.

Kondo, Y., S. Kondo, et al. (1997). "Involvement of p53 and WAF1/CIP1 in gamma-irradiation-induced apoptosis of retinoblastoma cells." *Experimental cell research* **236**: 51-6.

Korhonen, H. M., O. Meikar, et al. (2011). "Dicer is required for haploid male germ cell differentiation in mice." *PLoS ONE* **6**(9): e24821.

Kota, S. K. and S. Balasubramanian (2010). "Cancer therapy via modulation of micro RNA levels: a promising future." *Drug discovery today* **00**: 1-8.

Krol, J., I. Loedige, et al. (2010). "The widespread regulation of microRNA biogenesis, function and decay." *Nature reviews. Genetics* **11**: 597-610.

Kruse, J. P. and W. Gu (2009). "Modes of p53 regulation." *Cell* **137**: 609-622.

Krutzfeldt, J., N. Rajewsky, et al. (2005). "Silencing of microRNAs in vivo with 'antagomirs'." *Nature* **438**(7068): 685-9.

Kubbutat, M. H., S. N. Jones, et al. (1997). "Regulation of p53 stability by Mdm2." *Nature* **387**(6630): 299-303.

Kumar, M. S., J. Lu, et al. (2007). "Impaired microRNA processing enhances cellular transformation and tumorigenesis." *Nature genetics* **39**: 673-7.

Kumar, M. S., R. E. Pester, et al. (2009). "Dicer1 functions as a haploinsufficient tumor suppressor." *Genes & development* **23**: 2700-4.

Lambertz, I., D. Nittner, et al. (2010). "Monoallelic but not biallelic loss of Dicer1 promotes tumorigenesis in vivo." *Cell death and differentiation* **17**: 633-41.

Laurie, N. a., S. L. Donovan, et al. (2006). "Inactivation of the p53 pathway in retinoblastoma." *Nature* **444**: 61-6.

Laurie, N. a., J. K. Gray, et al. (2005). "Topotecan combination chemotherapy in two new rodent models of retinoblastoma." *Clinical cancer research : an official journal of the American Association for Cancer Research* **11**: 7569-78.

Le, M. T., C. Teh, et al. (2009). "MicroRNA-125b is a novel negative regulator of p53." *Genes Dev* **23**(7): 862-76.

Leal-Leal, C., M. Flores-Rojo, et al. (2004). "A multicentre report from the Mexican Retinoblastoma Group." *The British journal of ophthalmology* **88**: 1074-7.

Lee, E. Y., C. Y. Chang, et al. (1992). "Mice deficient for Rb are nonviable and show defects in neurogenesis and haematopoiesis." *Nature* **359**: 288-94.

Lee, E. Y., H. To, et al. (1988). "Inactivation of the retinoblastoma susceptibility gene in human breast cancers." *Science* **241**(4862): 218-21.

Lee, R. C., R. L. Feinbaum, et al. (1993). "The C. elegans heterochronic gene lin-4 encodes small RNAs with antisense complementarity to lin-14." *Cell* **75**: 843-54.

Lee, W. H., A. L. Murphree, et al. (1984). "Expression and amplification of the N-myc gene in primary retinoblastoma." *Nature* **309**(5967): 458-60.

Lee, W. H., J. Y. Shew, et al. (1987). "The retinoblastoma susceptibility gene encodes a nuclear phosphoprotein associated with DNA binding activity." *Nature* **329**: 642-5.

Lefever, S., J. Hellemans, et al. (2009). "RDML: structured language and reporting guidelines for real-time quantitative PCR data." *Nucleic acids research* **37**: 2065-9.

Lenz, G., G. W. Wright, et al. (2008). "Molecular subtypes of diffuse large B-cell lymphoma arise by distinct genetic pathways." *Proceedings of the National Academy of Sciences of the United States of America* **105**: 13520-5.

Levine, A. J., C. A. Finlay, et al. (2004). "P53 is a tumor suppressor gene." *Cell* **116**(2 Suppl): S67-9, 1 p following S69.

Levine, A. J., W. Hu, et al. (2006). "The P53 pathway: what questions remain to be explored?" *Cell Death Differ* **13**(6): 1027-36.

Levine, A. J. and M. Oren (2009). "The first 30 years of p53: growing ever more complex." *Nat Rev Cancer* **9**: 749-758.

Li, J., P. Smyth, et al. (2007). "Comparison of miRNA expression patterns using total RNA extracted from matched samples of formalin-fixed paraffin-embedded (FFPE) cells and snap frozen cells." *BMC biotechnology* **7**: 36.

Li, Y., L. M. Vecchiarelli-Federico, et al. (2012). "The miR-17-92 cluster expands multipotent hematopoietic progenitors while imbalanced expression of its individual oncogenic miRNAs promotes leukemia in mice." *Blood*.

Liu, I. S., J. D. Chen, et al. (1994). "Developmental expression of a novel murine homeobox gene (Chx10): evidence for roles in determination of the neuroretina and inner nuclear layer." *Neuron* **13**(2): 377-93.

Longworth, M. S. and N. J. Dyson (2010). "pRb, a local chromatin organizer with global possibilities." *Chromosoma* **119**: 1-11.

Loya, C. M., C. S. Lu, et al. (2009). "Transgenic microRNA inhibition with spatiotemporal specificity in intact organisms." *Nature methods* **6**: 897-903.

Lu, J., G. Getz, et al. (2005). "MicroRNA expression profiles classify human cancers." *Nature* **435**: 834-8.

Lucchesi, J. C. (1968). "Synthetic lethality and semi-lethality among functionally related mutants of Drosophila melanfgaster." *Genetics* **59**(1): 37-44.

Lujambio, A. and S. W. Lowe (2012). "The microcosmos of cancer." *Nature* **482**: 347-55.

Luo, J., A. Y. Nikolaev, et al. (2001). "Negative control of p53 by Sir2alpha promotes cell survival under stress." *Cell* **107**(2): 137-48.

Ma, C. X., S. Cai, et al. (2012). "Targeting Chk1 in p53-deficient triple-negative breast cancer is therapeutically beneficial in human-in-mouse tumor models." *J Clin Invest* **122**(4): 1541-52.

Ma, L., J. Teruya-Feldstein, et al. (2007). "Tumour invasion and metastasis initiated by microRNA-10b in breast cancer." *Nature* **449**: 682-8.

Ma, L., J. Young, et al. (2010). "miR-9, a MYC/MYCN-activated microRNA, regulates E-cadherin and cancer metastasis." *Nature cell biology* **12**: 247-56.

Maatouk, D. M., K. L. Loveland, et al. (2008). "Dicer1 is required for differentiation of the mouse male germline." *Biol Reprod* **79**(4): 696-703.

MacCarthy, a., G. J. Draper, et al. (2006). "Retinoblastoma incidence and survival in European children (1978-1997). Report from the Automated Childhood Cancer Information System project." *European journal of cancer (Oxford, England : 1990)* **42**: 2092-102.

MacPherson, D., K. Conkrite, et al. (2007). "Murine bilateral retinoblastoma exhibiting rapid-onset, metastatic progression and N-myc gene amplification." *The EMBO journal* **26**: 784-94.

MacPherson, D., J. Sage, et al. (2003). "Conditional mutation of Rb causes cell cycle defects without apoptosis in the central nervous system." *Mol Cell Biol* **23**(3): 1044-53.

Maetens, M., G. Doumont, et al. (2007). "Distinct roles of Mdm2 and Mdm4 in red cell production." *Blood* **109**: 2630-2633.

Mahajan, A., A. Crum, et al. (2011). "Ocular neoplastic disease." *Seminars in ultrasound, CT, and MR* **32**: 28-37.

Mahoney, M. C., W. S. Burnett, et al. (1990). "The epidemiology of ophthalmic malignancies in New York State." *Ophthalmology* **97**: 1143-7.

Marcelis, C. L., F. A. Hol, et al. (2008). "Genotype-phenotype correlations in MYCN-related Feingold syndrome." *Hum Mutat* **29**(9): 1125-32.

Marcus, D. M., S. E. Brooks, et al. (1998). "Trilateral retinoblastoma: insights into histogenesis and management." *Survey of ophthalmology* **43**: 59-70.

Marine, J.-C., S. Francoz, et al. (2006). "Keeping p53 in check: essential and synergistic functions of Mdm2 and Mdm4." *Cell death and differentiation* **13**: 927-34.

Marino, S., M. Vooijs, et al. (2000). "Induction of medulloblastomas in p53-null mutant mice by somatic inactivation of Rb in the external granular layer cells of the cerebellum." *Genes Dev* **14**(8): 994-1004.

Marquardt, T., R. Ashery-Padan, et al. (2001). "Pax6 is required for the multipotent state of retinal progenitor cells." *Cell* **105**(1): 43-55.

Matsubara, H., T. Takeuchi, et al. (2007). "Apoptosis induction by antisense oligonucleotides against miR-17-5p and miR-20a in lung cancers overexpressing miR-17-92." *Oncogene* **26**: 6099-105.

Mavrakis, K. J., A. L. Wolfe, et al. (2010). "Genome-wide RNA-mediated interference screen identifies miR-19 targets in Notch-induced T-cell acute lymphoblastic leukaemia." *Nature cell biology* **12**: 372-9.

Mayo, L. D. and D. B. Donner (2001). "A phosphatidylinositol 3-kinase/Akt pathway promotes translocation of Mdm2 from the cytoplasm to the nucleus." *Proc Natl Acad Sci U S A* **98**(20): 11598-603.

McEvoy, J., J. Flores-Otero, et al. (2011). "Coexpression of normally incompatible developmental pathways in retinoblastoma genesis." *Cancer cell* **20**: 260-75.

Menten, B., F. Pattyn, et al. (2005). "arrayCGHbase: an analysis platform for comparative genomic hybridization microarrays." *BMC bioinformatics* **6**: 124.

Merritt, W. M., Y. G. Lin, et al. (2008). "Dicer, Drosha, and outcomes in patients with ovarian cancer." *The New England journal of medicine* **359**: 2641-50.

Mestdagh, P., A.-K. Boström, et al. (2010). "The miR-17-92 MicroRNA Cluster Regulates Multiple Components of the TGF-β Pathway in Neuroblastoma." *Molecular cell* **40**: 762-73.

Mestdagh, P., T. Feys, et al. (2008). "High-throughput stem-loop RT-qPCR miRNA expression profiling using minute amounts of input RNA." *Nucleic acids research* **36**: e143.

Mestdagh, P., P. Van Vlierberghe, et al. (2009). "A novel and universal method for microRNA RT-qPCR data normalization." *Genome biology* **10**: R64.

Migliorini, D., D. Danovi, et al. (2002). "Hdmx recruitment into the nucleus by Hdm2 is essential for its ability to regulate p53 stability and transactivation." *J Biol Chem* **277**: 7318-7323.

Mitchell, P. S., R. K. Parkin, et al. (2008). "Circulating microRNAs as stable blood-based markers for cancer detection." *Proceedings of the National Academy of Sciences of the United States of America* **105**: 10513-8.

Momand, J., D. Jung, et al. (1998). "The MDM2 gene amplification database." *Nucleic Acids Res* **26**: 3453-3459.

Mott, J. L., S. Kobayashi, et al. (2007). "mir-29 regulates Mcl-1 protein expression and apoptosis." *Oncogene* **26**(42): 6133-40.

Mu, P., Y.-C. Han, et al. (2009). "Genetic dissection of the miR-17~92 cluster of microRNAs in Myc-induced B-cell lymphomas." *Genes & development* **23**: 2806-11.

Mudhasani, R., A. N. Imbalzano, et al. (2010). "An essential role for Dicer in adipocyte differentiation." *J Cell Biochem* **110**(4): 812-6.

Mudhasani, R., V. Puri, et al. (2011). "Dicer is required for the formation of white but not brown adipose tissue." *J Cell Physiol* **226**(5): 1399-406.

Mudhasani, R., Z. Zhu, et al. (2008). "Loss of miRNA biogenesis induces p19Arf-p53 signaling and senescence in primary cells." *The Journal of cell biology* **181**: 1055-63.

Murchison, E. P., J. F. Partridge, et al. (2005). "Characterization of Dicer-deficient murine embryonic stem cells." *Proceedings of the National Academy of Sciences of the United States of America* **102**: 12135-40.

Murphy, E. A., B. K. Majeti, et al. (2008). "Nanoparticle-mediated drug delivery to tumor vasculature suppresses metastasis." *Proc Natl Acad Sci U S A* **105**(27): 9343-8.

Murphy, M., A. Hinman, et al. (1996). "Wild-type p53 negatively regulates the expression of a microtubule-associated protein." *Genes Dev* **10**(23): 2971-80.

Muthusamy, V., C. Hobbs, et al. (2006). "Amplification of CDK4 and MDM2 in malignant melanoma." *Genes Chromosomes Cancer* **45**: 447-454.

Nelson, P. T., D. A. Baldwin, et al. (2006). "RAKE and LNA-ISH reveal microRNA expression and localization in archival human brain." *RNA (New York, N.Y.)* **12**: 187-91.

Niederlaender, E. (2006). "Causes of death in the EU." Retrieved 18/04/2012, from http://epp.eurostat.ec.europa.eu/cache/ITY_OFFPUB/KS-NK-06-010/EN/KS-NK-06-010-EN.PDF.

Nikitina, E. G., L. N. Urazova, et al. (2012). "MicroRNAs AND HUMAN CANCER." *Experimental oncology* **34**: 2-8.

Nork, T. M., G. L. Poulsen, et al. (1997). "p53 regulates apoptosis in human retinoblastoma." *Archives of ophthalmology* **115**: 213-9.

Nyamori, J. M., K. Kimani, et al. (2012). "The incidence and distribution of retinoblastoma in Kenya." *The British journal of ophthalmology* **96**: 141-3.

O'Donnell, K. A., E. A. Wentzel, et al. (2005). "c-Myc-regulated microRNAs modulate E2F1 expression." *Nature* **435**: 839-43.

O'Rourke, J. R., S. a. Georges, et al. (2007). "Essential role for Dicer during skeletal muscle development." *Developmental biology* **311**: 359-68.

Okamura, K., J. W. Hagen, et al. (2007). "The mirtron pathway generates microRNA-class regulatory RNAs in Drosophila." *Cell* **130**: 89-100.

Olive, V., M. J. Bennett, et al. (2009). "miR-19 is a key oncogenic component of mir-17-92." *Genes & development* **23**: 2839-49.

Olive, V., I. Jiang, et al. (2010). "mir-17-92, a cluster of miRNAs in the midst of the cancer network." *The international journal of biochemistry & cell biology* **42**: 1348-1354.

Olivier, M., S. P. Hussain, et al. (2004). "TP53 mutation spectra and load: a tool for generating hypotheses on the etiology of cancer." *IARC Sci Publ*(157): 247-70.

Osada, H. and T. Takahashi (2011). "let-7 and miR-17-92: small-sized major players in lung cancer development." *Cancer science* **102**: 9-17.

Ota, A., H. Tagawa, et al. (2004). "Identification and characterization of a novel gene, C13orf25, as a target for 13q31-q32 amplification in malignant lymphoma." *Cancer Res* **64**(9): 3087-95.

Owoeye, J. F. A., E. A. O. Afolayan, et al. (2006). "Retinoblastoma--a clinico-pathological study in Ilorin, Nigeria." *African journal of health sciences* **13**: 117-23.

Pampalakis, G., E. P. Diamandis, et al. (2010). "Down-regulation of dicer expression in ovarian cancer tissues." *Clinical biochemistry* **43**: 324-7.

Park, S. Y., J. H. Lee, et al. (2009). "miR-29 miRNAs activate p53 by targeting p85 alpha and CDC42." *Nat Struct Mol Biol* **16**(1): 23-9.

Pekarsky, Y., U. Santanam, et al. (2006). "Tcl1 expression in chronic lymphocytic leukemia is regulated by miR-29 and miR-181." *Cancer Res* **66**(24): 11590-3.

Petitjean, A., E. Mathe, et al. (2007). "Impact of mutant p53 functional properties on TP53 mutation patterns and tumor phenotype: lessons from recent developments in the IARC TP53 database." *Hum Mutat* **28**: 622-629.

Petrocca, F., A. Vecchione, et al. (2008a). "Emerging role of miR-106b-25/miR-17-92 clusters in the control of transforming growth factor beta signaling." *Cancer Res* **68**(20): 8191-4.

Petrocca, F., R. Visone, et al. (2008b). "E2F1-regulated microRNAs impair TGFbeta-dependent cell-cycle arrest and apoptosis in gastric cancer." *Cancer cell* **13**: 272-86.

Pickering, M. T., B. M. Stadler, et al. (2009). "miR-17 and miR-20a temper an E2F1-induced G1 checkpoint to regulate cell cycle progression." *Oncogene* **28**: 140-5.

Pinter, R. and R. Hindges (2010). "Perturbations of microRNA function in mouse dicer mutants produce retinal defects and lead to aberrant axon pathfinding at the optic chiasm." *PloS one* **5**: e10021.

Poché, R. a. and B. E. Reese (2009). "Retinal horizontal cells: challenging paradigms of neural development and cancer biology." *Development (Cambridge, England)* **136**: 2141-51.

Portela, A. and M. Esteller (2010). "Epigenetic modifications and human disease." *Nature biotechnology* **28**: 1057-68.

Potenza, N., U. Papa, et al. (2010). "A novel splice variant of the human dicer gene is expressed in neuroblastoma cells." *FEBS Lett* **584**(15): 3452-7.

Poulaki, V. and S. Mukai (2009). "Retinoblastoma: genetics and pathology." *International ophthalmology clinics* **49**: 155-64.

Ragazzini, P., G. Gamberi, et al. (2004). "Amplification of CDK4, MDM2, SAS and GLI genes in leiomyosarcoma, alveolar and embryonal rhabdomyosarcoma." *Histol Histopathol* **19**: 401-411.

Raj, L., T. Ide, et al. (2011). "Selective killing of cancer cells by a small molecule targeting the stress response to ROS." *Nature* **475**: 231-234.

Raver-Shapira, N., E. Marciano, et al. (2007). "Transcriptional activation of miR-34a contributes to p53-mediated apoptosis." *Mol Cell* **26**: 731-743.

Richter, S., K. Vandezande, et al. (2003). "Sensitive and efficient detection of RB1 gene mutations enhances care for families with retinoblastoma." *American journal of human genetics* **72**: 253-69.

Rodrigues, K. E. S., M. d. R. D. O. Latorre, et al. (2004). "[Delayed diagnosis in retinoblastoma]." *Jornal de pediatria* **80**: 511-6.

Rowan, S. and C. L. Cepko (2004). "Genetic analysis of the homeodomain transcription factor Chx10 in the retina using a novel multifunctional BAC transgenic mouse reporter." *Developmental biology* **271**: 388-402.

Ruby, J. G., C. H. Jan, et al. (2007). "Intronic microRNA precursors that bypass Drosha processing." *Nature* **448**: 83-6.

Ruzankina, Y., D. W. Schoppy, et al. (2009). "Tissue regenerative delays and synthetic lethality in adult mice after combined deletion of Atr and Trp53." *Nature genetics* **41**: 1144-9.

Sablina, A. a., A. V. Budanov, et al. (2005). "The antioxidant function of the p53 tumor suppressor." *Nature medicine* **11**: 1306-13.

Sachdeva, M., S. Zhu, et al. (2009). "p53 represses c-Myc through induction of the tumor suppressor miR-145." *Proc Natl Acad Sci U S A* **106**(9): 3207-12.

Sage, J. and A. Ventura (2011). "miR than meets the eye." *Genes & development* **25**: 1663-7.

Saito, Y., G. Liang, et al. (2006). "Specific activation of microRNA-127 with downregulation of the proto-oncogene BCL6 by chromatin-modifying drugs in human cancer cells." *Cancer cell* **9**: 435-43.

Schlamp, C. L., G. L. Poulsen, et al. (1997). "Nuclear exclusion of wild-type p53 in immortalized human retinoblastoma cells." *Journal of the National Cancer Institute* **89**: 1530-6.

Schulte, J. H., S. Horn, et al. (2008). "MYCN regulates oncogenic MicroRNAs in neuroblastoma." *International journal of cancer. Journal international du cancer* **122**: 699-704.

Seoane, M., P. Iglesias, et al. (2008). "Retinoblastoma loss modulates DNA damage response favoring tumor progression." *PLoS ONE* **3**(11): e3632.

Shamma, A., Y. Takegami, et al. (2009). "Rb Regulates DNA damage response and cellular senescence through E2F-dependent suppression of N-ras isoprenylation." *Cancer cell* **15**(4): 255-69.

Sherr, C. J. and F. McCormick (2002). "The RB and p53 pathways in cancer." *Cancer cell* **2**: 103-12.

Singh, M. K., M. M. Lu, et al. (2011). "MicroRNA-processing enzyme Dicer is required in epicardium for coronary vasculature development." *The Journal of biological chemistry* **286**: 41036-45.

Soussi, T. (2007). "p53 alterations in human cancer: more questions than answers." *Oncogene* **26**: 2145-56.

Soussi, T. and C. Béroud (2001). "Assessing TP53 status in human tumours to evaluate clinical outcome." *Nature reviews. Cancer* **1**: 233-40.

Squire, J., A. D. Goddard, et al. (1986). "Tumour induction by the retinoblastoma mutation is independent of N-myc expression." *Nature* **322**(6079): 555-7.

Suárez, Y., C. Fernández-Hernando, et al. (2008). "Dicer-dependent endothelial microRNAs are necessary for postnatal angiogenesis." *Proceedings of the National Academy of Sciences of the United States of America* **105**: 14082-7.

Suzuki, H. I. and K. Miyazono (2010). "Dynamics of microRNA biogenesis: crosstalk between p53 network and microRNA processing pathway." *Journal of molecular medicine (Berlin, Germany)* **88**: 1085-94.

Suzuki, H. I., K. Yamagata, et al. (2009). "Modulation of microRNA processing by p53." *Nature* **460**: 529-33.

Sylvestre, Y., V. De Guire, et al. (2007). "An E2F/miR-20a autoregulatory feedback loop." *The Journal of biological chemistry* **282**: 2135-43.

Talluri, S., C. E. Isaac, et al. (2010). "A G1 checkpoint mediated by the retinoblastoma protein that is dispensable in terminal differentiation but essential for senescence." *Molecular and cellular biology* **30**: 948-60.

Tamboli, A., M. J. Podgor, et al. (1990). "The incidence of retinoblastoma in the United States: 1974 through 1985." *Archives of ophthalmology* **108**: 128-32.

Tang, K.-F., H. Ren, et al. (2008). "Decreased Dicer expression elicits DNA damage and up-regulation of MICA and MICB." *The Journal of cell biology* **182**: 233-9.

Tanzer, A. and P. F. Stadler (2004). "Molecular evolution of a microRNA cluster." *J Mol Biol* **339**(2): 327-35.

Tarasov, V., P. Jung, et al. (2007). "Differential regulation of microRNAs by p53 revealed by massively parallel sequencing: miR-34a is a p53 target that induces apoptosis and G1-arrest." *Cell Cycle* **6**(13): 1586-93.

Tasdemir, E., M. C. Maiuri, et al. (2008). "Regulation of autophagy by cytoplasmic p53." *Nat Cell Biol* **10**: 676-687.

Tavazoie, S. F., C. Alarcón, et al. (2008). "Endogenous human microRNAs that suppress breast cancer metastasis." *Nature* **451**: 147-52.

Tazawa, H., N. Tsuchiya, et al. (2007). "Tumor-suppressive miR-34a induces senescence-like growth arrest through modulation of the E2F pathway in human colon cancer cells." *Proc Natl Acad Sci U S A* **104**(39): 15472-7.

Thomson, J. M., M. Newman, et al. (2006). "Extensive post-transcriptional regulation of microRNAs and its implications for cancer." *Genes & development* **20**: 2202-7.

Toledo, F. and G. M. Wahl (2006). "Regulating the p53 pathway: in vitro hypotheses, in vivo veritas." *Nature reviews. Cancer* **6**: 909-23.

Tong, A. H., M. Evangelista, et al. (2001). "Systematic genetic analysis with ordered arrays of yeast deletion mutants." *Science* **294**(5550): 2364-8.

Trichonas, G., Y. Murakami, et al. (2010). "Receptor interacting protein kinases mediate retinal detachment-induced photoreceptor necrosis and compensate for inhibition of apoptosis." *Proc Natl Acad Sci U S A* **107**(50): 21695-700.

Tronche, F., C. Kellendonk, et al. (1999). "Disruption of the glucocorticoid receptor gene in the nervous system results in reduced anxiety." *Nat Genet* **23**(1): 99-103.

Uziel, T., F. V. Karginov, et al. (2009). "The miR-17~92 cluster collaborates with the Sonic Hedgehog pathway in medulloblastoma." *Proceedings of the National Academy of Sciences of the United States of America* **106**: 2812-7.

Valastyan, S., F. Reinhardt, et al. (2009). "A pleiotropically acting microRNA, miR-31, inhibits breast cancer metastasis." *Cell* **137**: 1032-46.

van Bokhoven, H., J. Celli, et al. (2005). "MYCN haploinsufficiency is associated with reduced brain size and intestinal atresias in Feingold syndrome." *Nat Genet* **37**(5): 465-7.

van Haaften, G. and R. Agami (2010). "Tumorigenicity of the miR-17-92 cluster distilled." *Genes & development* **24**: 1-4.

van Kouwenhove, M., M. Kedde, et al. (2011). "MicroRNA regulation by RNA-binding proteins and its implications for cancer." *Nature reviews. Cancer* **11**: 644-56.

Varambally, S., Q. Cao, et al. (2008). "Genomic loss of microRNA-101 leads to overexpression of histone methyltransferase EZH2 in cancer." *Science* **322**(5908): 1695-9.

Ventura, A., A. G. Young, et al. (2008). "Targeted deletion reveals essential and overlapping functions of the miR-17 through 92 family of miRNA clusters." *Cell* **132**: 875-86.

Vogelstein, B., D. Lane, et al. (2000). "Surfing the p53 network." *Nature* **408**: 307-310.

Volinia, S., G. A. Calin, et al. (2006). "A microRNA expression signature of human solid tumors defines cancer gene targets." *Proc Natl Acad Sci U S A* **103**(7): 2257-61.

Vousden, K. H. and D. P. Lane (2007). "p53 in health and disease." *Nat Rev Mol Cell Biol* **8**: 275-283.

Vousden, K. H. and C. Prives (2009). "Blinded by the Light: The Growing Complexity of p53." *Cell* **137**: 413-431.

Vousden, K. H. and K. M. Ryan (2009). "p53 and metabolism." *Nat Rev Cancer* **9**: 691-700.

Wallace, V. A. (2006). "Cancer biology: second step to retinal tumours." *Nature* **444**: 45-6.

Weidle, U. H., D. Maisel, et al. (2011). "Synthetic lethality-based targets for discovery of new cancer therapeutics." *Cancer genomics & proteomics* **8**: 159-71.

Wightman, B., I. Ha, et al. (1993). "Posttranscriptional regulation of the heterochronic gene lin-14 by lin-4 mediates temporal pattern formation in C. elegans." *Cell* **75**: 855-62.

Windle, J. J., D. M. Albert, et al. (1990). "Retinoblastoma in transgenic mice." *Nature* **343**: 665-9.

Winter, J., S. Jung, et al. (2009). "Many roads to maturity: microRNA biogenesis pathways and their regulation." *Nature cell biology* **11**: 228-34.

Woods, K., J. M. Thomson, et al. (2007). "Direct regulation of an oncogenic micro-RNA cluster by E2F transcription factors." *The Journal of biological chemistry* **282**: 2130-4.

Xi, Y., G. Nakajima, et al. (2007). "Systematic analysis of microRNA expression of RNA extracted from fresh frozen and formalin-fixed paraffin-embedded samples." *RNA (New York, N.Y.)* **13**: 1668-74.

Xiao, C., L. Srinivasan, et al. (2008). "Lymphoproliferative disease and autoimmunity in mice with increased miR-17-92 expression in lymphocytes." *Nature immunology* **9**: 405-14.

Xiong, S., V. Pant, et al. (2010). "Spontaneous tumorigenesis in mice overexpressing the p53-negative regulator Mdm4." *Cancer research* **70**: 7148-54.

Xu, X. L., Y. Fang, et al. (2009). "Retinoblastoma has properties of a cone precursor tumor and depends upon cone-specific MDM2 signaling." *Cell* **137**: 1018-31.

Yamakuchi, M., M. Ferlito, et al. (2008). "miR-34a repression of SIRT1 regulates apoptosis." *Proc Natl Acad Sci U S A* **105**(36): 13421-6.

Yamakuchi, M., C. D. Lotterman, et al. "P53-induced microRNA-107 inhibits HIF-1 and tumor angiogenesis." *Proc Natl Acad Sci U S A* **107**(14): 6334-9.

Yan, H.-l., G. Xue, et al. (2009). "Repression of the miR-17-92 cluster by p53 has an important function in hypoxia-induced apoptosis." *The EMBO journal* **28**: 2719-32.

Yang, J.-S., T. Maurin, et al. (2010). "Conserved vertebrate mir-451 provides a platform for Dicer-independent, Ago2-mediated microRNA biogenesis." *Proceedings of the National Academy of Sciences of the United States of America* **107**: 15163-8.

Yi, R., D. O'Carroll, et al. (2006). "Morphogenesis in skin is governed by discrete sets of differentially expressed microRNAs." *Nature genetics* **38**: 356-62.

You, H., K. Yamamoto, et al. (2006). "Regulation of transactivation-independent proapoptotic activity of p53 by FOXO3a." *Proc Natl Acad Sci U S A* **103**(24): 9051-6.

Young, J. L., M. A. Smith, et al. (1999). "Retinoblastoma - SEER Pediatric Monograph." *ICCC V*.

Young, R. W. (1985). "Cell proliferation during postnatal development of the retina in the mouse." *Brain research* **353**: 229-39.

Zehir, A., L. L. Hua, et al. (2010). "Dicer is required for survival of differentiating neural crest cells." *Dev Biol* **340**(2): 459-67.

Zhang, C. C., J. M. Yang, et al. (1999). "DNA damage increases sensitivity to vinca alkaloids and decreases sensitivity to taxanes through p53-dependent repression of microtubule-associated protein 4." *Cancer Res* **59**(15): 3663-70.

Zhang, C. C., J. M. Yang, et al. (1998). "The role of MAP4 expression in the sensitivity to paclitaxel and resistance to vinca alkaloids in p53 mutant cells." *Oncogene* **16**(12): 1617-24.

Zhang, J., C. A. Benavente, et al. (2012). "A novel retinoblastoma therapy from genomic and epigenetic analyses." *Nature*.

Zhang, J., J. Gray, et al. (2004a). "Rb regulates proliferation and rod photoreceptor development in the mouse retina." *Nature genetics* **36**: 351-360.

Zhang, J., B. Schweers, et al. (2004b). "The first knockout mouse model of retinoblastoma." *Cell cycle (Georgetown, Tex.)* **3**: 952-9.

Zhou, B. P., Y. Liao, et al. (2001). "HER-2/neu induces p53 ubiquitination via Akt-mediated MDM2 phosphorylation." *Nat Cell Biol* **3**: 973-982.

Zhu, Q., W. Sun, et al. (2011). "Sponge transgenic mouse model reveals important roles for the microRNA-183 (miR-183)/96/182 cluster in postmitotic photoreceptors of the retina." *The Journal of biological chemistry* **286**: 31749-60.

List of Abbreviations

3’UTR	3’untranslated region
5’UTR	5’untranslated region
Ago2	Argonaute 2
AKT	v-akt murine thymoma viral oncogene homolog 1
AKT-2	v-akt murine thymoma viral oncogene homolog 2
AP	alkaline phosphatase
array CGH	array-comparative genomic hybridization
Atm	Ataxia telangiectasia mutated
Atr	Ataxia telangiectasia and Rad3 related protein
BAC	bacterial artificial chromosome
Bax	Bcl2-Associated X protein
BCIP	5-Bromo-4-chloro-3-indolyl-phosphate
Bcl2	B-cell lymphoma/leukemia-2 gene
BCL6	B-cell CLL/lymphoma 6
Bim	BCL2-like 11
bp	base pairs
BrdU	5-Bromo-2‘-deoxyUridine
Casp-3*	cleaved form of Caspase-3
Cdc2	cell division control 2
CDC7	cell division cycle 7 homolog
CDK	cyclin dependent kinase
CDK4	cyclin-dependent kinases 4
CDK6	cyclin-dependent kinases 6
cDNA	complementary deoxyribonucleic acid
Chk1	checkpoint Kinase 1
Chk2	checkpoint Kinase 2
Chx10	ceh-10 homeo domain containing homolog (C. elegans)
CLL	chronic lymphocytic leukemia
CpG	regions of DNA where a cytosine nucleotide occurs next to a guanine nucleotide
Cre	Cre recombinase
CTGF	connective tissue growth factor

CUL5	cullin 5
Da	Dalton
DAPI	4',6-diamidino-2-phenylindole
ddH_2O	double distilled water
DDR	DNA damage response
DGCR8	DiGeorge syndrome critical region gene 8
DicKO	*Chx10Cre*; *Dicer1*$^{lox/lox}$
DKO	*Chx10Cre; Rb1*$^{lox/lox}$*; p107*$^{-/-}$
DKO; Mdm4Tg	*Chx10Cre; Rb1*$^{lox/lox}$*; p107*$^{-/-}$*; Mdm4*^{Tg}
DKO; p53KO	*Chx10Cre; Rb1*$^{lox/lox}$*; p107*$^{-/-}$*; p53*$^{lox/lox}$
DKO; p53KO; miR-17~92KO	*Chx10Cre; Rb1*$^{lox/lox}$*; p107*$^{-/-}$*; p53*$^{lox/lox}$*; miR-17~92*$^{lox/lox}$
DLBCL	diffused B-Cell lymphoma
DMEM	Dulbecco's Modified Eagles Medium
DMSO	dimethyl sulfoxide
DNA	deoxyribonucleic acid
DNMT3A	DNA (cytosine-5-)-methyltransferase 3 alpha
DNMT3B	DNA (cytosine-5-)-methyltransferase 3 beta
dNTP	deoxyribonucleotid triphosphate
dor	deep orange *[Drosophila melanogaster]*
ds	double stranded
dsRBP	dsRNA-binding protein
E	embryonic day
E2	ubiquitin conjugating enzyme
E2F	E2F transcription factor
EGFR	epidermal growth factor receptor
ES cell(s)	embryonic stem cell(s)
EthOH	ethanol
EtOH	ethanol
Ex.	excised
FACS	fluorescence-activated cell sorting
FCS	fetal calf serum
Fl.	floxed
FOXO3a	forkhead box O3
GCL	ganglion cell layer

GFP	green fluorescence protein
h	hour
H&E	Haematoxylin & Eosin
H_2O	water
H3K27	lysine 27 on histone H3
HA-Ras	v-Ha-ras Harvey rat sarcoma viral oncogene homolog
HDM2	human orthologue of Murine double minute 2
HDMx/HDM4	human orthologue of Murine double minute x / 4
HIF1	hypoxia inducible factor 1
HIF-1beta	hypoxia inducible factor 1 beta
hnRNP	heterogeneous nuclear ribonucleoprotein
Hs	Homo sapiens
IHC	immunohistochemistry
INL	inner nuclear layer
INL	inner nuclear layer
IPL	inner plexiform layer
IRES	internal ribosomal entry side
kDa	kiloDalton
KO	knock-out
K-Ras	v-Ki-ras2 Kirsten rat sarcoma viral oncogene homolog
lincRNAs	long non-coding RNAs (long ncRNAs)
lncRNAs	long non-coding RNAs (long ncRNAs)
MAD2L1	MAD2 mitotic arrest deficient-like 1 (yeast)
MAP-4	microtubule-associated protein-4
Mdm2	Mouse/Murine double minute 2
Mdmx/Mdm4	Mouse/Murine double minute x / 4
$MgCl_2$	magnesium chloride
min	minute
miR	microRNA
miR-17~92	microRNA cluster *miR-17~92*
miR-17~92KO	*Chx10Cre; miR-17~92$^{lox/lox}$*
miRISC	RISC with incorporated miRNA
miRNA	microRNA
mirtrons	microRNA located in an intron

Mm	Mus musculus
mRNA	messenger ribonucleic acid
mTOR	mechanistic target of rapamycin
Myc/c-Myc	Myelocytomatosis (cellular) oncogene
MYCN	v-myc myelocytomatosis viral related oncogene, neuroblastoma derived (avian)
NAC	*N*-Acetyl-L-cysteine
NaCl	sodium chloride
NBT	4-Nitro blue tetrazolium chloride
ncRNA	non-coding ribonucleic acid
NFL	nerve fiber layer
NLS	nuclear localization signal
Notch1	Notch gene homolog 1 (Drosophila)
N-Ras	neuroblastoma RAS viral [V-Ras] oncogene homolog
NSCLC	non-small cell lung cancer
NSCLC	non-small cell lung cancer
nt	nucleotides
o/n	over night
OLM	outer limiting membrane
oncomiR-1	microRNA cluster *miR-17~92*
ONL	outer nuclear layer
ONL	outer nuclear layer
OPL	outer plexiform layer
OPL	outer plexiform layer
OS	outer segments
P	postnatal day
p.a.	pro analysi
p21	cyclin-dependent kinase inhibitor 1A (CDKN1A, Cip1)
p53	53 kDa tumour protein [*Homo sapiens* and *Mus musculus*]
p53KO	*Chx10Cre; p53$^{lox/lox}$*
p57	cyclin-dependent kinase inhibitor 1C (CDKN1C, Kip2)
p63	63 kDa tumour protein
p73	73 kDa tumour protein

PAI-1	plasminogen activator inhibitor-1
PBS	phosphate buffered saline
PCR	polymerase chain reaction
PCR2	polycomb repressive complex 2
PI3K	PI3 kinase
Pirh2	p53-induced RING-H2 domain
piRNAs	Piwi-interacting RNA
PR	photoreceptors
PTEN	phosphatase and tensin homolog
Puma	p53-upregulated modulator of apoptosis
Puro	puromycin
QKO	*Chx10Cre; $Rb1^{lox/lox}$; $p107^{-/-}$; $p53^{lox/lox}$; $Dicer1^{lox/lox}$*
qPCR	quantitative polymerase chain reaction
Ras	rat sarcoma viral oncogene homolog
Rb	retinoblastoma 1
Rb1	retinoblastoma 1
RBL15	retinoblastoma cell line 15
RE	responsive element
RING	really interesting new gene [domain]
RNA	ribonucleic acid
rNTP	ribonucleotide tri-phosphate
ROS	reactive oxygen species
RPC	retinal progenitor cell
RPE	retinal pigmented epithelium
rpm	rotation per minute
rRNA	ribosomal RNA
RT	room temperature
RT	room temperature
RT	reverse transcription
RT-qPCR	reverse transcription quantitative PCR
ry	rosy *[Drosophila melanogaster]*
sh	short hairpin
siRNA	small interfering RNA
SIRT1	silent information regulator 1

SMAD2	SMAD family member 2
SMAD4	SMAD family member 4
snoRNA	small nucleolar RNAs
SNP	single nucleotide polymorphism
TGFβ	transforming growth factor β
TGFβR2	transforming growth factor β receptor 2
TIGAR	TP53-induced glycolysis and apoptosis regulator (C12orf5)
TP53	tumor protein 53, gene encoding for human p53 protein
TRBP	human immunodeficiency virus transactivating response RNA-binding protein
Tris	tris(hydroxymethyl)aminomethane
tRNAs	transfer ribonucleic acid
Trp53	tumor related protein 53, gene encoding for murine p53 protein
Tsp1	tumor suppressor region 1
T-UCR	transcribed ultraconserved regions
UTR	untranslated region
Vinc	vinculin
w/o	without
WERI-Rb1	retinoblastoma cell line from Wills Eye Research Institute
wk	week
WT	*wild-type*
XPO5	Exportin 5
Y79	retinoblastoma cell line Y79
ZFP36	zinc finger protein 36, C3H type, homolog (mouse)
α-	anti- (used to indicate specificity of an antibody)

List of Figures and Tables

Addendum

Curriculum Vitae

Personal information

First Name: David

Surname: Nittner

E-mail: david.nittner@gmail.com

Born: 16/05/1981, Heidelberg

Citizenship: German

Education

2007-2012: PhD in Biotechnology
Faculty of Sciences, Ghent University, Belgium
Promoter Prof. Dr. Jean-Christophe Marine,
Laboratory for Molecular Cancer Biology, VIB-KU Leuven

2001-2007: Biochemistry at Eberhard Karls University Tübingen, Germany
Major subject: Biochemistry, final grade: 1.3 (very good)
Minors: Organic Chemistry and Microbiology
Diploma Thesis: final grade: 1.0 (very good)

2004-2005: Studies in Biochemistry at University of Oulu, Finland
(1 academic year)

2000: High school graduation, score: 1.0 (very good),
Justus-Knecht-Gymnasium, Bruchsal, Germany

Scholarships

2007-2011: "VIB International Ph.D. Program 2007"

Each year, VIB selects 4 candidates amongst participants from all over the world for a fully funded 4-year Ph.D. program with challenging interdisciplinary research projects.

2001-2003: "Jubiläums-Stipendium der Stiftung Stipendien-Fonds des Verbandes der Chemischen Industrie"

The scholarship selects students based on their grades and motivation to financially support them in their first years of chemistry or biochemistry studies.

Scientific courses

2012:	Course for Communication & Presentation Techniques, VIB
2009:	Course for qPCR experiment design and data-analysis, Biogazelle
2009:	Effective writing for life sciences research, VIB
2008/2009:	Basic course in laboratory animal science, Ghent University

Language Knowledge

German (native language), English (fluent), Dutch (fluent), French (basic knowledge)

Extracurricular Activities

Sports: Running marathons is my passion since 2008. Per year I participate in two international competitions. In 2010, I ran the London and New York marathons. In London, I could reach my aspired goal of 2 h 50 min for the 42.195 kilometers.

University: In 2010, I organized together with other Ph.D. students an international Ph.D. student symposium for 300 participants. During the time of one year to prepare for the symposium, I was responsible for creating the website, handling the registration process and managing the contacts with the international participants. Being in the close contact with over 50 international students, I was the one to answer all their questions, and help them to organize their trip to the symposium.

Publications

Nittner, D., I. Lambertz, et al. (submitted and under revision). "Synthetic lethality between *Rb1*, *p53* and *miR-17~92* uncovers a therapeutic strategy for retinoblastoma"

Lambertz, I., **D. Nittner**, et al. (2010). "Monoallelic but not biallelic loss of Dicer1 promotes tumorigenesis in vivo." *Cell death and differentiation* **17**: 633-41.

Mestdagh, P., E. Fredlund, F. Pattyn, A. Rihani, T. Van Maerken, J. Vermeulen, C. Kumps, B. Menten, K. De Preter, A. Schramm, J. Schulte, R. Noguera, G. Schleiermacher, I. Janoueix-Lerosey, G. Laureys, R. Powel, **D. Nittner**, J-C. Marine, M. Ringnér, F. Speleman, J. Vandesompele. (2010). "An integrative genomics screen uncovers ncRNA T-UCR functions in neuroblastoma tumours." *Oncogene* **29**: 3583-92.

Supplementary tables

Table S 1: Differential miRNA expression in *DKO; p53KO* mouse tumors compared to normal *WT* and *DKO* retina.

miRNA	Tumor vs. normal *WT* retina		Tumor vs. *DKO* retina	
	fold change	p value	fold change	p value
let-7a	0.7343	0.2731	0.8951	0.6916
let-7a*	5.5008	0.0196	5.4160	0.0219
let-7b	3.5353	0.0104	2.7801	0.0444
let-7c	3.3595	0.0292	2.4385	0.0688
let-7c-1*	4.7413	0.1266	3.8934	0.1699
let-7d	1.2341	0.2978	1.1728	0.4568
let-7d*	0.3691	0.0889	0.5310	0.1190
let-7e	1.2841	0.1645	1.3964	0.1413
let-7f	0.9447	0.7769	1.0098	0.9756
let-7g	1.1351	0.3763	1.3151	0.2585
let-7g*	2.6332	0.1036	4.1443	0.0723
let-7i	1.9470	0.0480	1.3034	0.2393
let-7i*	1.3935	0.5647	2.1864	0.2727
miR-1	0.7931	0.8285	0.9531	0.9756
miR-100	2.1246	0.2997	1.6061	0.5144
miR-101	2.4264	0.0290	2.8409	0.1323
miR-101b	2.2882	0.0312	2.5512	0.1502
miR-103	1.3049	0.3953	1.1150	0.7553
miR-106a	51.8873	0.0092	22.4349	0.0444
miR-106b	6.4755	0.0088	5.2269	0.0372
miR-106b*	9.8449	0.0057	7.6453	0.0937
miR-107	0.5165	0.0760	0.4898	0.0747
miR-10a	3.0074	0.1099	3.0074	0.1206
miR-122	2.4119	0.0683	1.8763	0.1940
miR-124*	0.3852	0.0930	2.1835	0.2348
miR-124a	0.2011	0.0131	0.4223	0.0905
miR-125a-3p	0.9347	0.8680	0.8781	0.7553
miR-125a-5p	1.5965	0.0813	1.3909	0.1699
miR-125b	1.0885	0.8860	0.8184	0.7691
miR-125b-1*	1.7703	0.4574	0.8311	0.8301
miR-125b*	5.2976	0.0623	4.6258	0.0846
miR-126	2.6622	0.0292	4.8792	0.0442
miR-126*	1.8118	0.0889	3.2637	0.0487
miR-127	0.7214	0.4563	0.7071	0.5144
miR-127-5p	0.6506	0.3709	1.0578	0.9399
miR-128a	0.6823	0.3889	0.6545	0.3985
miR-129	0.1129	0.0091	0.1619	0.0318
miR-129-3p	0.0960	0.1318	0.1375	0.1847
miR-130a	1.7142	0.0092	1.9926	0.0083
miR-130b	0.5842	0.2181	0.7669	0.5459
miR-130b*	0.6481	0.3506	0.9290	0.8843
miR-132	1.6104	0.0719	1.9958	0.0450
miR-133a	1.2096	0.8576	1.3416	0.7846
miR-133b	0.8194	0.8168	0.9131	0.9271
miR-134	2.5336	0.0828	2.1828	0.1324
miR-135a	0.9470	0.8970	0.7118	0.5144
miR-135b	2.6951	0.0569	2.0552	0.1018

miR-136	1.4548	0.3691	1.8247	0.3394
miR-136*	0.8886	0.8697	1.1953	0.8465
miR-137	4.2927	0.0293	3.8413	0.0625
miR-138	0.7746	0.4041	0.7345	0.3998
miR-138*	1.0670	0.8970	1.2778	0.6890
miR-139-5p	0.9318	0.8680	0.7975	0.6584
miR-140	2.7350	0.1081	3.0591	0.0936
miR-140-3p	2.7475	0.1102	3.5982	0.0819
miR-141	1.9100	0.2255	1.9100	0.2420
miR-141*	0.7391	0.3384	0.8206	0.3060
miR-142-3p	16.5844	0.0092	4.8252	0.0492
miR-142-5p	1.7644	0.2518	1.7644	0.2682
miR-143	0.9446	0.8674	1.9855	0.2727
miR-145	0.8744	0.4370	2.0195	0.2727
miR-146a	11.1182	0.0022	3.3848	0.1699
miR-146b	7.6094	0.0257	3.4858	0.1569
miR-146b*	5.4212	0.0341	3.3572	0.2727
miR-148a	1.4194	0.1722	1.5505	0.1702
miR-148b	0.4966	0.0192	0.7019	0.2607
miR-149	1.4135	0.5537	1.0701	0.9271
miR-150	1.0775	0.8500	1.6054	0.4218
miR-151	1.4434	0.1206	1.9562	0.0450
miR-152	1.8558	0.0773	2.1003	0.0759
miR-153	0.9731	0.9182	1.0123	0.9756
miR-154	0.4132	0.3501	0.2693	0.0487
miR-154*	1.4639	0.3501	1.4097	0.4255
miR-155	5.9336	0.0151	5.0468	0.1346
miR-15a	0.7947	0.3656	1.5964	0.1408
miR-15a*	6.4584	0.0151	7.1785	0.0330
miR-15b	5.4531	0.0425	4.6019	0.1193
miR-15b*	63.1923	0.0049	54.2893	0.0715
miR-16	3.0333	0.0311	5.1577	0.0219
miR-16*	33.0051	0.0049	18.2245	0.0688
miR-17	47.5831	0.0030	21.5527	0.0487
miR-17*	7.0508	0.0284	11.1288	0.0219
miR-181a	0.3894	0.0339	0.3790	0.0450
miR-181c	0.5412	0.1498	0.5453	0.1699
miR-182	0.0483	0.1722	0.2757	0.5144
miR-183	0.0159	0.1133	0.1063	0.2980
miR-183*	0.0554	0.1909	0.2661	0.5144
miR-184	0.7025	0.5190	0.7095	0.5857
miR-185	1.2938	0.2188	1.0978	0.6645
miR-186	7.4941	0.0022	6.9527	0.0083
miR-186*	8.5333	0.0151	9.9962	0.0167
miR-187	1.0276	0.9802	1.0086	0.9939
miR-188-5p	0.6680	0.4695	1.0183	0.9777
miR-18a	72.2779	0.0028	20.7957	0.0865
miR-18a*	7.4614	0.0233	5.8501	0.0318
miR-190	0.6081	0.4563	0.6424	0.6159
miR-190b	1.5011	0.8680	1.8966	0.8139
miR-191	1.5178	0.0030	2.7368	0.0010
miR-191*	1.0336	0.8168	1.8957	0.0318
miR-192	2.6147	0.0343	2.8721	0.0703
miR-193*	1.1542	0.8185	1.4449	0.6211
miR-193a-3p	3.3841	0.1265	2.5587	0.2219
miR-193b	2.2055	0.1048	1.3331	0.4568

miR-194	1.5270	0.1767	1.6877	0.2391
miR-195	3.3628	0.0074	2.8812	0.0219
miR-197	1.1711	0.4563	1.1711	0.5144
miR-199a-3p	3.2913	0.0929	3.0768	0.1047
miR-199b	2.0387	0.1778	2.4026	0.1413
miR-19a	9.9279	0.0102	13.1885	0.0219
miR-19a*	1.6706	0.1909	1.6706	0.2085
miR-19b	10.9491	0.0092	13.9927	0.0219
miR-200b	2.7644	0.2997	2.7644	0.3223
miR-200c	1.5509	0.3311	1.5509	0.3582
miR-202	1.3503	0.5042	1.2619	0.6645
miR-203*	1.5630	0.2250	1.5630	0.2415
miR-204	0.7206	0.3078	0.7933	0.5522
miR-205	15.4544	0.0312	10.8745	0.0450
miR-206	0.2143	0.1318	0.2207	0.1413
miR-20a	36.4913	0.0094	14.1815	0.0825
miR-20a*	12.6451	0.0311	12.6451	0.0450
miR-20b	45.1042	0.0098	17.6974	0.0723
miR-21	1.5302	0.2411	2.1148	0.0980
miR-21*	2.1784	0.2736	2.1784	0.2893
miR-210	1.0680	0.8680	1.8984	0.1526
miR-211	0.1019	0.0027	0.1843	0.1482
miR-212	2.0953	0.1217	2.9297	0.0326
miR-214	1.2490	0.3384	1.2490	0.3688
miR-214*	6.4445	0.0871	8.7361	0.0864
miR-215	5.7968	0.0574	5.7727	0.0219
miR-216b	0.4490	0.7461	0.4562	0.7643
miR-217	0.9178	0.9331	1.0956	0.9554
miR-218	3.3595	0.1235	4.3838	0.1120
miR-218-1*	1.2168	0.2997	1.0399	0.8565
miR-218-2*	5.3945	0.1267	5.3945	0.1413
miR-22	0.7261	0.2432	1.4681	0.5497
miR-22*	0.4397	0.0533	0.7141	0.5176
miR-221	1.4396	0.4041	1.0983	0.8579
miR-222	8.2335	0.0025	5.7609	0.0220
miR-224	1.6168	0.1281	2.4240	0.2832
miR-23b	0.5494	0.1318	0.5913	0.1847
miR-24	2.9351	0.0049	3.0090	0.0318
miR-24-2*	8.2626	0.0098	7.3800	0.0219
miR-25	3.3014	0.0092	3.9535	0.1474
miR-26a	0.9554	0.8680	1.1221	0.7553
miR-26b	0.6224	0.1874	1.3837	0.3910
miR-26b*	1.5731	0.1645	2.5132	0.0300
miR-27a	2.1282	0.0292	1.8542	0.0860
miR-27a*	14.5024	0.0106	8.4701	0.0457
miR-27b	0.5640	0.2101	0.7368	0.4947
miR-27b*	2.0195	0.1909	3.2211	0.0898
miR-28	2.5363	0.0117	2.1815	0.0219
miR-28*	3.3344	0.0103	2.6166	0.0937
miR-292-3p	0.7568	0.4627	1.4678	0.2892
miR-294	0.2846	0.0250	0.4608	0.4454
miR-296	0.5796	0.3397	0.5533	0.3365
miR-296-3p	2.7937	0.1417	2.7396	0.1569
miR-297a*	1.9717	0.1133	2.0102	0.1205
miR-298	4.0789	0.1011	2.6628	0.2099
miR-29a	1.1064	0.8649	1.0470	0.9615

miR-29a*	0.9828	0.9757	1.1067	0.9208
miR-29b	0.5328	0.3384	0.6453	0.6137
miR-29b*	1.1289	0.4044	1.1197	0.6893
miR-29c*	0.6357	0.3501	1.2751	0.7094
miR-300*	0.7057	0.4281	0.8751	0.8465
miR-301	4.1720	0.0250	4.1757	0.0372
miR-301b	3.7319	0.0256	3.8783	0.0330
miR-30a-3p	1.1817	0.5681	1.5120	0.2099
miR-30a-5p	0.7641	0.3703	1.1129	0.7934
miR-30b*	0.7432	0.2334	1.5592	0.3985
miR-30c	1.1867	0.3852	1.7333	0.1271
miR-30c-2*	0.2883	0.3703	0.6800	0.7794
miR-30d	0.7540	0.2660	0.9910	0.9777
miR-30e	1.0462	0.8016	1.6850	0.1738
miR-30e-3p	1.3122	0.2997	1.7629	0.0905
miR-31	1.2583	0.3397	0.8821	0.7352
miR-31*	1.3022	0.3622	0.9979	0.9924
miR-32	1.9687	0.1281	2.7879	0.0833
miR-320	1.6826	0.1217	1.5497	0.1699
miR-322*	3.1865	0.0588	4.0280	0.0487
miR-323-3p	1.3858	0.3116	1.1266	0.7191
miR-324-3p	1.6934	0.1513	1.3461	0.3743
miR-324-5p	1.3863	0.3709	1.3679	0.4275
miR-326	1.3396	0.4122	1.0486	0.6903
miR-328	0.4018	0.1217	0.3415	0.1011
miR-329	0.3920	0.0196	0.3923	0.0219
miR-330	0.3767	0.0476	0.4108	0.0860
miR-330-5p	0.2085	0.0211	0.2448	0.0689
miR-331	1.2152	0.3953	1.1564	0.5555
miR-331-5p	1.3294	0.2010	1.0971	0.4338
miR-335	0.3479	0.0915	0.6024	0.3636
miR-335*	0.4924	0.0813	1.1274	0.7268
miR-337-3p	0.9226	0.7470	0.9876	0.9777
miR-337-5p	1.1359	0.5503	0.9754	0.9423
miR-338-3p	1.2643	0.4811	1.0472	0.9271
miR-339-3p	1.5126	0.1059	3.0514	0.0219
miR-339-5p	0.7180	0.1998	0.9097	0.7143
miR-33a*	2.5816	0.0468	3.9783	0.0372
miR-340	3.1883	0.0716	3.0848	0.0833
miR-340*	2.6673	0.0682	2.6100	0.0763
miR-342-3p	3.9970	0.0174	3.7537	0.0219
miR-342-5p	2.5007	0.0667	2.4875	0.0817
miR-344	1.6552	0.1761	1.2855	0.4487
miR-345-3p	0.9222	0.8285	1.1359	0.7643
miR-345-5p	0.6874	0.2997	0.9324	0.8465
miR-34b-3p	10.5575	0.0012	5.1247	0.0833
miR-34b-5p	7.0634	0.0022	3.8219	0.0083
miR-34c	5.7071	0.0049	2.6295	0.0487
miR-34c*	3.7234	0.0049	3.3042	0.0444
miR-350	2.2071	0.0293	2.0651	0.0819
miR-361	0.5523	0.0656	0.5858	0.1214
miR-362-3p	0.6335	0.0374	1.1960	0.7203
miR-362-5p	2.2219	0.0912	2.7138	0.0450
miR-365	0.8246	0.5950	0.7838	0.6083
miR-369-3p	0.8199	0.6528	0.6843	0.4192
miR-369-5p	0.6617	0.3361	0.5250	0.2043

miR-370	1.7933	0.1722	1.4955	0.3212
miR-374-5p	14.9008	0.0027	18.4684	0.0083
miR-375	0.0266	0.0467	0.0307	0.0487
miR-376a	1.3294	0.5299	1.2748	0.6645
miR-376a*	1.4886	0.3292	1.7458	0.3626
miR-376b	1.6428	0.3687	1.2536	0.7136
miR-376b*	1.5275	0.3501	1.6135	0.3985
miR-376c	4.8004	0.0250	4.8834	0.0300
miR-379	2.5920	0.0293	2.1666	0.0457
miR-380-5p	1.8584	0.0683	1.8048	0.1413
miR-381	0.8404	0.7837	0.8379	0.7934
miR-382	0.6801	0.3775	0.6645	0.4057
miR-383	0.6043	0.5705	0.6580	0.6926
miR-384-3p	0.8303	0.4775	0.7495	0.5145
miR-384-5p	1.2635	0.3564	1.2569	0.5555
miR-409-3p	1.6686	0.0868	1.4113	0.1879
miR-409-5p	0.2638	0.0306	0.2331	0.0318
miR-410	0.7411	0.4093	0.8080	0.5970
miR-411	3.5429	0.0131	2.9358	0.0219
miR-411*	2.4803	0.0061	2.5100	0.0450
miR-412	0.7690	0.4695	0.7296	0.4586
miR-423-5p	0.4878	0.2733	0.7424	0.6472
miR-424	3.4286	0.0233	2.5949	0.0490
miR-425	1.3858	0.1909	2.2440	0.0444
miR-431	2.8831	0.0518	2.9146	0.1391
miR-433	0.3933	0.1513	0.3600	0.1413
miR-434-3p	0.9034	0.7678	0.8936	0.7826
miR-434-5p	1.6132	0.3109	1.3946	0.4898
miR-448	0.4229	0.1217	0.2486	0.0492
miR-449	102.6824	0.0049	56.6108	0.0889
miR-449b	128.9933	0.0049	44.6129	0.1167
miR-450a	1.3816	0.1832	0.8302	0.5852
miR-465a-3p	1.9942	0.2733	1.9942	0.2892
miR-466d-3p	1.5854	0.2334	1.5854	0.2495
miR-467*	1.7238	0.0365	1.9223	0.0372
miR-467b	1.5423	0.1483	1.5060	0.0823
miR-467c	5.2525	0.0030	3.6882	0.1018
miR-467d	4.9590	0.0196	3.4905	0.1250
miR-467e	1.1449	0.5450	0.9649	0.9199
miR-470*	0.4613	0.2716	0.8217	0.7643
miR-483*	41.7572	0.1541	16.1906	0.2749
miR-484	2.6004	0.0049	2.2506	0.0220
miR-485-3p	1.2244	0.4916	1.2009	0.5767
miR-485-5p	0.7589	0.4563	0.7212	0.5522
miR-487b	1.0686	0.9036	0.5106	0.4921
miR-488*	2.3999	0.0574	2.0392	0.0864
miR-489	2.2370	0.4399	2.0157	0.5522
miR-491	1.6681	0.1217	1.5264	0.1877
miR-493	2.2887	0.2186	2.2394	0.2421
miR-494	1.9198	0.0656	1.4901	0.1764
miR-495	0.7644	0.4395	0.6721	0.3743
miR-496	0.4349	0.1244	0.3695	0.0901
miR-497	5.1815	0.0092	2.7618	0.0901
miR-500	0.8217	0.4250	1.0723	0.8146
miR-501*	0.5962	0.1398	1.2069	0.6760
miR-503	1.7119	0.1803	1.7119	0.1940

miR-503*	3.1265	0.0468	3.2433	0.0487
miR-504	0.3589	0.2920	0.5071	0.5522
miR-532	2.1214	0.0467	2.2806	0.0450
miR-532-3p	1.7822	0.0110	1.6072	0.0318
miR-541	2.9426	0.0772	2.4917	0.1250
miR-542-3p	0.8553	0.4775	1.3062	0.4038
miR-542-5p	0.9508	0.9020	1.4242	0.2543
miR-543	0.5247	0.0872	0.4468	0.0763
miR-544	0.3454	0.0889	0.3507	0.1413
miR-547	2.5416	0.0884	2.2172	0.1250
miR-551b	0.2835	0.2874	0.2770	0.2928
miR-574-3p	2.9735	0.0074	2.5155	0.0450
miR-582-3p	4.1656	0.0574	4.1383	0.0701
miR-582-5p	1.3990	0.4563	1.1743	0.7553
miR-592	2.2891	0.2716	1.7788	0.4338
miR-598	0.4261	0.0683	0.4089	0.0888
miR-652	0.6363	0.1941	0.7003	0.2909
miR-665	1.7008	0.1909	1.0357	0.9554
miR-666	0.4730	0.1166	0.4074	0.0876
miR-667	0.7111	0.3361	0.6420	0.2585
miR-668	0.2907	0.1786	0.2467	0.1535
miR-669a	1.4495	0.1660	1.2224	0.4946
miR-671-3p	1.3742	0.1434	1.3055	0.2099
miR-672	8.9835	0.0018	4.0319	0.0763
miR-673	2.4923	0.0209	2.0431	0.0604
miR-673-3p	1.6356	0.3691	1.6356	0.4046
miR-674	1.1551	0.5945	1.1184	0.7553
miR-674*	2.2261	0.0284	2.1755	0.0282
miR-676	1.5830	0.2887	0.9890	0.9779
miR-676*	1.9311	0.1219	1.4014	0.3743
miR-677	2.1661	0.0138	1.2682	0.6760
miR-678	0.9520	0.8285	0.9243	0.7352
miR-680	1.9958	0.1592	1.9958	0.1702
miR-682	2.0112	0.2733	1.6844	0.4063
miR-684	1.7926	0.2386	1.1392	0.8807
miR-685	2.3250	0.3852	2.6443	0.3743
miR-690	2.3387	0.0196	2.7334	0.0288
miR-694	1.8394	0.0293	1.4077	0.0882
miR-699	1.0298	0.8860	1.3836	0.2058
miR-7*	2.0955	0.0574	3.1629	0.0450
miR-700	1.1777	0.5450	1.3504	0.1346
miR-701	8.3604	0.0161	7.5597	0.0219
miR-702	0.2960	0.0355	0.3671	0.0860
miR-704	0.4986	0.0761	0.6174	0.0763
miR-706	3.3156	0.0341	3.2128	0.0487
miR-708	1.8625	0.5470	1.6621	0.6760
miR-709	2.4107	0.0196	2.2799	0.0330
miR-720	3.1417	0.0463	3.1122	0.0905
miR-721	1.0120	0.9323	1.0280	0.9271
miR-741	1.1971	0.3564	1.1971	0.3938
miR-744	1.4084	0.2518	1.4167	0.2607
miR-744*	1.7295	0.2997	2.3688	0.0708
miR-760	1.4771	0.0912	1.3503	0.0825
miR-764-5p	0.8487	0.3703	0.7525	0.1843
miR-770-3p	0.6794	0.2997	0.5244	0.1239
miR-770-5p	0.2056	0.0918	0.1670	0.0846

miR-7b	0.6986	0.4297	0.5830	0.4129
miR-802	0.4849	0.3775	0.6832	0.6740
miR-804	1.8326	0.4343	2.2498	0.2274
miR-805	7.4550	0.0110	8.3450	0.0219
miR-872	1.3403	0.3892	2.6172	0.0779
miR-872*	1.6538	0.1434	3.6208	0.0083
miR-873	0.4791	0.2982	0.9641	0.9777
miR-875-5p	0.5021	0.1206	0.8471	0.6893
miR-877*	0.6536	0.1235	0.7066	0.2099
miR-878-3p	1.0921	0.4641	0.7632	0.6595
miR-879	1.1180	0.8680	1.6459	0.3582
miR-879*	2.8325	0.0635	2.7528	0.0330
miR-881*	1.3792	0.4641	1.3792	0.5208
miR-9	1.1033	0.8783	0.9257	0.9271
miR-9*	1.8695	0.4482	2.6427	0.3140
miR-92	2.9358	0.0637	5.7739	0.0700
miR-93	30.5877	0.0022	9.4910	0.1257
miR-93*	7.5854	0.0018	5.8683	0.0833
miR-96	0.0107	0.0689	0.0924	0.2099
miR-99a	1.9748	0.3428	1.5377	0.5522
miR-99b	0.5731	0.0281	0.6997	0.1413
miR-99b*	2.2428	0.0199	2.2471	0.0444

Table S 2: Differential miRNA expression in human tumors.

miRNA	tumor vs. normal retina	
	fold change	p value
hsa-let-7a	0.3553790	0.0001386
hsa-let-7b	0.0960455	0.0000072
hsa-let-7c	0.0857961	0.0000072
hsa-let-7d	0.2603711	0.0001386
hsa-let-7e	1.0728688	0.7750257
hsa-let-7f	0.3486576	0.0004307
hsa-let-7g	0.2515795	0.0000072
hsa-let-7i	0.3123420	0.0000401
hsa-mir-1	0.0590332	0.0004940
hsa-mir-100	0.0859554	0.0000072
hsa-mir-101	0.3470506	0.0003348
hsa-mir-103	2.7203751	0.0000072
hsa-miR-105	1.5746551	0.0994383
hsa-mir-106a	22.4668082	0.0000072
hsa-mir-106b	10.6402635	0.0000072
hsa-mir-10a	2.1920179	0.0461181
hsa-mir-10b	1.3439072	0.7415661
hsa-mir-124a	0.0900642	0.0004307
hsa-mir-125a	0.5231962	0.0022645
hsa-mir-125b	0.0787872	0.0000072
hsa-miR-126	0.4573023	0.2427086
hsa-mir-126*	0.6257817	0.2560278
hsa-mir-127	0.0342777	0.0000072
hsa-mir-128a	0.7824566	0.1386128
hsa-mir-128b	0.3295381	0.0004307
hsa-mir-129	0.2818393	0.0000072
hsa-mir-130a	2.2543328	0.0133951
hsa-mir-130b	21.4342907	0.0000072
hsa-mir-132	1.4948522	0.0054634
hsa-mir-133a	0.0436029	0.0001854
hsa-mir-133b	0.0646316	0.0003348

hsa-mir-134	0.0437214	0.0000072
hsa-mir-135a	0.6860929	0.3268279
hsa-mir-135b	2.4677787	0.0153996
hsa-mir-136	0.2058798	0.0000414
hsa-mir-137	0.1190246	0.0320335
hsa-mir-139	0.4108590	0.0013856
hsa-mir-140	0.4407683	0.0089737
hsa-mir-142-3p	1.0044799	0.8537212
hsa-mir-142-5p	1.1893089	0.4895443
hsa-mir-143	0.4121620	0.0002512
hsa-mir-145	1.2121639	0.2697602
hsa-mir-146a	0.6846331	0.1935018
hsa-miR-146b	0.4938285	0.0548053
hsa-mir-147	1.0210604	0.7262167
hsa-mir-148a	0.4356479	0.0015263
hsa-mir-148b	0.8043338	0.3088958
hsa-mir-149	1.0112901	0.9077094
hsa-mir-150	0.5041007	0.0227267
hsa-mir-151	1.0735959	0.4655902
hsa-mir-152	0.2517561	0.0000072
hsa-mir-153	0.3954751	0.0117662
hsa-mir-155	2.1348908	0.0174956
hsa-mir-15a	2.0636355	0.0090042
hsa-mir-15b	26.1777272	0.0000072
hsa-mir-16	7.0069907	0.0000072
hsa-mir-17-3p	2.9472995	0.0002512
hsa-mir-17-5p	26.3119159	0.0004307
hsa-mir-181a	0.4125044	0.0018715
hsa-mir-181b	0.4559957	0.0041878
hsa-mir-181c	0.3884647	0.0001854
hsa-mir-181d	0.7031880	0.1270344
hsa-mir-182	0.3523287	0.0004307
hsa-mir-182*	0.4255779	0.0174956
hsa-mir-183	0.5743967	0.0285932
hsa-mir-184	0.0639815	0.0000072
hsa-miR-185	1.5415554	0.1270344
hsa-mir-186	1.8543890	0.0012406
hsa-mir-187	0.4648131	0.3936791
hsa-mir-188	0.8880624	0.7262167
hsa-mir-189	0.1689350	0.0003023
hsa-mir-18a	79.0815882	0.0000072
hsa-mir-18a*	63.9114703	0.0000072
hsa-mir-190	1.6401400	0.2889012
hsa-mir-191	1.1047789	0.2697602
hsa-mir-192	0.1462240	0.0000072
hsa-mir-193a	1.1678983	0.6746585
hsa-mir-193b	4.2090245	0.0001386
hsa-mir-194	0.2090721	0.0000072
hsa-mir-195	2.8573946	0.0001854
hsa-mir-196a	16.7342353	0.0004307
hsa-mir-196b	17.7581272	0.0004307
hsa-mir-197	3.3116927	0.0000072
hsa-mir-199a*	0.5500008	0.1084375
hsa-mir-19a	6.8875133	0.0000072
hsa-mir-19b	4.4937336	0.0000130
hsa-mir-200b	0.4279177	0.0037847
hsa-mir-200c	1.4157987	0.0174956
hsa-mir-202	1.1245744	0.2636806
hsa-mir-203	0.8355882	0.4895443
hsa-mir-204	0.0370652	0.0000072
hsa-mir-205	0.5367589	0.0758117
hsa-mir-206	0.9580725	0.7750257

hsa-mir-20a	26.4811479	0.0000072
hsa-mir-20b	14.1612372	0.0000072
hsa-mir-21	0.5765650	0.0133951
hsa-mir-210	0.9628572	0.9906034
hsa-mir-211	0.0248280	0.0004307
hsa-mir-213	0.4836200	0.2476658
hsa-mir-214	1.3894380	0.1270344
hsa-mir-216	2.3210745	0.0093918
hsa-mir-217	7.8132242	0.0000130
hsa-mir-218	0.2517909	0.0076255
hsa-mir-219	0.9463152	0.9601050
hsa-mir-22	0.0525316	0.0000072
hsa-mir-221	1.4094766	0.5272094
hsa-mir-222	1.0933970	0.6746585
hsa-mir-223	0.8953460	0.8537212
hsa-mir-224	291.8648249	0.0000072
hsa-mir-23b	0.4200482	0.0000244
hsa-mir-24	0.6389637	0.0490670
hsa-mir-25	15.6401857	0.0000072
hsa-mir-26a	0.5955367	0.0442740
hsa-mir-26b	0.5583957	0.0320335
hsa-mir-27a	0.3573996	0.0002512
hsa-mir-27b	0.3622524	0.0000072
hsa-mir-28	1.0319090	0.6477827
hsa-mir-296	2.1351466	0.0001386
hsa-mir-29a	0.0421722	0.0000072
hsa-mir-29b	0.0482461	0.0002102
hsa-mir-29c	0.0288659	0.0000072
hsa-mir-301	7.4250278	0.0004307
hsa-mir-302a	0.8393894	0.5682995
hsa-mir-302b	0.6734236	0.5268989
hsa-mir-302c	1.1932806	0.7750257
hsa-mir-30a-3p	0.1480078	0.0000072
hsa-mir-30a-5p	0.5313676	0.0006314
hsa-mir-30b	0.5458853	0.0133951
hsa-mir-30c	0.5593936	0.0039131
hsa-mir-30d	0.7681248	0.5367022
hsa-mir-30e-3p	0.2106057	0.0000401
hsa-mir-31	0.0210180	0.0004307
hsa-mir-32	1.7654894	0.0442740
hsa-mir-320	1.1200035	0.3483077
hsa-mir-323	0.3336934	0.0014135
hsa-mir-324-3p	1.2634500	0.2505400
hsa-mir-324-5p	1.9327812	0.0022645
hsa-mir-328	0.3347539	0.0001386
hsa-mir-329	0.0523792	0.0007761
hsa-mir-33	0.4896823	0.0913180
hsa-mir-330	0.0952696	0.0004307
hsa-mir-331	1.2051349	0.0678533
hsa-mir-335	0.3110579	0.0000649
hsa-mir-337	0.2086231	0.0090042
hsa-mir-338	0.9519232	0.7262167
hsa-mir-339	0.9702796	0.9906034
hsa-mir-340	4.3996595	0.0000401
hsa-mir-342	1.2049924	0.2697602
hsa-mir-345	2.2335974	0.0006314
hsa-mir-34a	3.2932512	0.0025184
hsa-mir-34b	2.1809079	0.0040426
hsa-mir-34c	11.4800940	0.0004307
hsa-mir-361	1.6448550	0.0001854
hsa-mir-362	4.6667567	0.0000972
hsa-mir-363	0.7669028	0.2697602

hsa-mir-365	3.1851319	0.0004307
hsa-mir-367	0.7884866	0.7071706
hsa-mir-368	0.2349716	0.0001012
hsa-mir-369-3p	0.0275169	0.0009109
hsa-mir-369-5p	0.0836195	0.0025184
hsa-mir-370	0.0747683	0.0006069
hsa-mir-371	0.4841878	0.1084375
hsa-mir-372	0.5430670	0.0441516
hsa-mir-373	0.9509754	0.6211617
hsa-mir-374	1.9916325	0.0818948
hsa-mir-375	1.2503536	0.8537212
hsa-mir-376a	0.0768353	0.0004940
hsa-miR-376a*	0.0968149	0.0000094
hsa-mir-378	0.1296273	0.0000072
hsa-mir-379	0.0395695	0.0002512
hsa-miR-380-5p	0.0380046	0.0006955
hsa-mir-381	0.4618507	0.0254578
hsa-mir-382	0.0307304	0.0001797
hsa-mir-383	0.0283853	0.0004940
hsa-mir-409-5p	0.3510641	0.0004843
hsa-mir-410	0.0522818	0.0012406
hsa-mir-411	0.0505212	0.0022499
hsa-mir-422a	0.1910191	0.0000972
hsa-mir-422b	0.1233889	0.0005558
hsa-mir-423	1.2842344	0.0093918
hsa-mir-424	0.3742888	0.0262440
hsa-mir-425	1.2801425	0.0244766
hsa-miR-425-5p	1.6253638	0.0320335
hsa-mir-429	0.3929063	0.0099459
hsa-mir-432	0.0528755	0.0033238
hsa-mir-432*	0.2765759	0.0016392
hsa-mir-433	0.0306924	0.0003174
hsa-mir-449	155.4346758	0.0004307
hsa-mir-449b	16.6971009	0.0004307
hsa-mir-451	0.4633213	0.0133951
hsa-mir-452*	50.0864717	0.0004307
hsa-mir-455	0.7951811	0.6211617
hsa-miR-484	1.1778933	0.5251131
hsa-mir-485-3p	0.1108984	0.0006314
hsa-mir-486	5.9867152	0.0000072
hsa-mir-487a	0.3434609	0.0000149
hsa-mir-487b	0.0359722	0.0007474
hsa-miR-488	0.2012242	0.0000972
hsa-mir-489	0.3190519	0.0090042
hsa-mir-491	0.3652790	0.0008133
hsa-mir-493-3p	0.6859919	0.0025978
hsa-mir-495	0.0384973	0.0007635
hsa-mir-496	0.3300278	0.0047903
hsa-mir-497	0.2185559	0.0007416
hsa-mir-500	3.2597784	0.0144688
hsa-mir-501	4.7999094	0.0040426
hsa-mir-502	4.9972275	0.0037847
hsa-miR-504	0.4893946	0.0158425
hsa-mir-511	1.9985553	0.0379916
hsa-mir-516-3p	2.6945762	0.0007761
hsa-mir-517c	0.6986132	0.2560278
hsa-mir-518b	0.6868402	0.2479639
hsa-mir-520b	1.6296476	0.0251097
hsa-mir-520c	0.7075127	0.3202043
hsa-mir-520d	1.1469034	0.9344157
hsa-mir-520f	1.1115869	0.9077094
hsa-mir-520g	1.3021177	0.9077094

hsa-mir-524	1.4398430	0.1241732
hsa-mir-526b*	1.0973129	1.0000000
hsa-miR-532	3.4935996	0.0009837
hsa-mir-539	0.0521890	0.0007761
hsa-mir-542-3p	0.1440279	0.0012424
hsa-mir-544	2.6205227	0.0221123
hsa-miR-545	1.0114619	0.9077094
hsa-miR-548a	2.0565578	0.0251097
hsa-miR-548c	1.4529841	0.4903598
hsa-mir-548d	67.9436778	0.0004307
hsa-mir-550	7.7678215	0.0000072
hsa-mir-551b	1.8929614	0.0748287
hsa-miR-556	1.4084918	0.1016451
hsa-mir-563	1.8360975	0.2233519
hsa-mir-564	0.8040403	0.6903335
hsa-mir-565	1.8602223	0.0442740
hsa-mir-572	1.5724844	0.1178823
hsa-mir-574	1.7388258	0.0400753
hsa-miR-576	3.4604257	0.0093918
hsa-miR-579	1.4555087	0.1787665
hsa-mir-580	1.6740452	0.0758117
hsa-mir-586	3.5635258	0.0041651
hsa-miR-589	2.7391901	0.0224632
hsa-miR-591	1.7820383	0.3261438
hsa-miR-592	3.6849267	0.0039131
hsa-miR-594	5.9532556	0.0018715
hsa-miR-597	1.0740736	0.9344157
hsa-mir-601	1.5690454	0.2090724
hsa-mir-604	0.8915881	0.8537212
hsa-miR-606	0.9303786	0.8316354
hsa-mir-610	1.6714297	0.0490670
hsa-mir-616	1.1399930	0.4655902
hsa-miR-617	0.9964456	1.0000000
hsa-miR-618	0.5560727	0.1178823
hsa-mir-624	0.7160710	0.3845464
hsa-mir-627	1.1708924	0.8537212
hsa-miR-628	1.7607653	0.0691615
hsa-miR-629	13.7301513	0.0000072
hsa-mir-630	0.9105617	0.6477827
hsa-mir-632	2.1906110	0.0285932
hsa-miR-638	1.3605807	0.4308006
hsa-mir-639	1.2894402	0.7278872
hsa-miR-641	1.1797699	0.7750257
hsa-miR-642	0.6771290	0.8537212
hsa-mir-643	1.3567365	0.1505697
hsa-miR-645	0.6528589	0.0400753
hsa-mir-650	1.3372344	0.4175414
hsa-mir-651	2.8328623	0.0056996
hsa-miR-653	0.3308879	0.0025086
hsa-mir-655	0.0624041	0.0020042
hsa-mir-656	0.1359565	0.0001735
hsa-mir-660	1.7528527	0.0610666
hsa-mir-7	42.6616607	0.0000072
hsa-mir-9	0.2639609	0.0000649
hsa-mir-9*	0.1931189	0.0000244
hsa-mir-92	6.4057347	0.0000072
hsa-mir-93	23.3811787	0.0000072
hsa-mir-95	2.1807093	0.0323956
hsa-mir-96	0.1514806	0.0000130
hsa-mir-98	0.3501880	0.0323956
hsa-mir-99a	0.0903338	0.0000072
hsa-mir-99b	1.4656772	0.0076255

Table S 3: List of miRNAs that are upregulated both in mouse and human tumors.

miRNAs	Murine tumour vs. normal retina	Human tumour vs. normal retina	Mouse Validated targets according to http://mirecords.biolead.org/	Human Validated targets according to http://mirecords.biolead.org/	Predicted Targets by at least 4 different algorithms according to miRNA body map (http://mellfire.ugent.be/public/body_map/)	Other putative targets - PubMed
miR-449b	128.99	16.70	-	-	none	-
miR-449	102.68	155.43	**E2F5**	-	ACCN1, ADRA1D, ANK3, BTBD11, CCNE2, CLIP3, DBC1, DLL1, DOCK8, E2F5, FAM76A, FGD6, FKBP1B, FUT8, LEF1, LMBR1L, MYCN, NUMBL, PALLD, PGM1, PKNOX1, PKP4, PLN, UBE2NL, XYLT1	**DLL-1, NOTCH-1**
miR-18a	72.28	79.08	-	-	BTG3, BTN1A1, C20orf30, C7orf42, CAD, DSG4, ESCO2, ESR1, HIF1A, IRF2, ITGA2, KCNH7, KIAA1012, MAP7D1, NKIRAS1, PCID2, PDE4D, PLA2G1B, PNLIPRP3, RAB9A, RAD51AP1, RBBP8, RFC4, SEC23IP, TBPL1, TNFAIP3 (A20), TOR1B, TRADD, TRPC4, TXK, UBTD2, ZNF536	**DLL-1, NOTCH-1**
miR-106a	51.89	22.47	**MYLIP, ARID4B, LOC100048439**	**VEGFA, RB1, RUNX1, APP**	none	K-Ras
miR-17-5p	47.58	26.31	RB2 (p130)	NCOA3, VEGFA, RUNX1, CCND1	**ARID4B, ATAD2, ATG12, ATP12A, C1orf63, C7orf43, CRIPT, DDX51, DHTKD1, DIP2A, DOCK4, E2F5, ENTPD4, ERBB3, FOXQ1, GAB1, GALNTL2, GLO1, GPR6, ITGB8, KIAA1191, KPNA2, LAPTM4A, LONP2, LRRC45, MAP3K8, MAP3K9, MAPK9, MCHR2, METAP1, MINK1, MMP3, MUC17, MYCN, NRBP1, NUP35, PBK, PBLD, PDDC1, POLQ, PON2, POU6F1, PTPN4, RCCD1, SACS, SC4MOL, SLC46A3, SPTY2D1, STAT3, STK17B, TBC1D2 TLE4, TMEM138, TMUB2, TRIM8, TRIP11, TRPV6, TSHZ3, UBE2B, VDAC1, VSX1, WEE1, ZNFX1**	
miR-20b	45.10	14.16	**MYLIP, ARID4B, LOC100048439**	**VEGFA**	CCL1, DDX5, SLC40A1, STK33	HBP1
miR-20a	36.49	26.48	ZBTB7A, STAT3	**VEGFA, E2F1, RUNX1, CCND1**	AGTPBP1, CAPRIN2, CROT, KIAA0922, MAGI3, MASTL, MTCH2, NTN4, PFKP, TRIP10, TSG101, VLDLR	
miR-93	30.59	23.38	**STAT3**	**E2F1, VEGFA, CDKN1A (p21Cip1)**	FGD5, OSR1, TRIM3	
miR-19b	10.95	4.49	**MYLIP, LOC100048439**	-	FAM69A, PCDH10, SOX4, ZC3HAV1L	
miR-19a	9.93	6.89	-	**PTEN**	>100	
miR-186	7.49	1.85	-	-	>100	
miR-18a*	7.46	63.91	-	-	none	
miR-34b	7.06	2.18	-	-	>100	**DLL-1**

miR-17*	7.05	2.95	-	-	none	CREB
miR-106b	6.48	10.64	-	**E2F1, VEGFA, CDKN1A (p21Cip1), ITCH**	ACPL2, BAMBI	
miR-155	5.93	2.13	SFPI1, MYB, RHEB, BAT5, JARID2, TRP53INP1, IKBKE, FADD, RIPK1, MAF, AICDA, SOCS1	AGTR1, BACH1 (FANCJ), LDOC1, MATR3, TM6SF1, RHOA, ETS1, MEIS1	DHX40, NARS, RCN2, SDCBP, SYPL1, TP53INP1, TRIM32, TRIP13	
miR-34c	5.71	11.48	-	-	B3GALNT1, MET, MFAP4, PPP2R5A, RRAS, TMEM55A, XBP1	**DLL-1**
miR-15b	5.45	26.18	-	BCL2, CCNE1	ATXN7L1, C14orf129, CHORDC1, EFCAB5, EIF2B2, FAM91A1, GLT1D1, ITPR1, MAP2K1, MBNL2, MKNK1, PDIA6, RECK, RSPO3, SFRS16, SPRYD3	**DLL-1**
miR-301	4.17	7.43	-	-	ABHD3, ACPL2, BAI3, BTBD3, C3orf64, CASP8, CENPO, CSMD1, DUS4L, F3, FBXO9, FSTL5, GADD45A, GAP43, GTF2H1, HABP4, HHEX, KIAA1217, MAT2B, NME7, NPTN, NUP133, PLAA, PSD, PTH, RAPGEF4, SAP18 SLAIN1, SNX2, USP28, WNT1	**DLL-1**
miR-195	3.36	2.86	-	-	ATP10B, CDC23, IKBKB, NFATC3, PCMT1, PEX13, PPAP2A, RBM6, RUNX1T1, ZBTB34	**MEOX2**
miR-25	3.30	15.64	-	-	ACADL, ADARB2, ADCY3, ADM, AP1AR, ARHGEF17, CDH10, CHKA, CHST1, CLDN11, COL1A2, DNAJB12, EGR2, GOLGA4, HIPK3, LMO2, MOBKL2A, NFIA, PCDH11X, PPCS, RNF4, TMEM87A, ZNF287	
miR-16	3.03	7.01	-	**CCND1**	CCNT2	**PTEN, BIM, MITF**
miR-92	2.94	6.41	**MYLIP, LOC100048439**	-	FAM70A, GPR172B, NKX2-4, SETD5	
miR-532	2.12	3.49	-	-	ADORA1, ARPC3, BPHL, C1orf144, C2orf24, CARHSP1, CFD, CFLAR, CHD3, CIRBP, CSF3, CTNNA2, ETNK2, FAM83E, GALNT6, GCNT1, GORASP1, GP6, HIPK2, HTR3B, IGFBP4, IRX1, LIMK2, MTMR12, MYOM3, NMT2 OASL, OTUD7B, PRDM7, PTK6, SIAH2, SLC25A42, SLCO4A1, SMARCD2, SRRM2, TAF15, TM2D3, TMEM100, TMEM101, TNFSF11, TRAF2, TRAPPC4, TTC8, USP48, WFDC1, ZNF74	**BIM, p63**
miR-130a	1.71	2.25	-	TAC1, CSF1, MAFB, MEOX2, HOXA5	CALM2, CASD1, CCDC85A, CCT6A, CD69, CEP55, CHD9, CLCN5, CLUL1, CSK, CXCL6, DSG1, DYNC1LI2, DYNLL2, ELK3, ENPP5, EREG, FRMD6, HPRT1, IL15, INHBB, KIAA0802, KLHL20, MASTL, MED12L, MEOX2, MET, MMP10, MPHOSPH9, MUM1L1, NPAT, PHF3, PRR15, PSAP, RAB34, RAB40B, RBM25, RPS6KA5, SEC23B, SMARCD2, ST8SIA3, SYT16, TGOLN2, TMEM9B, TNRC6A, TRIM3, VPS37A, WDR20, WDR47	**DLL-1**

Publications

Nittner, D., I. Lambertz, et al. (submitted and under revision). "Synthetic lethality between *Rb1*, *p53* and *miR17~92* uncovers a therapeutic strategy for retinoblastoma"

Lambertz, I., D. Nittner, et al. (2010). "Monoallelic but not biallelic loss of Dicer1 promotes tumorigenesis in vivo." *Cell death and differentiation* **17**: 633-41.

Mestdagh, P., E. Fredlund, et al. (2010). "An integrative genomics screen uncovers ncRNA T-UCR functions in neuroblastoma tumours." *Oncogene* **29**: 3583-92.